

# Transfer Printing Techniques for Materials Assembly and Micro/Nanodevice Fabrication

Andrew Carlson, Audrey M. Bowen, Yonggang Huang,\* Ralph G. Nuzzo,\* and John A. Rogers\*

Transfer printing represents a set of techniques for deterministic assembly of micro- and nanomaterials into spatially organized, functional arrangements with two and three-dimensional layouts. Such processes provide versatile routes not only to test structures and vehicles for scientific studies but also to high-performance, heterogeneously integrated functional systems, including those in flexible electronics, three-dimensional and/or curvilinear optoelectronics, and bio-integrated sensing and therapeutic devices. This article summarizes recent advances in a variety of transfer printing techniques, ranging from the mechanics and materials aspects that govern their operation to engineering features of their use in systems with varying levels of complexity. A concluding section presents perspectives on opportunities for basic and applied research, and on emerging use of these methods in high throughput, industrial-scale manufacturing.

## 1. Introduction

This Review addresses the current literature and recent developments in transfer printing, a potentially transformational approach to materials assembly and micro-/nanofabrication with far-ranging fields of use. At the heart of the method is the use of highly parallel protocols to print 'inks', here defined as a diversity of material classes with a wide range of geometries and configurations having broadly adaptable levels of functional integration, into the precise architectures required by devices. Recent rapid progress in the field has expanded the competencies of transfer printing, in terms of both the range of materials

for patterning and scope of applications enabled. Inspired by the scalability and cost advantage of various forms of commercial printing and soft lithography,<sup>[1–4]</sup> transfer printing has evolved into a sophisticated approach to materials assembly and device fabrication. As the content of this Review will illustrate, essentially any class of material can be developed in the form of an ink appropriate for transfer printing-based fabrication schemes—from complex molecular scale materials (self-assembled monolayers (SAMs),<sup>[1–4]</sup> nanotubes and graphene,<sup>[5–8]</sup> functional polymers,<sup>[9–11]</sup> DNA,<sup>[12–14]</sup> photoresists,<sup>[15]</sup> etc.), to high performance hard materials (single-crystalline inorganic semiconductors,<sup>[16–20]</sup> metals,<sup>[21–24]</sup> oxide thin films,<sup>[25,26]</sup> etc.), to fully integrated device structures (thin film transistors (TFTs),<sup>[16,27–30]</sup> light emitting diodes (LEDs),<sup>[31,32]</sup> complementary metal oxide semiconductor (CMOS) circuits,<sup>[33–35]</sup> sensing arrays,<sup>[36,37]</sup> solar cells,<sup>[38,39]</sup> etc.). Demonstrations of unique material constructs and devices created by advanced forms of transfer printing appear in **Figure 1**. These examples illustrate functional integration of some of the materials and geometries discussed in detail throughout this Review and show how the myriad capabilities inherent to transfer printing can enable new fabrication routes such as multidimensional assembly (Figure 1a),<sup>[40]</sup> large-area deployment of nanostructured materials (Figure 1b),<sup>[41]</sup> and manufacture of passive (Figure 1c-d)<sup>[42,43]</sup> and active (Figure 1e-f)<sup>[44–46]</sup> devices in light-weight, flexible, and curvilinear formats.

The printing protocols discussed in this Review directly address the adaptation of a wide range of material classes - in many cases, the highest performance materials known for specific applications - to challenging and unusual environments. **Figure 2** shows three distinct categories of transfer: additive transfer, subtractive transfer, and deterministic assembly; all printing techniques discussed in the following utilize one or more these methods. The third protocol is particularly powerful, due to its natural compatibility with high performance, single crystalline semiconductor materials (such as Si, GaAs, GaN, InP, etc.)<sup>[16,18,20,47,48]</sup> in micro- or nanostructured forms. Transfer printing such materials with a soft, elastomeric stamp enables their deterministic assembly onto nearly any type of substrate, at room temperature, with high yields and accurately registered placement, in rapid, parallel fashion. When repeated, this process provides a high resolution large-area assembly technique, with capabilities in two or three dimensional layouts and

Prof. J. A. Rogers, A. Carlson  
Department of Materials Science and Engineering  
Fredrick Seitz Materials Research Laboratory  
Beckman Institute for Advanced Science and Technology  
University of Illinois at Urbana-Champaign  
Urbana, IL, USA  
E-mail: jrogers@illinois.edu

Prof. R. G. Nuzzo, Dr. A. M. Bowen  
Department of Chemistry  
University of Illinois at Urbana-Champaign  
Urbana, IL, USA  
E-mail: r-nuzzo@illinois.edu

Prof. Y. Huang  
Department of Mechanical Engineering  
Department of Civil and Environmental Engineering  
Northwestern University  
Evanston, IL, USA  
E-mail: y-huang@northwestern.edu



DOI: 10.1002/adma.201201386

in heterogeneous levels of materials integration, all of which lie beyond the competency of any other method.<sup>[1,3,4]</sup>

In all three schemes of Figure 2 a molded stamp, or one whose surface chemistry is adjusted in a patterned way to control adhesion, affects physical mass transfer between two intrinsically different substrates. The first two have the additional feature that the stamp itself plays a critical role in the structuring of relevant materials into forms with desired lateral geometries. We refer to the first case (Figure 2a) as *additive transfer*, an effective modality for manipulating many types of organic and inorganic materials,<sup>[49–58]</sup> in which transfer occurs between an entire ink layer, or selected parts of it, that have been deposited on the surface of a stamp, and a receiving substrate. Inking of the stamp can be achieved through a variety of methods, from solution casting to physical vapor deposition, as discussed throughout the sections of this Review.<sup>[15,59–61]</sup> Layers printed by additive techniques can provide different functions, such as forming integrated device components or serving as etch masks for subsequent processing.<sup>[32,62–64]</sup>

The second method, *subtractive transfer*, shown schematically in Figure 2b, utilizes a stamp to selectively retrieve regions of a blanket film. This printing modality can be used to directly pattern an active layer or to open windows in etch masks, allowing access to underlying layers of materials for subsequent processing.<sup>[65,66]</sup> As in the case of additive printing, chemical modification of the receiver, heat, or thin intermediate polymeric adhesion promoting layers between the stamp and ink can aid the transfer.<sup>[66,67]</sup> Unlike additive printing, this mode requires cohesive fracture of the ink layer and, therefore, an additional set of considerations in engineering design. In some instances, *subtractive transfer* represents the inking step for the *additive transfer* process. Such methods, or more conventional processing or growth techniques, can form defined structures on a donor substrate, for use in *deterministic assembly* techniques, shown in Figure 2c. This strategy is valuable, in part, because it dramatically expands the materials possibilities in fabrication by separating growth and processing of the inks from the stamp and the receiving substrate. These methods often rely on a dynamic, reversible modulation of adhesion forces to the stamp, using techniques described in the next section.

A key advantage of the procedures outlined in Figure 2 is that they enable rapid delivery of materials in sparse or dense layouts over large substrate areas, specifically via multiple stamp inking and printing cycles. Several variants of sequential inking and printing can be used: in the first method, delineated ink structures on a donor wafer can be translated directly to a receiver, either by use of a stamp with a flat surface or one in which the surface relief pattern is directly matched to the format of the donor ink. Final layouts for the donor are determined during processing of the ink and can exploit precise positioning and size control available to the lithographic fabrication steps used to construct the ink.<sup>[68,69]</sup> A second method utilizes molded relief on a stamp to determine pitch, layout, and critical dimensions of the printed inks, independent of the configuration on the donor substrate. **Figures 3a–c** demonstrate a case of area expansion in which densely packed thin plates of compound semiconductor (here in the form of epitaxial stacks of materials designed for light emitting diodes) on the



**Andrew Carlson** received his BS and MS degrees in Materials Science and Engineering from Stanford University in 2006. He is currently a Ph.D. candidate in the Materials Science and Engineering department at the University of Illinois at Champaign-Urbana, working in the Rogers research group. His graduate work

has explored the physics of adhesion between low and high modulus materials, fabrication, manipulation, and assembly of multi-dimensional semiconductor nanomaterials, as well as materials and device designs for unconventional electronic systems.



**Audrey M. Bowen** received her BS in Materials Science and Engineering from Cornell University in 2005 and her PhD in Materials Chemistry from the University of Illinois at Urbana-Champaign in 2011. She completed her graduate work with Ralph Nuzzo, focusing on the development of various soft lithography based fabrication

techniques, including non-planar and 3D photo-patterning. Bowen is currently a process development engineer at Intel Corporation.



**Professor John A. Rogers** obtained BA and BS degrees in chemistry and physics from the University of Texas, Austin, in 1989. From MIT, he received S.M. degrees in physics and chemistry in 1992 and a Ph.D. in physical chemistry in 1995. He currently holds the Flory-Founder Chair in Engineering at the University of Illinois

at Urbana-Champaign. Rogers' research includes fundamental and applied aspects of materials and patterning techniques for unusual electronic and photonic devices, with an emphasis on bio-integrated and bio-inspired systems

donor are selectively retrieved with a microstructured stamp and printed, with expanded pitch, across a sparsely populated area on the target.<sup>[31]</sup> Printing in this manner enables transformation of the donor wafer geometry upon translation to the

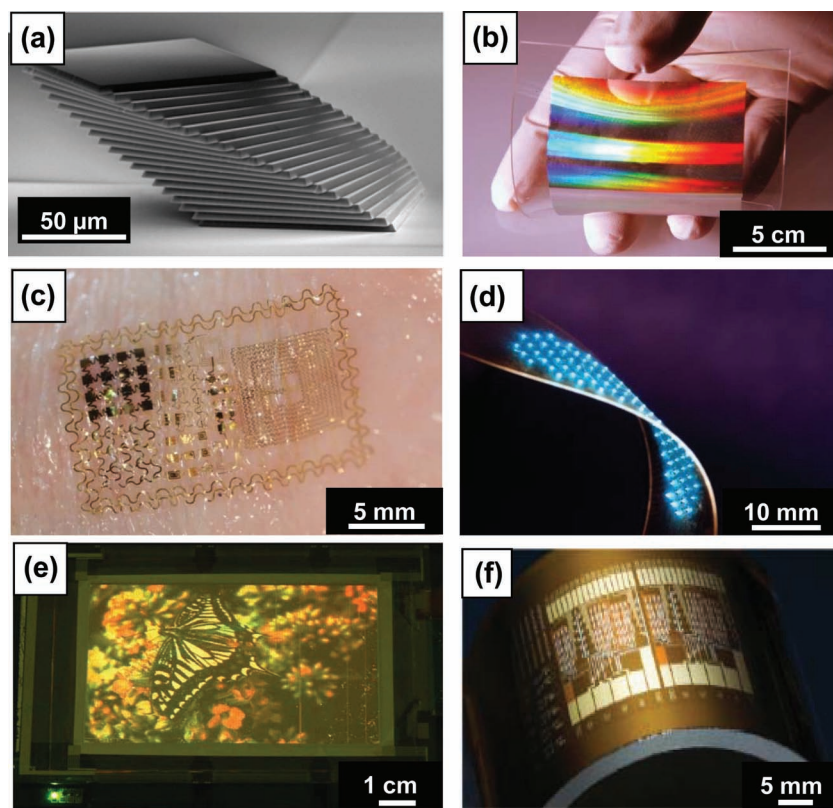


**Figure 1.** Representative examples of unusual constructs, devices and integrated systems enabled by the techniques of transfer printing. (a) SEM image of a printed multilayer stack of silicon platelets. Reproduced with permission from Ref. [40]. Copyright 2010 National Academy of Sciences. (b) Photograph of a large area (10 cm x 10 cm) negative index metamaterial (NIM) comprised of alternating layers of Ag and MgF<sub>2</sub> in a nanoscale fishnet pattern printed onto a flexible substrate. Reproduced with permission from Ref. [41]. Copyright 2011 Nature Publishing Group. (c) Photograph of an 'epidermal' electronic device, conformally laminated onto the surface of the skin. The key components of the system, from radio frequency antennae, inductive coils, inductors, capacitors, silicon diodes, strain gauges, light emitting diodes (LEDs), temperature sensors, electrophysiological sensors and field effect transistors, are all fabricated by transfer printing. (d) Image of a mechanically flexed array of ultrathin, microscale, blue LEDs printed from a source wafer onto a thin strip of plastic. Reproduced with permission from Ref. [43]. Copyright 2011 National Academy of Sciences. (e) Picture of a 4-inch, full-color quantum dot (QD) LED display that uses printed collections of QDs in an active matrix configuration of 320 × 240 pixels. Reproduced with permission from Ref. [46]. Copyright 2011 Nature Publishing Group. (f) Photograph of a flexible integrated circuit (four-bit decoder composed of 88 transistors) that uses printed networks of single walled carbon nanotubes for the semiconductor. Reproduced with permission from Ref. [44]. Copyright 2008 Nature Publishing Group.

receiver, as demonstrated in Figures 3b-c where the pitch of the inks are expanded by ~7 times from the donor to the target array. This capability has several advantages, including efficient use of ink materials, precise control of ink spacing and density, and access to final layouts that are not restricted by the substrate size limitations of traditional lithography tools. Figures 3d-e show optical images of small 250 μm × 250 μm × 2.5 μm plates sparsely assembled over transparent substrates. Figure 3d presents an image of ~1600 such structures printed onto a plastic sheet that is subsequently wrapped around a glass cylinder. Figure 3e illustrates the same type of devices printed onto a glass substrate that rests above a sheet of paper with lettering and logos to demonstrate transparency and relative size scales.<sup>[31]</sup>

Some of the diverse materials classes, geometries, and printing modalities that have been reported in the literature over the last 15 years appear in Table 1 along with the general chemical or surface modification techniques adopted to facilitate printing. The following sections of this Review summarize recent progress, organized according to the materials classes of the inks, and beginning with the two-inorganic semiconductors and metals—that have been demonstrated at the highest levels of engineering sophistication. A concluding section outlines some of the most promising device and system-level applications, along with needs and opportunities to expand the scope of capabilities and modes of use. We start, however, with some general considerations related to the mechanics and materials aspects of the transfer process itself.

## 2. Materials Science and Mechanics of Transfer Printing

Effective transfer, using any of the three modes of Figure 2, relies, fundamentally, on control of adhesion and fracture mechanics at the critical interfaces between the ink/donor, the stamp/ink and the ink/receiver. A first consideration is the chemistry and generalized adhesion forces at these interfaces. In a broad sense, the only interface that should bond permanently is the one between the ink and the receiver substrate; all others should demonstrate reversible and, preferably, switchable adhesive behavior in a passive or active mode. The following discussion provides several general considerations for realizing these requirements. Detailed discussions and quantitative experimental and theoretical studies for many cases appear elsewhere. We focus on methods that are the most diverse and well-developed, which form the theoretical framework for describing the

widest expanse of printing techniques for *additive/subtractive transfer* and *deterministic assembly*. Specialized processes for each technique, such as incorporation of adhesive or release layers, use of oligomer diffusion, heat, light, or plasma activation in stamps to influence transfer, will be outlined in detail in subsequent sections and rely predominantly on adaptations to the methods outlined briefly here.

Separation/delamination processes in each of the three modalities of Figure 2 can be modeled as the initiation and propagation of interfacial cracks,<sup>[70,71]</sup> with each interface providing a competing fracture pathway that has a characteristic energy release rate  $G$ . For the case of *additive transfer*, the process is governed by delamination at the stamp/ink interface, which occurs when the interfacial energy release rate,  $G^{interface}$ ,

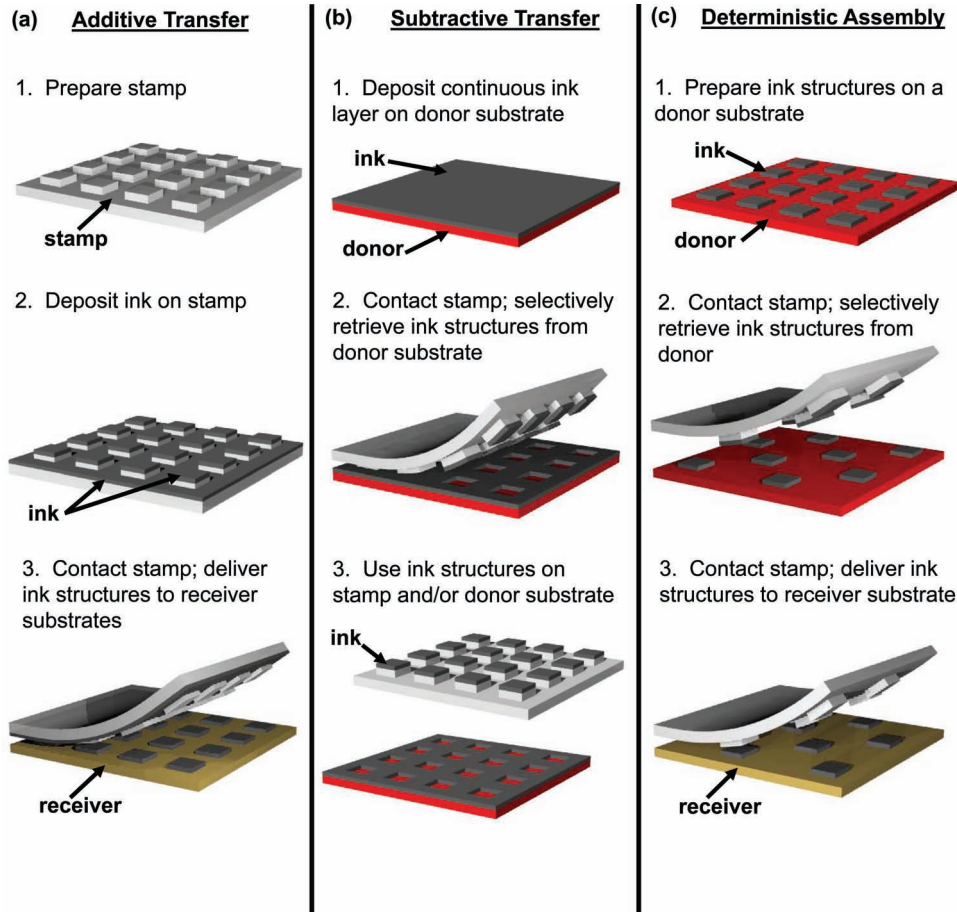


**Figure 2.** Schematic illustrations of three basic modes for transfer printing. (a) Additive transfer exploits a stamp that is 'inked' with a material of interest, using processes such as physical vapor deposition, solution casting/assembly, or physical transfer. Contacting such an inked stamp to a target substrate followed by peel-back affects transfer of material. (b) Subtractive transfer starts with a continuous film of material deposited on a donor substrate. A stamp brought into contact with the film selectively removes material in the areas of contact, leaving behind a patterned film on the donor and transferred material on the stamp. A stamp inked in this manner can then be used for additive transfer, as in (a). Alternatively, the patterned material on the donor itself can be used in further device processing. (c) Deterministic assembly involves contact of a stamp with a donor substrate that supports pre-fabricated micro or nanostructures. Peeling the stamp away leads to removal of selected structures from the donor substrate. Printing onto a receiving substrate completes the process. In all three cases, chemical, thermal and/or mechanical strategies facilitate the inking and printing processes, to enable high yield, efficient operation.

is equal to the work of adhesion between the stamp and ink,  $G_c^{stamp/ink}$  [72]

$$G_c^{interface} = G_c^{stamp/ink} \quad (1)$$

$G_c^{stamp/ink}$  depends on the choice of materials at the stamp/ink interface and is typically on the order of 0.1 N/m ~ 1 N/m whereas  $G_c^{interface}$  is influenced by stamp shape and elastic modulus, but generally increases with applied force; specific forms of  $G_c^{interface}$  can be found in the literature.<sup>[70,72,73]</sup> In contrast, during *subtractive transfer* (and the retrieval step in *deterministic assembly*), release at the interface between the ink/donor must occur. This release can involve cohesive fracture in the ink, in some other class of material that temporarily bonds the ink to the donor, or between the ink and the donor itself. In most cases, this ink/donor interface can be engineered to enable release onto unmodified surfaces of elastomeric stamps that are capable of soft, conformal contact, via the action of van der Waals or related forces. For separation to occur the energy

release rate must reach the fracture toughness of the ink/donor interface,<sup>[72]</sup> i.e.,  $G_c^{interface} = G_c^{ink/donor}$ , which is primarily a property of the ink material, ranging from ~1 N/m for inorganic semiconductors to as large as ~10<sup>4</sup> N/m for metals. As in the case of *additive transfer*, stamp modulus, geometry, and applied forces can affect the realized energy release rate.<sup>[65]</sup>

*Deterministic assembly* represents an interesting combination of the fracture mechanics described above for *additive* and *subtractive transfer*. In many instances, inking of a stamp via this modality can be likened to retrieval processes of *subtractive transfer* where the ink/donor interface must preferentially fail. Likewise, delivery of ink onto a receiver follows mechanical considerations similar to those for printing in *additive transfer*. A powerful and widely exploited strategy in *deterministic assembly* utilizes the rate-dependent effects of viscoelastic stamps, such as those made of poly(dimethylsiloxane) (PDMS).<sup>[16,18–20,25,27,28,30,38,47,68–70,74–80]</sup> Here, the velocity of separation of the stamp from a surface influences the adhesive strength, with

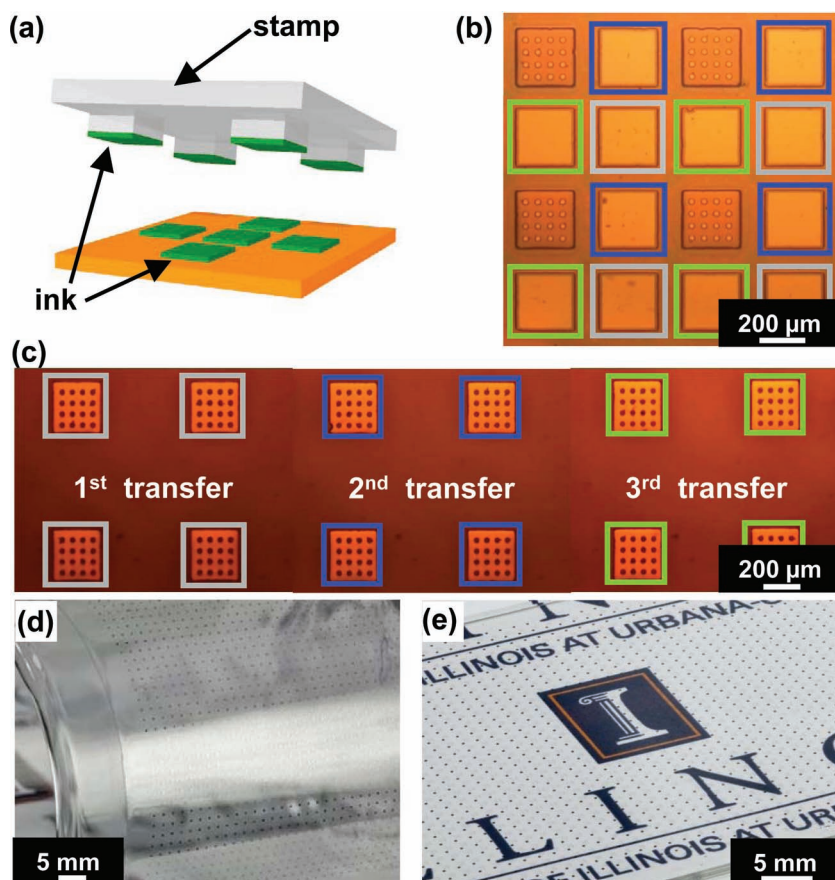


**Figure 3.** (a) Schematic illustration of the process of retrieving and printing selected sets of microstructures (i.e. ‘inks’ consisting of platelets designed as AlInGaP LEDs) with a stamp. (b) Optical micrograph of a donor substrate after three cycles of printing. Each colored box (gray, blue, green) highlights different sets of platelets retrieved in sequential cycles of printing. (c) Micrograph of a receiving substrate after printing from the donor substrate of (b), illustrating the concept of area expansion, in which dense arrays of microstructures are distributed into sparse configurations. The gray, blue and green boxes show platelets that correspond to those highlighted in a similar manner in (b). (d) Large-scale collection of structures (~1600 in a square array with pitch of 1.4 mm) printed onto a thin, flexible sheet of plastic, shown here wrapped onto a cylindrical glass substrate. (e) Similar collection of structures printed onto a plate of glass. Reproduced with permission from Ref. [31]. Copyright 2009 The American Association for Advancement of Science.

higher velocities yielding proportionally larger adhesion.<sup>[47]</sup> Ink retrieval and delivery can, therefore, occur efficiently at velocities on the order of 10 cm/s or greater and a few mm/s or less, respectively.<sup>[47]</sup> By modeling the retrieval and printing processes as the propagation of interfacial cracks, similar to the other printing techniques of Figure 2, criteria for predicting retrieval or printing can be established.<sup>[65]</sup> A general form of the steady-state energy release rate (following a tape peel test convention<sup>[47]</sup>) is given by:

$$G = \frac{F}{w} \quad (2)$$

where  $F$  is the force applied to the stamp in the normal direction and  $w$  is the stamp width. While  $G$  is a measure of the interfacial adhesive strength between the stamp and its contacting substrate, it differs from the interfacial work of adhe-

sion since it accounts for both interface bond breaking and viscoelastic energy dissipation surrounding the crack tip.<sup>[47,73,81–83]</sup> Separation at either the stamp/ink or ink/receiver interface corresponds to a  $G_c^{stamp/ink}$  and  $G_c^{ink/receiver}$ , respectively, leading to the simple relations:

$$G_c^{stamp/ink} < G_c^{ink/receiver} \text{ for printing} \quad (3a)$$

$$G_c^{stamp/ink} > G_c^{ink/receiver} \text{ for retrieval} \quad (3b)$$

The elastic nature of both the rigid ink and receiver substrate implies that  $G_c^{ink/receiver}$  is constant, to first approximation, with no dependence of interfacial strength on velocity. By contrast, the velocity dependence of the stamp energy release rate can be expressed as  $G_c^{stamp/ink} = G_c^{stamp/ink}(v)$ .<sup>[70,73,81–83]</sup> At a critical velocity,  $v_c$ , the energy release rates for both interfaces are equal, leading to the condition:

$$G_c^{stamp/ink}(v) = G_c^{ink/receiver} \quad (4)$$

that mark the transition from a retrieval to printing regime, as shown in Figure 4a. A general power-law relationship fits the rate-dependence, according to (5):

$$G_c^{stamp/ink}(v) = G_0 \left[ 1 + \left( \frac{v}{v_0} \right)^n \right] \quad (5)$$

where  $G_0$  is the zero-velocity energy release rate similar to a fatigue limit fracture energy,  $v$  is the separation velocity,  $v_0$  a reference velocity associated with  $G_0$ , and  $n$  the scaling parameter.<sup>[47,70,84]</sup> Rearranging Equation (5) provides an analytical expression for the critical separation velocity:

$$v_c = v_0 \left[ \frac{G_c^{stamp/ink} - G_0}{G_0} \right]^{1/n} \quad (6)$$

A number of other techniques have been developed to further enhance the efficacy of *deterministic assembly* including use of pulsed lasers to realize transfer by initiating separation of the stamp/ink interface due to large thermal mismatch between the ink and stamp materials;<sup>[85]</sup> surface relief structures to achieve large surface contact between the stamp and ink, and therefore large  $G$  to promote transfer;<sup>[40,86,87]</sup> and mechanical loading protocols that give different  $G$  for the same peel force, to control transfer.<sup>[88]</sup> These last two (i.e., altering the surface structure of the stamp and the nature of loading forces) have proven to be particularly valuable. As an example of the former, PDMS stamps with pyramidal microtips at the corners of the contacting regions can be designed to allow reversible, pressure-controlled contact areas, and thereby switch the available adhesion strength.<sup>[40]</sup> Figure 4b shows scanning electron microscope (SEM) images of such a stamp, in high and low adhesion states (ON and OFF, respectively) against a platelet of silicon as the ink.

**Table 1.** Representative materials classes, structure geometries, transfer protocols and associated surface modifications that have been demonstrated in transfer printing.

Materials Class	Ink Structure	Common Transfer Protocols	Common Surface Modifications
Inorganic semiconductors (Section 3)	• Nanomembranes, nanoribbons, platelets and bars	• Additive transfer	• Heat
	• Nanowires	• Subtractive transfer	• UV-Ozone or plasma modification
	• Quantum Dots	• Deterministic assembly	• Adhesives
Metals (Section 4)	• Thin films in flat and structured forms	• Additive transfer	• Heat
	• Nanowires	• Subtractive transfer	• Pressure
	• Nanoparticles		• Adhesives • Water • SAMs
Carbon (Section 5)	• Nanomembranes and thin films	• Additive transfer	• Heat
	• Nanotubes	• Subtractive transfer • Deterministic assembly	• Adhesives • Pressure
Organic materials (Section 6)	• Nanomembranes and thin films	• Additive transfer	• UV-Ozone or plasma modification
	• Self-assembled microstructures and/or domains	• Subtractive transfer	• Adhesives
			• SAMs
Colloids (Section 7)	• Nanomembranes and thin films	• Additive transfer	• Heat
	• Self-assembled microstructures and/or domains	• Subtractive transfer	• Plasma modification
	• Nanoparticles/clusters	• Deterministic assembly	• Adhesives • Water
Biological materials (Section 8)	• Nanomembranes and thin films	• Additive transfer	• Adhesives
	• Self-assembled microstructures		• SAMs
	• Macromolecular configurations		• Biocapture

Quantitative measurements reveal the exceptional capabilities of this approach for switching adhesion, particularly when combined with the viscoelastic effects described above (Figure 4b).<sup>[40]</sup> Similar types of operation are possible with other schemes, including shear loading and various bio-inspired sur-

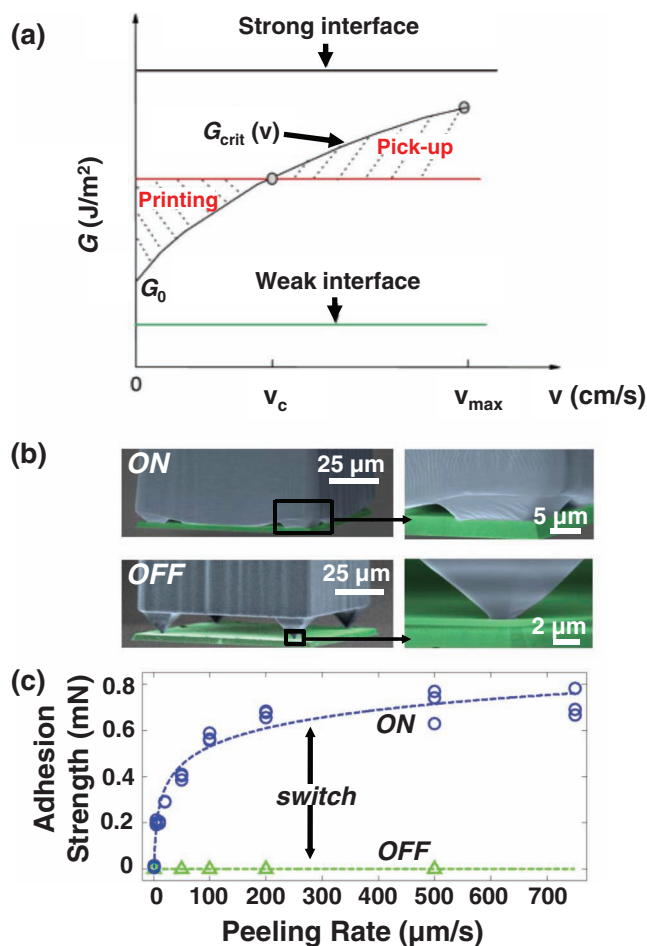


**Figure 4.** (a) Schematic diagram of critical energy release rates for the stamp/ink and ink/receiver interfaces of a model printing experiment consisting of a stamp, continuous ink film, and receiver substrate. The intersection of the horizontal line in the middle with the monotonically increasing curve represents the critical peel velocity,  $v_c$ , for kinetically controlled transfer printing. The horizontal lines at the bottom and top represent very weak and very strong film/receiver interfaces, respectively, corresponding to conditions for which only retrieval or printing can be realized. Reproduced with permission from Ref. [70]. Copyright 2007 American Chemical Society. (b) Colored SEM images of microstructured elastomeric surfaces bearing pyramidal microtips in the ‘adhesion ON’ (top panel) and ‘adhesion OFF’ (bottom panel) states, in which the ‘ink’ platelets appear green. Panels on the right show high magnification images of individual microtips in each state. The extreme differences in contact area provide high levels of adhesion switching between OFF and ON states. (c) Pull-off force as a function of delamination velocity for microtipped stamps in the ON and OFF states. When in full contact, the compressed stamp has a strong rate-dependent behavior due to the viscoelastic nature of the stamp. When only contacting at the microtips, adhesive forces are minimized. Reproduced with permission from Ref. [103]. Copyright 2011 Nature Publishing Group.

face structures. For the case of shear-assisted transfer, targeted loading of a microstructured PDMS stamp can induce strong interfacial moments between the stamp surface and a rigid ink (e.g., a silicon platelet) that locally weaken stamp adhesion around the molded surface relief. Increasing shear strains in the stamp can effectively modulate the total stamp adhesive

strength to negligible levels, enabling efficient delivery of inks into a variety of configurations.<sup>[88]</sup> In fact, many of the advanced devices described in Section 10 exploit one or more of the enhancements outlined above and serve as demonstrations of the robust assembly capabilities enabled by printing.

### 3. Inorganic Semiconductors

In many functional devices, the semiconductor represents often the most enabling, and challenging, material. Performance is generally highest with high purity, single crystalline inorganic materials. When implemented with micro- and nanostructures of such classes of semiconductors, *deterministic assembly* (Figure 2) provides a simple, yet powerful pathway to useful system or device configurations that cannot be achieved through any other technique. A recent, promising direction involves advanced electronic materials grown and processed on a substrate and then transferred over large areas in step-and-repeat type processes,<sup>[47,89]</sup> (Figure 3), while preserving spatial orientation and electronic properties, to yield integrated circuits on sheets of plastic or slabs of rubber. This strategy bypasses the standard requirement that materials which comprise the circuit must be compatible with all of the processes used in integrated fabrication.<sup>[4,30]</sup> While a wide variety of methods exist for forming inorganic semiconducting inks,<sup>[18,20]</sup> this Review focuses mainly on techniques for transfer printing such structures, with an emphasis on single-crystalline materials, organized according to their structural forms.

#### 3.1. Nanomembranes, Nanoribbons, Platelets and Bars

The earliest reports of transfer printing of inorganic semiconductors used structures of silicon with thicknesses ranging from a few nm's to a few tens of microns and lateral dimensions between tens of nm's and mm's, derived from silicon-on-insulator (SOI) wafers and referred to originally as microstructured silicon ( $\mu\text{-Si}$ ). Fabrication involves anisotropic wet chemical etching, or dry etching, of selected exposed regions of the top layer silicon, and then undercut removal of the buried oxide with hydrofluoric acid to release silicon structures<sup>[16,27,30,90,91]</sup> in various geometries and sizes, most commonly nanoribbons/nanomembranes (NMs) or microbars/plates, optimized for incorporation into transistors and solar cells, respectively. Van der Waals forces tether the silicon structures to the underlying wafer, in their lithographically defined locations, for use in the *deterministic assembly* process of Figure 2. Comparative literature analysis indicates that stamp-mediated transfers of this type provide much greater degrees of alignment and placement control than are possible with other printing or assembly techniques based on solution casting.<sup>[16,17,59]</sup> Recent research advances have greatly increased the sophistication of silicon ink geometries, with an example in Figure 5a.<sup>[16]</sup> While silicon can be created in this manner easily, the high cost of SOI might represent a disadvantage for certain applications. Newer processing schemes allow the fabrication directly from low cost bulk silicon wafers.<sup>[28,68,76]</sup> These procedures, when repetitively applied, can efficiently utilize material through the entire thickness of the wafer.<sup>[28,68]</sup> A single wafer can yield large quantities

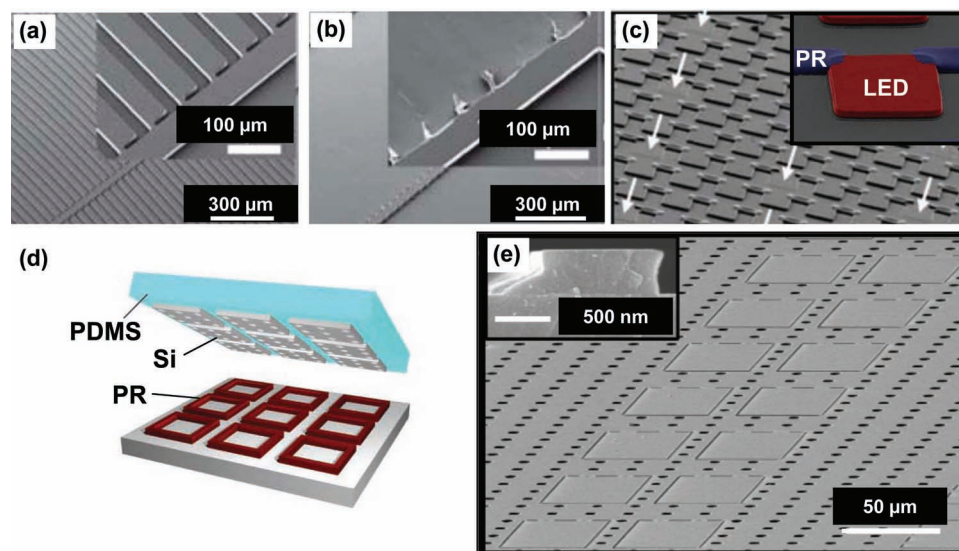


**Figure 5.** (a) SEM image of silicon microbar photovoltaic cells, undercut etched but tethered via ‘anchors’ at their endpoints to an underlying silicon wafer. (b) SEM image of the wafer after retrieving the cells with a stamp. The insets in (a) and (b) provide magnified views of the anchor regions. Reproduced with permission from Ref. [39]. Copyright 2010 The Royal Society of Chemistry. (c) SEM image of a GaAs wafer with an array of undercut etched, microscale AlInGaP LEDs in ultrathin layouts, anchored to the underlying wafer with patterns of photoresist. Here, the white arrows indicate the positions of LEDs that were retrieved with a stamp. The inset shows a colorized, angled-view SEM image. A pair of photoresist (PR) anchors (blue) at the two far corners holds the LED (red) above the GaAs wafer (grey) in the suspended configuration of a diving board, to facilitate retrieval with a stamp. Reproduced with permission from Ref. [31]. Copyright 2009 The American Association for Advancement of Science. (d) Schematic illustration of silicon structures retrieved from a substrate to which they were anchored with PR features around their perimeters. (e) SEM image of the PR structures in (d) after transfer printing. The inset shows a cross-sectional view of one such structure. Reproduced with permission from Ref. [94]. Copyright 2011 John Wiley and Sons.

of  $\mu\text{s-Si}$ , as much as several hundred square feet of Si ribbons from 1 ft<sup>2</sup> of starting material.<sup>[28,76]</sup>

A significant additional advancement in design involves the use of anchoring schemes that retain precise spatial layouts of the undercut  $\mu\text{s-Si}$  prior to and during transfer, with levels of control that cannot be achieved with the original schemes based on van der Waals adhesion.<sup>[92]</sup> In addition to holding the inks in place, anchors must fracture easily during delamination of the stamp. Early generations of such anchors consisted of vertical columns of buried oxide designed to remain after undercutting an SOI wafer.<sup>[18,20,30,69,93]</sup> The loads associated with stamp contact can fracture such anchors, to facilitate effective retrieval.<sup>[93]</sup> One disadvantage of this design is that small oxide particulates can remain on the  $\mu\text{s-Si}$  after anchor fracture; in many cases, their removal requires an additional HF etching step.<sup>[93]</sup> Optimized designs feature anchors that lie in the plane of the device and are significantly easier to fabricate and refine.<sup>[29]</sup> These anchors may consist of the same material as the ink ('homogeneous' anchors)<sup>[92]</sup>, as shown in images of Figure 5a,b collected before and after printing. In other cases, anchors of a distinct material ('heterogeneous' anchors), such as the photoresist posts highlighted in Figure 5c, can be used.<sup>[31,94]</sup> The colorized SEM of Figure 5c demonstrates a version of these anchors in a "diving board" configuration where support is provided only on one side of the ink.<sup>[31]</sup> Figure 5d, e show another type of photoresist anchor, referred to as a perimeter pedestal, which exists underneath the ink layer around its periphery.<sup>[94]</sup> These anchors are sufficiently strong to withstand undercut etching, but can be significantly easier to fracture than homogeneous anchors, thereby facilitating retrieval. Additionally, from the standpoint of materials utilization, such schemes provide pathways for highly efficient use of the ink, through formation of dense arrays of structures. Figure 5c presents one such layout, from which selected layers are retrieved as in Figure 3a.

As discussed in Section 2, printing depends on exploiting the differential adhesion developed between the stamp/ink interface and the ink/substrate interface through chemical and/or dynamic mechanisms. As an example of the first possibility, hydroxyl groups formed on the  $\mu\text{s-Si}$  surface and an oxide-bearing layer on the receiving substrate can lead to  $-\text{Si-O-Si}-$  bonds at the interface, upon contact.<sup>[56,95–98]</sup> Alternatively, a separate adhesive layer can be used. Partially cured polymers such as photodefinable epoxies (SU-8),<sup>[30]</sup> polyimide (PI),<sup>[27,74]</sup> or benzocyclobutene (BCB)<sup>[34]</sup> can flow around the  $\mu\text{s-Si}$  edges and, when cured, create strong bonding forces that promote efficient transfer, in a way that simultaneously planarizes the top surface to facilitate the formation of electrical interconnects, for example.<sup>[38,39]</sup> The adhesive can also serve as an integrated component (e.g., as a gate dielectric), although with modest performance compared to that possible with dielectrics, such as thermal oxide, grown directly on the silicon.<sup>[30]</sup> For demanding applications, devices (such as silicon transistors) can be fabricated in their entirety prior to release from the donor wafer onto the stamp.<sup>[16,27,28,30,69]</sup> Integrated circuits printed in this way perform extremely well<sup>[34,74]</sup> and will be discussed in subsequent sections of this Review. Similar classes of materials and devices can be printed directly, using the donor wafer itself as the stamp, as demonstrated in both strained<sup>[99–101]</sup> and unstrained silicon NMs.<sup>[102]</sup> The use of the wafer is convenient, but brings

some disadvantages—it is generally opaque, rigid and difficult to handle in the context of an automated tool, and is not easily implemented in a step and repeat mode—compared to stamp-based approaches. Nevertheless, the simplicity of this method makes it useful for research purposes, in devices such as thin film transistors<sup>[101,103]</sup> and ultracompact Fano filters.<sup>[102–104]</sup>

Many other semiconductors can be processed as inks in a conceptually similar manner to the examples of silicon provided above.<sup>[17,19,29,48,75,77,78,103,105]</sup> Demonstrated cases include III-V materials, such as single-crystalline GaAs, GaN and InP, of interest due to their high electron mobilities, high saturated drift velocities, direct band gaps, and tolerance to a large range of operation and process temperatures.<sup>[78]</sup> Complex and diverse forms of compound semiconductor inks (e.g., GaAs and InP nanowires and nanoribbons)<sup>[77,78,105]</sup> can be produced from wafers using processes comparable to those described for the fabrication of silicon micro/nanostructures from bulk Si wafers. An example is the fabrication of the GaAs (or InP) nanowires/ribbons by anisotropic chemical etching. Newer approaches exploit more conventional forms of wafer level fabrication in conjunction with heterogeneous anchors<sup>[31]</sup> and sacrificial epitaxial layers that can be selectively removed by undercut etching, to yield compound semiconductor inks.<sup>[31,92,106]</sup> In an alternative approach, sheets or platelets of AlGaIn/GaN (used to fabricate HEMTs)<sup>[29]</sup> or GaN/AlN grown on bulk silicon wafers with (111) orientation can be released by anisotropic undercut etching of the Si<sup>[17]</sup>. Many classes of devices, from photodetectors,<sup>[35,106]</sup> to light emitting diodes,<sup>[31]</sup> solar cells<sup>[106]</sup> and transistors<sup>[35]</sup> are possible, in which formation of ohmic contacts can be accomplished on the donor wafer prior to retrieval, again separating the required high temperature processes from the temperature sensitive plastic substrates, for example. Large area coverage can be achieved through multiple inking and printing steps.<sup>[19,48,75]</sup>

Related protocols can affect heterogeneous and/or three dimensional integration by fabricating semiconductor inks from multiple types of wafers and then repeating the printing processes.<sup>[35,107]</sup> In certain such cases, the electrical/optical/thermal properties of the interfaces between the different materials and/or the receiving substrate can be important. Although surface modifications and/or adhesives can be effective for transfer, they often alter, in unwanted ways, these critical interface characteristics. For these situations, adhesiveless schemes for *deterministic assembly*, such as those described in Section 2, are important. For structures that are not easily printed via manually controlled speeds, automated transfer printing tools can be employed. Such toolsets allow finer optimization of the strain-rate dependent adhesion than can be accomplished by hand, as well as more accurate placement of printed objects. Examples of the capabilities of such tools are discussed briefly in Section 10.5.

Other approaches to printing of inorganic semiconductors exploit *subtractive transfer* techniques. One example, based on nanocontact electrification, utilizes the charged surface of a structured PDMS stamp to remove layers of silicon (up to 5 mm lateral dimensions) from a patterned donor substrate.<sup>[108]</sup> Levels of surface charge on the PDMS are precisely maintained through plasma activation and soaking in either acidic or basic solutions to form protonated or deprotonated surfaces while

control over the stamp surface relief ensures only selected regions of silicon are subtractively removed. In an advanced form of this technique, patterned silicon retrieved with charged PMDS is subsequently transferred to other stamps, provided that the new stamps have higher charge density.<sup>[108]</sup>

Another interesting example of *subtractive transfer*, referred to as dry-removal soft lithography,<sup>[109–111]</sup> uses a PDMS stamp to retrieve porous silicon microstructures from a bulk donor wafer. Pressing a stamp into contact and then peeling it away retrieves silicon, in its porous form, in isolated features on the raised regions of relief on the stamp. A transparent hydrophobic polymer poly[(vinyl butyral)-*co*-(vinyl alcohol)-*co*-(vinyl acetate)] (PVB) can be drop cast, cured, and then peeled off of the stamp, to remove the silicon structures.<sup>[109]</sup> The optical properties of the porous silicon surface are unaltered by this process, and the transferred materials can be further integrated into a variety of optical devices.<sup>[112–115]</sup> One demonstration exploits porous Si as a freestanding Bragg mirror<sup>[115–120]</sup> supported on a transparent polymeric substrate. Similar patterning schemes can produce arrays of porous silicon photonic crystals and free-standing thin porous silicon micro-hole arrays.<sup>[110,119,120]</sup>

### 3.2. Nanowires

One-dimensional inorganic semiconductors, i.e., nanowires, offer an interesting collection of electronic and optoelectronic properties that also enable the fabrication of useful devices embedding design rules down to the molecular scale. The availability of techniques to manipulate the size, structure, composition, and morphology of such nanowires makes them useful as building blocks for various applications in the fields of electronics,<sup>[121–123]</sup> photonics,<sup>[124,125]</sup> sensors,<sup>[126–128]</sup> and energy conversion (specifically battery electrodes and heterojunctions in photovoltaics).<sup>[129]</sup> Although top-down approaches such as those described in the previous section can provide access to such materials, some of the most widely explored methods rely on synthetic growth techniques. Integration into devices can occur directly through precise control over size and position of the resulting nanowires, in their as-grown configurations. An alternative involves separate steps of synthesis followed by organized assembly. The first option can be addressed, to some extent, with approaches that use CVD growth from ordered catalyst arrays<sup>[130–132]</sup> fabricated by such techniques as AFM lithography, electron-beam lithography, nanosphere lithography, nanoimprint lithography, self-assembled templates.<sup>[133,134]</sup> The conditions, however, often preclude the use of low temperature substrates. Also, scaling to large areas will be challenging. The second approach of organized assembly typically relies on controlled precipitation of nanowires separately formed by hydrothermal/solvothermal processes, solution-liquid-solid (SLS) or vapor-liquid-solid (VLS) methods, solution-phase techniques based on capping reagents, or low temperature aqueous-solution processes.<sup>[132,133]</sup> Although certain degrees of alignment and positioning can be achieved through the application of electric fields,<sup>[135]</sup> microfluidic flows,<sup>[136]</sup> directed adsorption through surface patterning with self-assembled monolayers,<sup>[137]</sup> and magnetic-force-driven self-assembly,<sup>[138]</sup> these methods, in their current forms, are only useful for organizing nanowires

over relatively small areas, with modest levels of control. The practical development of nanowire-based technologies demands improved precision in patterning and alignment, with methods that are compatible with conventional microfabrication processes and which can be scaled up for production. Transfer printing is well positioned to address these limitations. To pattern single and multilayer nanowire assemblies, arrays are most commonly formed on a donor substrate or in a reaction vessel that is specifically optimized for nanowire growth, followed by transfer to a desired receiving substrate. Such printing-based transfers have now been demonstrated for many classes of nanowires, including those based on III-V semiconductors and group IV materials.<sup>[107,121,123,124,139,140]</sup>

One of the most powerful printing schemes in this context falls into the *deterministic assembly* category, in which nanowire transfer to a variety of unusual flexible and rigid substrates is achieved through adhesive tapes or via direct contact to the receiver surface. In the former case, nanowire arrays, meshes, and even complete devices can undergo single or multiple transfers for assembly into complex layouts.<sup>[139]</sup> These transfers typically rely on PDMS or thermal tapes whose adhesive properties are easy to modulate during retrieval and delivery; often the tape structure itself is incorporated into the final device architecture. Nanowire assemblies transferred onto diverse substrates such as Petri dishes and insulating surfaces demonstrate the printing capabilities.<sup>[139]</sup> An alternative method to using tapes as a transfer media instead utilizes a directional sliding process<sup>[107,121,123,141,142]</sup> in which a substrate with a dense, nanowire deposit is dragged across a receiving substrate that supports patterns of photoresist, areas of differing surface energy, or charge.<sup>[143]</sup> As the nanowires are sheared by the sliding contact, they detach from the growth substrate surface and adhere to the receiver through either van der Waals forces or more specific chemical interactions. Sufficiently strong bonding interactions can be achieved easily in practice, as demonstrated in the example given in **Figure 6a**.<sup>[123]</sup> Selective functionalization of a surface with SAMs, and therefore sites of preferential adhesion, provides a means to affect a hierarchical patterning in the printed nanowires. For example, organofluorine modified surfaces resist nanowire deposition, while amine-terminated SAM surfaces enable high efficiency transfers.<sup>[141,142]</sup> Chemical modifications of this type also allow control over the densities of the nanowires in transferred arrays.<sup>[141]</sup> More recent variations of the process utilize a lubricant, to facilitate contact between the donor and receiving substrates, thereby minimizing fracture, detachment, and misalignment of the nanowires during transfer.<sup>[141]</sup>

As with other forms of transfer printing, this process can be implemented in a roller format, in which a cylindrical growth substrate connects to a wheel assembly to accomplish the frictional sliding transfers.<sup>[143,144]</sup> The initially randomly oriented crystalline nanowires on the cylinder can be transferred to and aligned with a variety of rigid or flexible receiving substrates (i.e., Si, glass, plastic, paper) using this method.<sup>[123,141,144]</sup> In the example shown, the rolling mechanism has a slightly smaller radius than the inked cylindrical substrate, which results in the necessary sliding motion. Silicon, InAs, and Ge nanowires are among the materials that have been contact printed successfully by this method.<sup>[121]</sup> Large-scale heterogeneous integration of

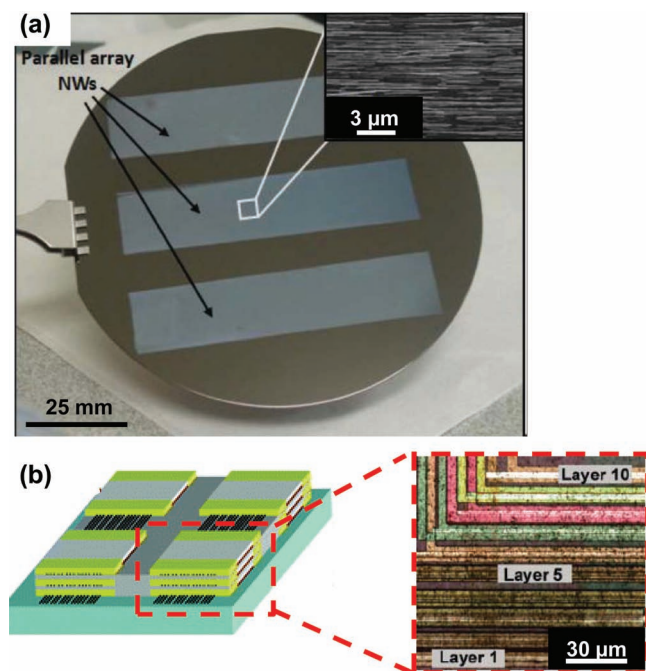


**Figure 6.** (a) Photograph of parallel arrays of aligned Ge nanowires (NWs; diameters  $\sim 30$  nm) assembled on a 4 inch diameter silicon wafer by transfer printing. The inset provides an SEM image of a region of the printed NWs, showing a density of  $\sim 7$  NW/ $\mu\text{m}$ . Reproduced with permission from Ref. [143]. Copyright 2009 John Wiley and Sons. (b) Three-dimensional NW circuit fabricated by multiple cycles of printing, device fabrication, and interlayer deposition. Optical microscope image of 10 layers of Ge/Si NW field effect transistors. Each device is offset to facilitate imaging. Reproduced with permission from Ref. [123]. Copyright 2007 American Chemical Society.

CdSe and Ge/Si core/shell nanowires into model ‘all nanowire’ circuits that are able to detect and amplify optical signals, or applied pressure with high sensitivity and precision have also been demonstrated.<sup>[107]</sup> The latter is presented in some detail in Section 10.2.

Multilayers of nanowires are also possible, in a transfer mode that involves spin-cast polymer buffer layers to provide electrical isolation and promote adhesion upon subsequent transfers. Patterning and rinsing away of select regions of the buffer layer allows control over the density and alignment, down to the single-wire level.<sup>[123,143]</sup> Such schemes can be adapted for fabrication of 3-D integrated circuits with combinations of materials and/or substrates that involve incompatible processing/growth conditions. Figure 6b provides a representative schematic illustration and an optical image of a 10 layer stack of nanowires printed in this way; each layer is offset to provide full view of the stack.<sup>[123]</sup>

Nanowires dispersed in solvents or synthesized by sol-gel methods (e.g.,  $\text{V}_2\text{O}_5$  nanowires)<sup>[145]</sup> require an inking step based on solution casting. Recent work reports that controlled drying can align wires relative to the features of relief on the stamp, and that this alignment can be retained in the subsequent transfers, in a form of *additive transfer*.<sup>[146]</sup> The character of the transfer printing also can be varied by modifying the surface properties of the stamps to control nanowire

wetting in different regions.<sup>[147]</sup> In a similar method, arrays of GaAs nanowires coated with a thin film of gold can be retrieved with PDMS-supported thermal release tape, as part of a *subtractive transfer* process.<sup>[148]</sup> Here, the gold serves as a sacrificial ‘carrier’ film that this is etched away to expose the nanowire array (in this example, now heterogeneously integrated on silicon).

### 3.3. Quantum Dots

Quantum dots (QDs) represent another important class of semiconductor structure.<sup>[149–152]</sup> Due to their excellent luminescent properties, high photoluminescence efficiency, good external quantum efficiency, photochemical stability, and the ability to tune color emission over a wide range of wavelengths but with narrow linewidths, colloidal semiconductor QDs of materials such as CdS, CdSe, ZnS, and ZnSe, are being intensively investigated for use as components of electroluminescent devices,<sup>[153–158]</sup> such as light-emitting diodes, in lighting applications and full-color flat panel display technologies. The active region in one design for these devices embeds an ordered array of QDs atop a hole-transporting organic semiconducting material. Formation of the QD layer can occur through spin coating or drop casting from solution, electrodeposition,<sup>[159]</sup> Langmuir-Schaefer transfer,<sup>[160–162]</sup> and controlled phase separation.<sup>[163]</sup> Transfer printing enables integration into devices, on substrates of interest, in a way that also provides a convenient mechanism for laterally patterning the materials in layouts designed for pixilation in a display, for example. In one published case, QDs assemble into a close-packed film by solvent evaporation and, once dry, are retrieved, by conformal contact with the raised regions of relief on a PDMS stamp, in a process that resembles *subtractive transfer*. The inked stamp can then transfer patterns of QDs onto a receiving substrate, comprised of a conducting polymer film (or small molecule semiconductor) that also acts as an adhesive.<sup>[164]</sup> The schematic in **Figure 7a** depicts a sophisticated version of this type of process.<sup>[46]</sup> A donor substrate is first rendered hydrophobic through the formation of an octadecyltrichlorosilane monolayer on its surface, a property that promotes even spreading of a solution of aliphatic capped QDs.<sup>[46]</sup> Next, the solvent is evaporated and the structured PDMS stamp is brought into conformal contact with the QD film and peeled back quickly under optimized applied pressure.<sup>[46]</sup> The QDs are picked up onto the stamp in the areas of contact, and the inked stamp is then used to print the QD pattern onto a substrate containing a pre-fabricated TFT array coated with an organic hole-transporting layer by slowly removing the stamp from the substrate surface, to exploit rate-dependent adhesion physics described in Section 2.<sup>[46,47]</sup> Examples of representative printed QD patterns are shown in Figures 7b,c.

Inking by direct spin coating of QDs onto PDMS stamps has proven more problematic due to the imperfect films that result and the adverse interactions that can occur between the stamp and the necessary solvents. By protecting the surface of the PDMS with a coating of epoxy or parylene,<sup>[165]</sup> QD suspensions can be directly spin-cast onto the PDMS stamp without undesirable swelling. These protective coatings also lower the surface energy of the stamp, allowing even spreading of the

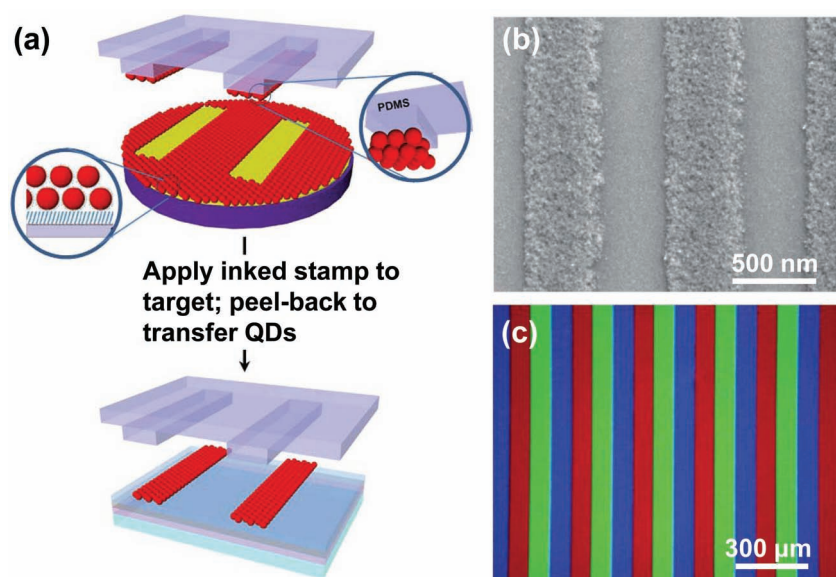


**Figure 7.** (a) Schematic illustration of a transfer printing process for patterning thin layers of quantum dots (QDs). Here, QD layers are retrieved from solution-cast assemblies on functionalized substrates. Red (R), green (G) and blue (B) emissive materials are printed in a sequential, aligned process. (b) SEM image of stripes of QDs printed onto a glass substrate. (c) Fluorescence micrograph of RGB stripes on a glass substrate. Reproduced with permission from Ref. [46]. Copyright 2011 Nature Publishing Group.

colloidal dispersion as well as easy release from the stamp to the receiving substrate. This technique has been used to fabricate white electroluminescence hybrid LEDs using red, blue, and green emitting CdSe/ZnS QDs (with variable diameters).<sup>[166]</sup> Multicolored LEDs are also possible using multiple registered printing steps to deposit, with precise placement, QDs of differing spectral emission side-by-side on the same substrate.<sup>[165]</sup>

In addition to their use in electroluminescent displays, QDs can also serve as sources of illumination on tips designed for atomic force and near-field scanning optical microscopy. Both kinds of integration can be accomplished with transfer printing.<sup>[167–169]</sup> In these cases, the tips themselves are used to retrieve small scale arrays of QDs, where the area that is transferred is dictated by the applied force and depth of the penetration of the tip into a QD film. This process is adaptable to many types of nanostructured surfaces, with applications in fiber optics, sensors, quantum logic devices, as well as nanoscale magnetometry.<sup>[170]</sup>

## 4. Metals

Semiconductor materials must, in most cases, be combined with metals to yield useful devices. Metals can also, of course, themselves be useful as electrodes, antenna structures, and as critical constituents of metamaterials and plasmonic devices. In many cases, the required feature resolution, layouts and/or materials choices can be uniquely addressed by techniques of transfer printing. The following sections describe examples, organized according to origins of the metal structures, as with the discussion of semiconductors.

### 4.1. Metal Films in Flat and Structured Forms

One of the first examples of metal transfer printing represented a form of *additive transfer*.<sup>[21,23,49,52,171–176]</sup> Figure 8a shows an early embodiment, referred to as nanotransfer printing (nTP), where a SAM (from a 3-mercaptopropyltrimethoxysilane) on a silicon substrate facilitates transfer of a layer of gold deposited on a PDMS stamp by electron beam evaporation with a collimated source.<sup>[177]</sup> Related chemistries (SAMs formed by 1,8-octanedithiol functionalization of a GaAs substrate<sup>[173]</sup>) are also possible, as in Figure 8b. For surfaces that present silanol groups, depositing a Ti film on the surface of the gold<sup>[49]</sup> enables formation of a native oxide<sup>[178]</sup> that can promote formation of interfacial Ti-O-Si bonds as a result of reactions similar to those that have been used to bond PDMS and SiO<sub>2</sub>.<sup>[98,179–181]</sup> Related schemes are applicable for SiO<sub>2</sub> treated surfaces<sup>[182]</sup> and Al films, in which interfacial Si-O-Al bonds form, in ways that can be enhanced by thin layers of water that form capillary bridges to pull the surfaces together as the water evaporates.<sup>[183,184]</sup> Heating can facilitate

these and other interface chemistries. In extreme cases of laser-induced heating, the thermal mechanism itself can weaken the adhesion and, in some cases, actively eject the metal from the surface. This process can be used with a stamp<sup>[185]</sup> or with a flat plate<sup>[186,187]</sup>, in non-contact modes where resolution of the transferred metal features is determined by the pattern of exposure light.<sup>[187,188]</sup> Recent demonstrations of one such process, laser decal transfer (LDT),<sup>[187]</sup> indicate suitability for assembling single and multiple layers of metallic interconnect bridges where regions of silver paste are printed to span natural gaps in contact electrodes.<sup>[186,187]</sup> The resulting 2D and 3D printed structures are self-supporting and can be patterned in a variety of shapes and thicknesses with geometries (<10 μm) below the current capabilities of commonly used interconnect techniques such as wirebonding.<sup>[186]</sup>

Heating can be particularly valuable when used with a thermoplastic adhesive (e.g., polymethylmethacrylate, PMMA or polystyrene).<sup>[189,190]</sup> Here, contacting an inked stamp against a substrate coated with such an adhesive layer, heating to temperatures above the glass transition, and then cooling the system and peeling the stamp away leaves a metal pattern embedded in and bonded to the polymer. Two-layer printed structures are possible (e.g., by printing a flat metal film on the surface of a patterned metal film in which some areas of the polymer adhesive are exposed),<sup>[189,190]</sup> for use as vertical interconnects in devices on plastic substrates.<sup>[191]</sup> The method can also be used to invert a stacked integrated structure, as demonstrated in the printing of metal/polymer bi-layers on polymeric substrates.<sup>[192]</sup> Plasticizing solvent vapor can decrease the glass transition temperature, to further facilitate printing in this mode.<sup>[193]</sup>

In a conceptually similar technique, mechanical loading of a flexible stamp can affect transfer for systems in which

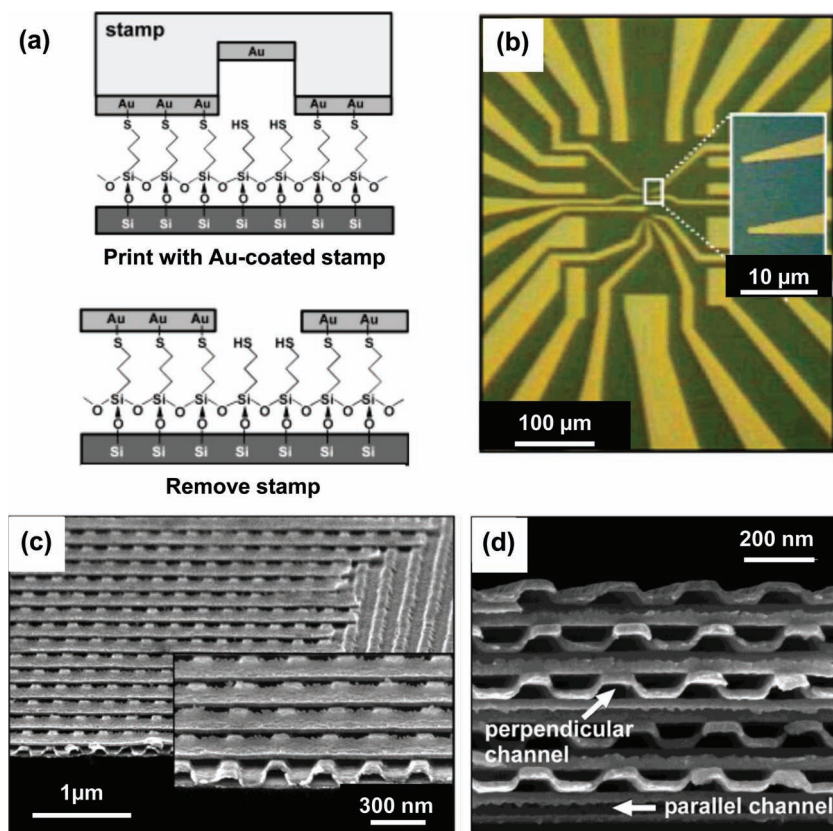


**Figure 8.** (a) Schematic illustration of a process for printing thin layers of gold using a self-assembled monolayer of 3-mercaptopropyltrimethoxysilane as an adhesive on a silicon wafer. (b) Optical micrograph of a pattern of gold printed in this way. Reproduced with permission from Ref. [21]. Copyright 2002 American Chemical Society. (c) SEM image of three-dimensional structures formed by printing gold lines (20 nm thick, 300 nm wide) onto printed nanochannel structures of gold. (d) SEM cross sectional view of a sample with 10 consecutively printed nanochannels of gold. Here, the stamps used for each printing step were rotated by 90° with respect to the direction of the channels of the underlying layer. In (c) and (d), the first structure of gold adheres to a GaAs substrate via covalent bonds to a dithiol monolayer. Cold welding bonds the subsequent gold layers to each other. Reproduced with permission from Ref. [52]. Copyright 2003 American Chemical Society.

additional adhesive layers are undesirable. For example, controlled buckling of micro and nanoscale patterned relief on polystyrene stamps, at elevated temperatures, can enable transfer of imprinted gold sheets to -OH bearing silicon surfaces. Free-standing gold patterns are then “developed” by sonication in toluene during which regions of highly stressed gold fracture and wash away, leaving select hierarchically nanopatterned regions on the surface.<sup>[194]</sup> An extreme example of deformation-assisted transfer involves stamps that are themselves soluble. Methods of this type have been explored with poly(vinyl alcohol) (PVA) stamps,<sup>[195]</sup> in which metal is transferred, or more precisely left behind, when the PVA is removed by dissolution in water.

*Subtractive transfer* of metal films is also possible with the collection of strategies described above, in some cases where additional control of the adhesion is afforded by viscoelastic effects described previously.<sup>[47,70,196,197]</sup> The resulting fracture interfaces can be quite sharp and well defined, when applied in an optimized way to suitable materials and film thicknesses. One of the earliest examples of this patterning exploited cold

welding between a Mg:Ag cathode and Cr/Ag coated stamp to selectively remove layers of metal-covered organic semiconductors. The separated regions (cathode and organic) define the pixel layouts for organic light-emitting diodes (OLED) comprising a 17 × 17 monochrome passive matrix display.<sup>[198]</sup> Patterned structures resulting from related modalities can also provide a variety of other useful functionalities, such as contacts to classes of devices like those based on organic semiconductors that are incompatible with traditional microelectronic fabrication techniques.<sup>[196,199,200]</sup>

An important capability of *additive transfer* is that conformally coating the stamp with a metal can lead to 3D structures upon transfer. Implementing the process in multiple cycles on a single region of a substrate yields hierarchical 3D multilayers, as shown in examples of Figures 8c-d where the transfers are facilitated by cold welding associated with gold-gold contacts.<sup>[171,198,201,202]</sup> When slightly modified, these printing strategies are equally effective at generating 3D structures with other metal inks. Incorporating anti-adhesion layers between the stamp and metal serves to weaken the stamp interface, thereby facilitating release. Likewise, thin metallic ‘strike layers’ on the receiver provide sites for enhanced cold welding, but can be easily removed after transfer.<sup>[201,203]</sup> Incorporating one or both of these additional layers can increase the diversity of available metallic inks. An alternative strategy to using repetitive printing steps to create 3D structures is to generate complex, multilayer assemblies by sequential deposition of different materials onto a single stamp. In such cases, the entire multilayer can be printed in a single

step.<sup>[52,201]</sup> Examples include printed metal-insulator-metal capacitors<sup>[21]</sup> and negative index metamaterials,<sup>[41]</sup> the latter of which are described in some detail in Section 9.2.

In favorable cases, resolution of the most well developed additive methods is limited by the grain size of the deposited metal and its thickness; 5 nm edge resolution and 70 nm feature sizes have been demonstrated.<sup>[21,49,173]</sup> Such outcomes require careful control over the process, both at the level of the stamp and the deposited metals. As an example of attention to the latter, stress releasing features in multilayer stacks, such as alternating gold and alkane-dithiol monolayers, have been shown to reduce defects associated with cracking.<sup>[204]</sup> The conditions for depositing metals onto the stamps also require attention.<sup>[52]</sup> Cumulative heating, for example, can lead to unwanted effects due to the large differences in coefficients of thermal expansion (CTE) between the metal and the PDMS.<sup>[205–208]</sup> The use of high modulus supports with low CTE can minimize such effects, and at the same time reduce mechanical sagging and buckling into the recessed regions due to thermal cycling of the stamp

and film.<sup>[24,171]</sup> Similar outcomes can be achieved using different formulations of the stamp material. For example, PDMS variants with a 5 to 10 fold increase in elastic modulus can be used.<sup>[171]</sup> Perfluorinated polyethers (PFPE) offer similar advantages in mechanics, together with highly non-adherent surfaces that can facilitate transfer.<sup>[209,210]</sup>

In certain instances, stamps can be built using high-modulus, non-elastomeric materials, as a way to further minimize mechanical deformations during transfer. Early work showed the ability to accomplish metal transfers with etched substrates of GaAs and glass.<sup>[21,49]</sup> The main disadvantage of these types of stamps is that achieving conformal contact with the target substrate can be difficult, compared to elastomers such as PDMS or PFPE. In part for this reason, polyurethane acrylate (PUA) polymers have attracted some attention, in stamp configurations that involve flexible backing layers.<sup>[32,50,211]</sup> Gold, for example, can be printed via transfer from a PUA stamp using a (3-mercaptopropyl) trimethoxysilane (MPTMS) functionalized surface (e.g., indium-tin-oxide, ITO),<sup>[175]</sup> or into a partially cured polyurethane coatings on a receiving substrate (e.g., on polyethylene terephthalate, PET).<sup>[211]</sup> Such procedures can be used to form a number of interesting metal patterns with challenging design rules, including metal nanocones,<sup>[175]</sup> and in two-step transfers that allow selective printing of metal patterns of different feature sizes from a single stamp. In the latter case, a first transfer prints metal from the raised regions of relief; the second step involves imprinting into a polymer film and simultaneously transferring metal from the recessed regions.<sup>[211,212]</sup>

The materials science of the stamps can be important in other ways, as observed in the case of printing of copper. Here, unlike many other metals, which are unaltered by the transfer process, copper loses its conductivity when printed by nTP.<sup>[23]</sup> In this case, mobile oligomers in the PDMS stamps<sup>[213–215]</sup> diffuse from near the surface of the stamp into the bulk of the copper film, specifically between the copper grains, thereby disrupting pathways for conductive percolation. To mitigate this effect, the PDMS can be leached extensively in a high swelling organic solvent<sup>[23,213]</sup> to eliminate the oligomers. In a completely different strategy, these oligomers are used to advantage, as release agents in the transfer. In particular, mild heating (50–80 °C) induces mobile oligomers to migrate from the PDMS stamp, causing a reduction in interfacial adhesion strength between the stamp and metal film due to its inherent low surface energy (~19.8 mJ/m<sup>2</sup>).<sup>[214,216–219]</sup> Using control mechanisms afforded by regulation of temperature, contact time, surface energies of each surface, and substrate roughness, transfer can be accomplished without reliance on specific forms of surface chemistry other than those of nominally weak non-covalent interactions.<sup>[53]</sup>

An important feature of these collective sets of transfer schemes is that they enable metal patterning on unusual or exotic substrates and in environments that would be challenging using traditional techniques. For example, silver patterns can be transferred from a nanopatterned PMMA stamp onto a flat MPTMS modified PDMS substrate<sup>[174]</sup> as a route to creating large-area, conformal metal-bearing surfaces. Conductive layers similarly deposited onto pre- or post-strained PDMS surfaces can be laterally deformed to modify the spacing between surface

features. Such actuable nanostructures have been suggested for use in surface enhanced Raman spectroscopy (SERS) or surface plasmon resonance (SPR) sensors.<sup>[220,221]</sup> Transfer can also be used to integrate patterned metal layers with organic semiconductors.<sup>[53,198,203,222]</sup> A recent additional example involved MPTMS treated electroactive (cotton cellulose) paper<sup>[223–226]</sup> as a substrate for transfer of arrays of gold electrodes.<sup>[227,228]</sup> Paper is a challenging substrate for patterning fine feature sizes, as it is not robust to the wet chemical processes that are necessary for conventional photolithography. Metals can be used as the desired materials, as described above, or as interfacial layers to facilitate transfer, as demonstrated with thin films of gold.<sup>[24]</sup> Such layers can also reduce degradation due to the oxidation of air sensitive materials.<sup>[24]</sup>

In addition to flat surfaces, metal transfer printing is compatible with non-planar substrates,<sup>[22]</sup> which are difficult or impossible to process using other approaches.<sup>[22,229,230]</sup> To demonstrate this capability as a variant of *deterministic assembly*, a PDMS-supported thiolene film can retrieve pre-patterned gold structures and transfer them to a curvilinear substrate. The thiolene transfer film can then be removed by oxygen plasma cleaning. By using a flat stamp as a transfer element, the pattern does not suffer from the same types of limitations that result from mechanical instabilities of structured PDMS stamps with challenging design rules.<sup>[22,231]</sup> A number of other transfer chemistries have been developed to facilitate this form of nTP, including the use of hydroxamic or phosphonic acid SAMs that strongly bond to the native oxides formed on metals.<sup>[232,233]</sup>

Apart from developing unique device architectures, metal transfer techniques such as nTP or *deterministic assembly* can enable fundamental investigation of interfacial physics. Recent studies into the nature of electrical contacts to semiconductor devices<sup>[172,173,234]</sup> and interfacial thermal conductance of printed metallic films<sup>[235]</sup> represent two interesting examples. In the former, electrical performance of Au/1,8-octanedithiol/GaAs junctions (top-contact Au electrodes delivered via nTP) were compared to similar devices fabricated by direct evaporation of Au onto GaAs or 1,8-octanedithiol treated GaAs substrates.<sup>[234]</sup> It was shown that electrodes directly evaporated onto a device surface resulted in direct contact between the Au and GaAs (electrical shorts) which dominated the electrical performance of current-voltage characteristics, were difficult to reproduce on a large scale, and in some cases masked the transport characteristics of the molecular layer.<sup>[172,234]</sup> The printed devices, in contrast, did not display the electrical shorting behavior and indicated that the dithiol layer behaved as an insulating tunnel barrier and effective hole transport layer.<sup>[172]</sup> Key insights into the density of states (DOS) and molecular ordering at contact were also obtained from the printed junctions.<sup>[234]</sup> In another example, layers of gold (100 nm thick) assembled via *deterministic assembly* were characterized using time-domain thermoreflectance (TDTR) to evaluate thermal conductance of interfaces with common device materials such as Si, SiO<sub>2</sub>, Cr, and Al<sub>2</sub>O<sub>3</sub>.<sup>[235]</sup> Surprisingly, the measured conductance of printed films was >10% of the thermal conductance for the corresponding interface formed by sputter-deposition.<sup>[235]</sup> The results indicate that thermal conductance of transferred films will not usually be a limiting factor in thermal management of devices assembled via transfer printing-based techniques.

#### 4.2. Nanowires, Nanorods and Nanoparticles

Nanostructured forms of metals are of interest for a wide array of applications, ranging from plasmonics and broader areas of optics, to biology and catalysis; for this reason they are a natural area of interest in transfer printing. For such structures to function in a useful manner, precise control over their placement must be achieved. Many of the transfer protocols described in the previous section for metallic films can also be adapted to the transfer of nanowires, nanorods and nanoparticles. *Deterministic assembly* of nanowires onto non-planar substrates has been demonstrated through transfer of a polymeric carrier layer in which the nanostructures were embedded. Removal of the carrier material via plasma etching after transfer released the metallic nanowires, completing the printing process.<sup>[222]</sup> Alternatively, metallic nanowires can remain embedded in the polymeric carrier layer which becomes part of a final device. Recent work shows that nanoimprint lithography (NIL) and polymer-assisted lift-off (PALO) can generate sub- $100 \times 100 \text{ nm}^2$  multilayer crossbar junctions that utilize printed Au nanowires embedded in PMMA films as top electrodes.<sup>[236]</sup> The resulting junctions are stable, demonstrate both Ohmic and Schottky-type contacts depending on the junction materials, and have some of the smallest stable junction areas recorded.

Other transfer methods follow a more direct printing approach via the *additive transfer* modality in which thin metal wires are transferred from the raised and recessed regions of a rigid stamp in a series of sequential prints.<sup>[237]</sup> Here, nanostructured silicon stamps coated with thin layers of Au/Cr are brought into contact under pressure and heat with a PET surface.<sup>[189]</sup> Thin nanowire strips are transferred in this mode to the PET surface from the raised regions of the stamp.<sup>[237]</sup> After transfer, the same stamp can subsequently be used to emboss a photocurable resin supported on a separate PET substrate. On removal, the Au/Cr nanowires patterns from the recesses transfer to the PET/resin substrate;<sup>[237]</sup> dry etching can be used to remove residual resin layers in modes similar to those used in nanoimprint lithography.<sup>[238–240]</sup> An interesting alternative takes advantage explicitly of 3D relief that can be molded into a stamp (soft or rigid) surface.<sup>[176]</sup> This process, known as nanotransfer edge printing,<sup>[176,241,242]</sup> can pattern narrow metal features through a two-step process that affords the selective transfer of metals from the sidewall regions of relief on the stamp. Resulting patterned features have shown nanowires with widths of 20 nm extending over  $\sim 0.5 \text{ cm}$  with pitch defined by the stamp. Multiple edge transfers have been sequentially applied to generate complex and multilayer arrangements.<sup>[176]</sup>

A conceptually similar approach, known as superlattice nanowire pattern transfer (SNAP)<sup>[243,244]</sup>, represents an *additive transfer* mode for printing nanowires of platinum, chromium, gold, aluminum, titanium,

and nickel.<sup>[243]</sup> In this process, stamps are fabricated through molecular beam epitaxial (MBE) growth of alternating layers of GaAs and AlGaAs. Buffered HF preferentially etches the AlGaAs layers to depths of  $\sim 40 \text{ nm}$ ; angled evaporation directly onto the etched surface results in metal layers predominantly on the protruding GaAs ridges.<sup>[243–245]</sup> The metal coated regions define the geometry of the nanowires and the etched AlGaAs layers the wire separation; atom-level control afforded by MBE provides extreme levels of precision for defining nanowire size and layout. Contacting the resulting stamp with a thin (10 nm) layer of thermally curable epoxy supported on an oxidized silicon wafer,<sup>[243]</sup> curing and then removing the stamp transfers the metallic features onto the receiver surface. The resulting nanowires can be used as-printed or they can form an etch mask for patterning the underlying receiver substrate.<sup>[243–246]</sup> Pt nanowires 8 nm in diameter with a pitch of 16 nm have been demonstrated, in single layers, multilayers, cross-bar formats, or even suspended across micrometer-scale gaps in the supporting substrate, as possible components in nanomechanical resonators or nanoscale electronic devices.<sup>[243,244]</sup>

For the case of metal nanoparticles, long range pattern control and individual particle placement in patterns deposited directly from a colloidal suspension generally require that the receiving substrate is first patterned in a way that controls the deposition process typically via self or directed assembly.<sup>[247,248]</sup> An advanced form of *additive transfer*, shown in Figure 9a,<sup>[60]</sup> provides an alternative approach - a direct delivery of nanoparticles from colloidal suspensions into recessed regions of stamps. Colloidal suspensions are used to directly ink stamps through rigorous control over particle transport variables such as the

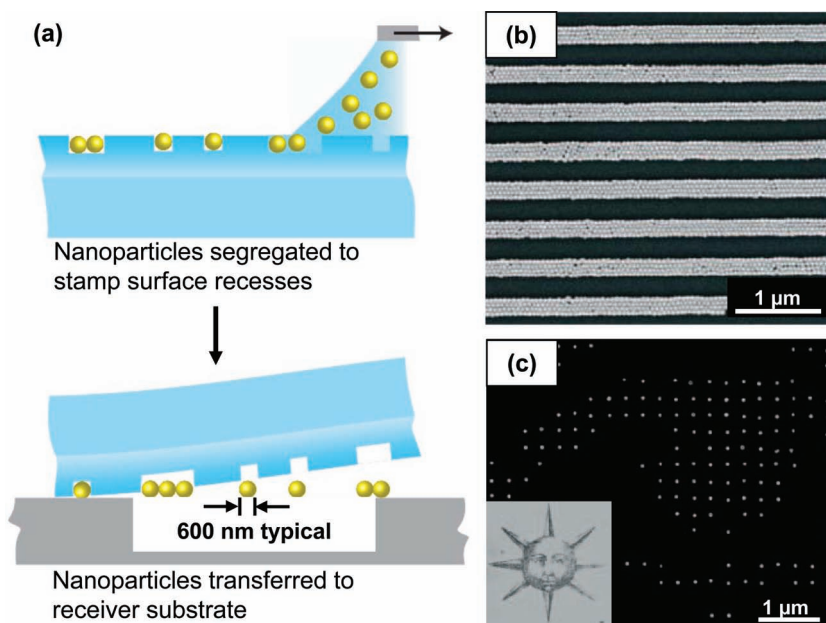


**Figure 9.** (a) Schematic representation of transfer printing of metallic nanoparticles, in a process that involves casting a solution suspension of the particles onto the surface of a stamp. Assemblies of particles in the recessed regions can be transferred onto a receiver substrate. (b) SEM images of 200-nm-wide lines of close-packed 60-nm particles of gold. (c) High magnification SEM image of a sparse (280 nm pitch) collection of 60-nm particles of gold in the layout of an illustration of the sun (inset). Reproduced with permission from Ref. [60]. Copyright 2007 Nature Publishing Group.

contact angles, temperature, and particle concentrations. When the process is optimized, the particles trap in the recessed regions of the stamps, and the excess particles are removed by the motion of the meniscus. The inked stamps, once dry, are then contacted to the surface of the receiving substrate, and the particles transferred via a gradient adhesion mechanism.<sup>[60]</sup> The resulting patterns mimic those of the relief features, taking the form of lines and complex patterns of particles with single particle resolution, as shown in examples given in Figures 9b,c.

## 5. Carbon

In pure, covalently bonded frameworks, carbon offers a remarkable array of superlative properties, in the form of diamond, tubes/fibers and graphene/graphite. These materials lie at the center of broad efforts in research, where end applications demand integration into mechanical, thermal or electronic systems. The techniques of transfer printing are useful for manipulating each of these three classes of carbon, as described in the following.

### 5.1. Thin Film Diamond

Transfer printing, in the *deterministic assembly* mode, is immediately applicable to various classes of thin film diamond and diamond-like carbon films, using the same types of ideas and processes described in previous sections. Ultra-nanocrystalline diamond (UNCD), deposited by CVD onto SiO<sub>2</sub>/Si, is emerging as an interesting class of material for use in thermal management, as well as for functional elements in microelectromechanical systems (MEMS),<sup>[249,250]</sup> optoelectronics, and biological sensors where its highly unreactive, biocompatible surfaces are important.<sup>[250–253]</sup> Transfer printing of UNCD is possible by using adapted versions of the procedures developed for  $\mu$ s-Si derived from SOI. Here, UNCD inks can be patterned directly by oxygen plasma RIE<sup>[25]</sup> to delineate desired lateral dimensions, followed by undercut etching of the SiO<sub>2</sub> with HF to free micro/nanostructures of UNCD, tethered with homogeneous anchors, for printing by rate-dependent retrieval and transfer<sup>[47]</sup> (adhesiveless or using a BCB adhesive). Material in this form can be easily integrated into other systems. As a simple example, printed ribbons of UNCD were used to facilitate thermal spreading when integrated directly on top of heat-generating devices on plastic.<sup>[25]</sup>

### 5.2. Graphene

Graphene, a 2-dimensional semi-metallic material made up of one atomic layer of hexagonal arrangements of carbon atoms, can also be manipulated by the techniques of transfer printing. The details depend on the synthetic routes for the graphene.<sup>[254–257]</sup> The most widely used approaches involve mechanical or chemical exfoliation<sup>[254–256]</sup> of graphite, graphitization of SiC<sup>[257]</sup> or CVD on catalytic metal films<sup>[257–259]</sup>. In the latter two methods, the growth substrates are often not desirable for envisioned applications, or even for fundamental study. For example, the metal films needed for CVD growth provide

low resistance transport pathways that lay in parallel with the overlying graphene coating. For graphene formed on SiC, the areas are limited by the available sizes of the wafers. In these and many other situations, an ability to transfer the films from the growth substrate to a different surface, either selectively or in uniform sheets, is needed.<sup>[260]</sup> The mechanical exfoliation approach launched the field, and can be thought of as a transfer printing procedure, although poorly controlled and performed with Scotch™ tape as a stamp.<sup>[260]</sup> Early work also demonstrated the use of PDMS stamps in a related type of mode.<sup>[47]</sup> More sophisticated versions use either a piece of graphite with features of relief etched onto its surface to yield a kind of stamp,<sup>[261,262]</sup> or a separate stamp of silicon<sup>[263]</sup> in a process in which *subtractive transfer* against graphite inks the stamp and *additive transfer* represents the printing step. Graphene sheets, in this case, are cut from near surface region of the graphite by high stress gradients that form at the edges of the stamp due to applied pressure. Separation exfoliates thin layers of graphene that remain adhered to the raised features of relief on the stamp. Printing with applied pressure onto a target surface, such as oxygen plasma cleaned SiO<sub>2</sub>, completes the process.<sup>[262,263]</sup>

By contrast to mechanical exfoliation, chemical schemes typically produce bulk quantities of single or few layer graphene pieces in solution suspension.<sup>[264]</sup> In the simplest method, printing can be performed using *subtractive transfer* of a film consisting of flakes of graphene formed by casting onto a solid substrate or by passing the suspension through a filter.<sup>[265,266]</sup> PDMS stamps brought into conformal contact can retrieve collections of flakes from selected regions of such films, for patterned transfer to a substrate such as silicon. In some cases, transfer can be enhanced by heating (2 hours at 50 °C or 30 minutes at 75 °C) to drive PDMS oligomers to the surface to improve release, as described previously the case of metal transfer printing.<sup>[265]</sup> *Additive transfer* can also be utilized to assemble graphene infiltrated polymer layers from solution.<sup>[256,257,267]</sup> In one interesting example, graphene-electrolyte multilayers were fabricated in a layer-by-layer process.<sup>[268]</sup> Here, solutions of graphene in sulfonated polystyrene (PSP) alternate with layers of poly-(diallyldimethylammonium chloride) (PDAC) on a structured PDMS stamp which is inked through repeated dipping and rinsing steps in the oppositely charged solutions. Laminating the inked stamp to a polyelectrolyte-treated SiO<sub>2</sub> surface for one hour followed by gentle delamination transfers the graphene/PSP-PDAC layers in geometries matching the surface relief of the PDMS stamp.<sup>[268]</sup> Sequential inking and printing steps can be used to fabricate large-area patterns of the multilayer assemblies.

For uniform layers of graphene on SiC, printing can also be useful. Often, thin polymer or metal films serve as sacrificial 'carriers' to facilitate transfer, as described in the case of nanowires in Section 3.2. PDMS, thermal release tapes, dissolvable layers of PMMA or other types of stamps can be used effectively in this procedure, with several demonstrated examples.<sup>[258,259,269–271]</sup> Of particular interest is the ability to print, one layer at a time, individual or few-layer graphene sheets removed from multilayer deposits formed on SiC.<sup>[272,273]</sup> Related printing schemes are also useful in the case of CVD graphene, where release can be facilitated by removal of the underlying metal films by etching.<sup>[274]</sup> In one example, the substrate (e.g.,

a plastic such as PET) and the graphene film are brought into contact with each other and heated above the  $T_g$  of the polymer substrate ( $T_g$  of PET is 170 °C) under applied pressure (500 psi).<sup>[274]</sup> The resulting plastic flow establishes conformal contact of the polymer with the graphene sheet, to mediate transfer. This technique is quite versatile and can be used to reproducibly transfer a wide array of thicknesses (ranging from a single graphene sheet to more bulk-like quantities of graphite).<sup>[274]</sup> Other, related methods use PDMS or PDMS-supported thermally sensitive tapes to transfer CVD graphene films onto flexible or stretchable substrates.<sup>[259,270]</sup> This procedure involves contacting the graphene film with the tape or PDMS, releasing the graphene from the growth substrate by ultra-sonication or etching, and then placing the inked stamp onto a receiving substrate. For the case of thermal tape, heating to ~120 °C dramatically decreases the strength of adhesion, thereby transferring the graphene; an example of wafer-scale graphene printed onto a rubber substrate this way is shown in Figure 10a.<sup>[270]</sup> For stamps without additional thermal release tape layers, kinetic effects similar to those described for *deterministic assembly* can be used to directly transfer sheets of graphene to the receiver.<sup>[259]</sup> The graphene sheets can be patterned before or after transfer, as shown in the image in Figure 10b. These and similar techniques can be integrated into roll-to-roll type processes to generate large-area sheets of high quality graphene. Recent implementation of roller-type applications have demonstrated over 30" (diagonal) sheets of graphene mounted on PET, as shown in Figure 10c.<sup>[269]</sup>

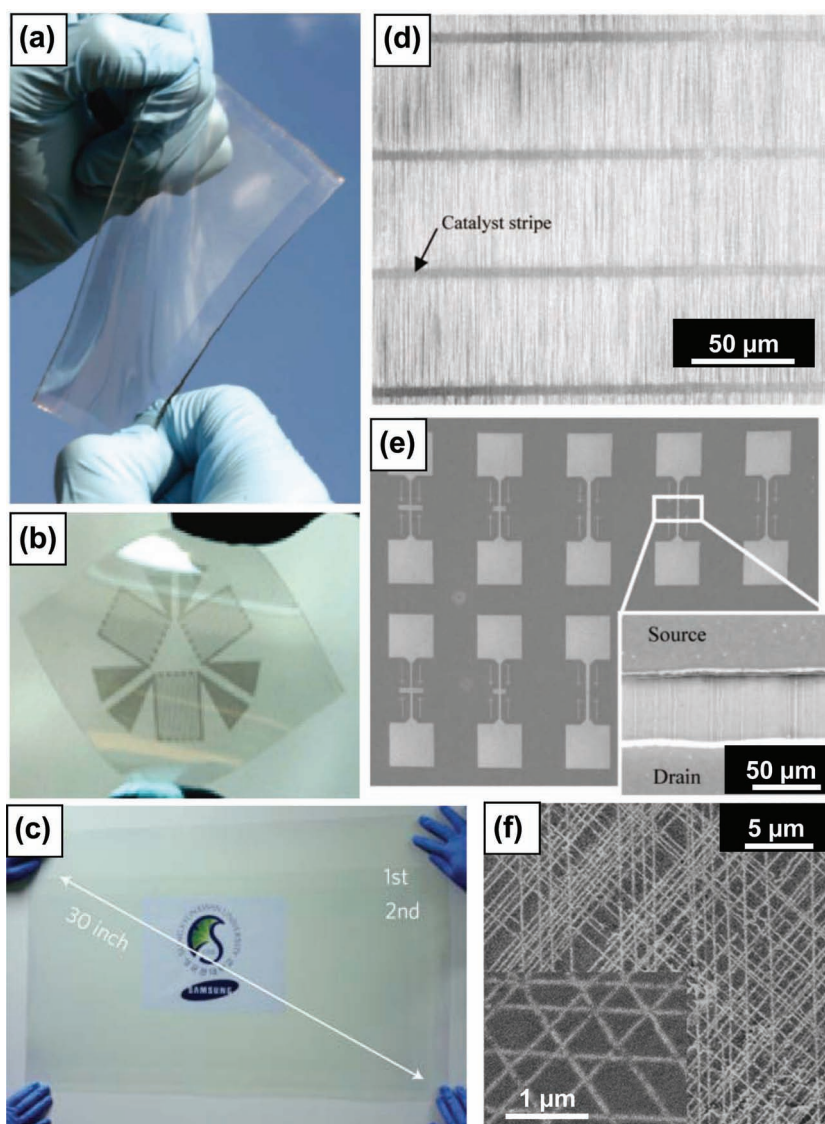


**Figure 10.** Printed patterns of graphene and single walled carbon nanotubes (SWNTs). (a) Large area film of graphene formed by chemical vapor deposition and then printed onto a PDMS substrate. (b) A three-element rosette strain gauge pattern formed with graphene printed onto a sheet of PDMS. Reproduced with permission from Ref. [270]. Copyright 2010 American Chemical Society. (c) Large-area graphene film transferred onto a 35-inch sheet of PET, by a continuous, roll-to-roll process. Reproduced with permission from Ref. [269]. Copyright 2010 Nature Publishing Group. (d) SEM image of aligned SWNTs grown on a quartz substrate and then printed onto a glass plate coated with a thin layer of epoxy. (e) SEM image of an array of devices built with arrays of SWNTs printed onto a glass plate. The inset provides an SEM image of SWNTs bridging a pair of ITO electrodes in a representative device. Reproduced with permission from Ref. [287]. Copyright 2009 American Chemical Society. (f) SEM image of overlapping, aligned arrays of SWNTs in a triangle lattice, formed by multiple cycles of printing. The inset gives a magnified view. Reproduced with permission from Ref. [283]. Copyright 2007 American Chemical Society.

### 5.3. Carbon Nanotubes

Like graphene, carbon nanotubes, particularly single-walled nanotubes (SWNTs), are of significant interest due to their excellent electronic, thermal, and mechanical properties.<sup>[5]</sup> Films consisting of random networks or aligned arrays of SWNTs represent realistic routes to integration in practical devices. The advantage of such arrangements is that they mitigate the consequences of the heterogeneity of the electronic properties associated with directly synthesized SWNTs via statistical averaging effects, and they also enable large current carrying capacities.<sup>[275]</sup> Such films are often deposited by casting from solution or they are directly grown by CVD, both in layouts that are suitable for integration into planar device geometries, for applications ranging from field effect transistors<sup>[6,44,276]</sup> and related semiconductor components to transparent electrodes for use as

conductors in organic light emitting diodes and solar cells.<sup>[277]</sup> Transfer printing represents one of the most promising ways to achieve integration. In one class of approach, solution deposition techniques can be used to coat PDMS stamps with SWNTs, in random or aligned configurations.<sup>[59,278]</sup> Stamps inked in this way can print patterns of SWNTs with controlled densities, in

some cases on amine terminated gold surfaces to mediate the transfer through electrostatic interactions.<sup>[278]</sup> When inked with higher concentrations of SWNTs, the stamps can be reused multiple times without re-inking.<sup>[278]</sup> Due to the elastomeric nature of the PDMS, this approach is also useful for transferring patterned SWNT films to the surfaces of non-planar substrates.<sup>[59]</sup>

Printing processes for dry, pre-formed films of SWNTs can also be effective.<sup>[279–281]</sup> In a simple form of transfer printing using a PDMS stamp, a solution of SWNTs passed through an alumina filtration membrane traps the SWNTs at the surface of the membrane as the solvent is pulled through the pores.<sup>[282]</sup> A PDMS stamp can peel the loosely bound film of SWNTs off of the surface of the membrane, similar to related approaches with graphene, as described in the previous section. The inked stamp is then used to print the SWNT film onto a receiving substrate (i.e., glass, flexible polyester, PET, PMMA, silicon, etc.) by applying pressure and heat for a short time (100 °C for 1 minute<sup>[277]</sup> or 80 °C for 10 min<sup>[282]</sup>). Once printed, the transferred films are strongly bound to the substrate, with adhesion sufficient to pass Scotch™ tape adhesion tests.<sup>[282]</sup> Alternatively, metal or polymer layers can act as sacrificial ‘carriers’. The resulting films, with SWNTs embedded on their surfaces, can then be processed and transferred using techniques described in previous sections. The final step involves removal of the film to leave only the SWNTs behind. Many demonstrations have been reported in such processes that use PDMS as the stamp, in single or multi-layer geometries.<sup>[6,45,283–286]</sup> In other examples, thermal release tapes can be used instead of PDMS.<sup>[287]</sup> A notable feature is the retention of alignment in arrays of SWNTs grown on substrates such as quartz, thereby enabling SWNT arrays, crossbars or more complex layouts to be achieved by printing.<sup>[283]</sup> Figure 10d shows aligned arrays of SWNTs for fabrication of transistors. Here, grown SWNTs span pre-patterned source and drain electrodes that can enable devices with varying channel widths, as illustrated in Figure 10e.<sup>[283]</sup> The same method can be adapted to printing of an individual SWNT that bridges two electrodes.<sup>[288]</sup> This type of configuration is difficult to achieve without the use of transfer printing, as it would require multiple corrosive etching steps that would compromise the electronic properties of the nanotube. By repeating the transfer printing step multiple times, it is possible to print multiple overlapping or suspended SWNTs per device (Figure 10 f).<sup>[288,289]</sup> This same type of approach can be applied to other classes of nanomaterials<sup>[290]</sup>, even fragile systems, with no resulting damage.

## 6. Organic Materials

Organic small molecule materials and polymers can serve as alternatives to or can be used in conjunction with the classes of

inorganic semiconductors, metals and carbon-based systems described in the previous sections. Semiconducting, metallic and dielectric properties are possible, with appropriate chemistries and doping techniques. The methods of transfer printing are well suited and well developed for manipulating all such types of organics. The following subsections present some examples, starting with organic semiconductors, then PDMS and various other polymers.

### 6.1. Organic Semiconductors

Organic semiconducting materials represent valuable classes of ink for transfer printing because of their critical roles in organic active electronic and optoelectronic devices, including in certain applications where films of SWNTs or sheets of graphene are also thought to be useful. The ability to pattern and transfer organic semiconductors at high spatial resolution, without sacrificing their electrical properties or altering the characteristics of the receiving substrates, is imperative.<sup>[4,10,222]</sup> Notable examples of transfer printing such materials are given in Figure 11. Solvent-free, direct methods are of interest because they eliminate constraints due to requirements on solvent compatibility. The most

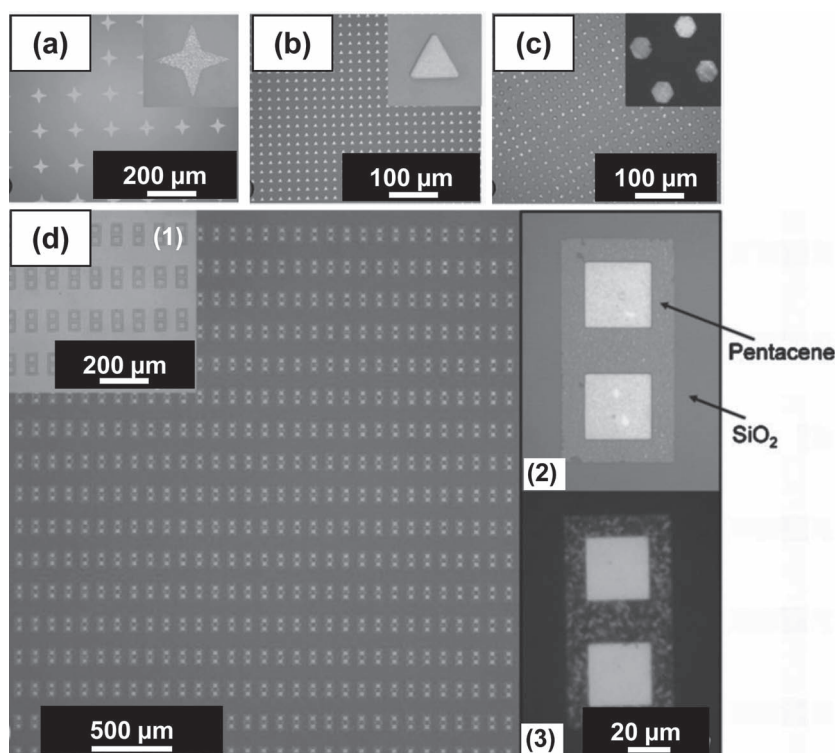


**Figure 11.** Transfer printed patterns of solution- and vapor-deposited small-molecule organic semiconductors, and their use in bottom-contact thin film transistors with self-aligned electrodes. Optical micrographs of printed patterns of films of (a) pentacene and (b) hexathiopentacene (HTP) formed by vapor deposition. (c) Micrographs of 5,5'-bis(4-tert-butylphenyl)-2,2'-bithiophene (dtb-P2TP) deposited by dip-coating and then transfer printing. The inset is a view through crossed polarizers. (d) Micrographs showing printed bottom-contact pentacene transistors. Inset (1): Pentacene film on Au before transfer. Insets (2,3): Magnified (2) and cross-polarized (3) optical micrographs of the final devices. Reproduced with permission from Ref. [304]. Copyright 2009 John Wiley and Sons.

well developed of such techniques use scanned lasers, in a process of thermal imaging.<sup>[291]</sup> Local, laser-induced heating decomposes materials at the interface between a donor substrate and a uniform coating of material to be printed, in a manner that releases selectively those heated regions onto a receiving substrate. An example of conducting polymers printed in this way is dinonyl-naphthalene sulfonic acid doped polyaniline (DNNSA-PANI), a material useful for its properties as an environmentally and thermally stable conducting polymer.<sup>[292]</sup> Repetitive application of this process enables multilayer devices.<sup>[291,293]</sup> A sophisticated version, termed Laser Induced Thermal Imaging (LITI), enables efficient delivery of active material stacks for complex device structures. This process has proven highly effective in fabrication of LCD color filters and OLED displays, with multi-color OLEDs being transferred simultaneously to a receiver plane.<sup>[294]</sup>

*Additive transfer* processes with stamps eliminate both the need for a laser and the constraints associated with heating, to deliver organic films to a receiving substrate by exploiting favorable van der Waals interactions,<sup>[295]</sup> specific surface chemistries that induce strong bonding,<sup>[296]</sup> or adhesiveless modes. Films of the organic semiconductor pentacene can, as an example of the last method, be printed with PDMS stamps directly onto ITO electrodes.<sup>[297]</sup> A water soluble sacrificial layer deposited on the surface of a donor substrate can facilitate release, if necessary.<sup>[298]</sup> Other schemes to enhance transfer use heat and pressure, as demonstrated in the printing of poly(3,4-ethylenedioxythiophene) (PEDOT) onto pentacene.<sup>[299]</sup> Similar ideas can be implemented to transfer all of the separate components of an organic thin film transistor (OTFT), including the metal, polymer, and organic semiconductor layers, occasionally with the assistance of intervening adhesive layers.<sup>[300–302]</sup> Also, printed bi-layers of poly(3,4-ethylenedioxythiophene) poly(styrenesulfonate) (PEDOT:PSS) and Au to N,N'-di(naphthalene-1-yl)-N,N'-diphenylbenzidine (NPB) can form OLEDs.<sup>[303]</sup> Entire OLED devices can be transferred in this way,<sup>[32,62–64]</sup> in which multiple printing steps yield arrays of red, green and blue OLEDs.

*Subtractive transfer* is also possible; one example uses an organic semiconductor film deposited on a substrate that supports a patterned film of gold.<sup>[304]</sup> Contacting a flat stamp and then peeling it away removes only material on top of the gold features, due to comparatively poor adhesion in these locations. Figure 11d shows an array of patterned pentacene field effect transistors (FETs), illustrating the ability to fabricate complete organic electronic devices by this method.<sup>[304]</sup> It is also possible, for select solution-processible organic semiconductors, to use *subtractive transfer* in which a PDMS stamp selectively retrieves contacted areas of a uniform film by means of diffusion into the stamp.<sup>[305]</sup>

As a final example, transfer printing can create patterns that guide assembly of organic semiconducting films from solution. A hydrophobic pattern can be defined on a substrate simply by transfer printing PDMS oligomers, using approaches described previously.<sup>[306]</sup> The associated spatial modulation in surface energy directs deposition during dip coating, thereby forming a pattern of solution processed organic materials such as PEDOT.<sup>[307]</sup>

## 6.2. PDMS

In addition to PDMS oligomers, it is possible to print solid two and three dimensional structures of PDMS, onto both planar and non-planar surfaces.<sup>[57]</sup> The methods, known as decal transfer lithography,<sup>[55–57,308]</sup> take two forms: selective pattern release (SPaR) and cohesive mechanical failure (CMF). SPaR prints a thin releasable patterned film of PDMS from a PDMS stamp, while CMF prints features that fracture from the bulk of a stamp.<sup>[56]</sup> Both rely on the ability of PDMS exposed to ozone and atomic oxygen generated by ultraviolet light (referred to as UVO treatment) to form an irreversible seal with an oxide bearing surface that can present hydroxyl groups, through bonding chemistries similar to those described previously.<sup>[56,96,309]</sup> Substrates that do not normally present surface hydroxyl groups can be coated with thin films of SiO<sub>2</sub>, or related materials, to yield this type of chemistry; examples include substrates coated with copper or with a planarizing layer of photoresist (Microposit, Shipley 1805) overcoated with SiO<sub>2</sub>.<sup>[58,310]</sup> An alternative approach uses gold and silver films treated with MPTMS, to yield thiolate based SAMS with free siloxy groups (on hydrolysis) that can bind to modified PDMS.<sup>[58]</sup> In addition to oxygen plasma treatments as alternatives to UVO, buffered oxide etchant (BOE) and NaOH can modify the PDMS to yield similar surface chemistries.<sup>[311–313]</sup>

Photo-assisted polymer transfer lithography<sup>[314]</sup> uses light activated chemistry in films of titanium dioxide that are deposited onto the receiving substrate and annealed to form an anatase crystalline phase. Contacting a patterned PDMS stamp with this titania film and exposing it to  $\lambda = 463$  nm light promotes adhesion to the PDMS via photocatalytic reaction with the TiO<sub>2</sub> film.<sup>[314]</sup> The methyl groups in PDMS are thought to be decomposed by electron-hole pairs generated in the TiO<sub>2</sub>, thereby causing the remaining siloxane groups to react with the TiO<sub>2</sub> film. Printing proceeds as for the other PDMS transfer methods, but through the formation of strong Si-O-Ti bonds, instead of siloxane bonds. Other variants are also possible. For example, treating a PDMS stamp with an O<sub>2</sub> plasma can induce bonding to a planar thin film of PDMS on a separate substrate.<sup>[315]</sup> Upon peel back, the contacted areas of the PDMS film are removed, in a form of *subtractive transfer*.

As with oligomers, printed PDMS can form hydrophobic patterns for local control over wettability.<sup>[313]</sup> The PDMS structures also, however, have sufficient thickness to serve as effective masks for dry reactive ion etching processes. High aspect ratio PDMS features, which are often needed for deep etching, can be patterned using a closed form of SPaR (shown in Figure 12a) which transfers the desired pattern by means of a sacrificial connecting film.<sup>[54,56]</sup> This covering membrane stabilizes PDMS features that would otherwise be mechanically susceptible to collapse. Prior to use as an etch mask, this layer of PDMS is eliminated with a fluorine-containing reactive ion etch chemistry.<sup>[54]</sup> SEM images of representative printed PDMS resists appear in Figures 12b-c. After the etching of the underlying substrate is complete, the remaining PDMS can be removed with a tetrabutylammonium fluoride wet etchant.<sup>[54,316]</sup>

Another convenient method for printing PDMS, known as masterless soft lithography,<sup>[55]</sup> uses a microreactor mask placed in direct contact with a flat PDMS stamp, as a means to expose

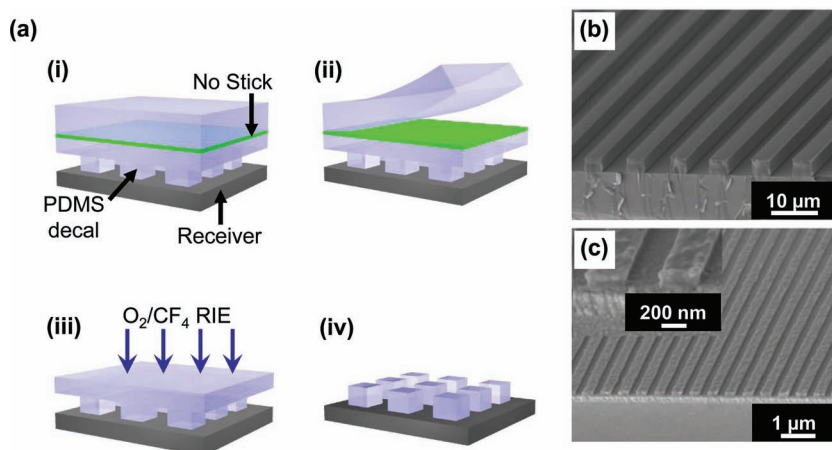


**Figure 12.** (a) Schematic illustration of a transfer printing process that combines a form of selective pattern release (SPaR) and decal transfer lithography to print structures of PDMS. (i) A selectively patterned stamp that separates surface relief (stabilized by a thin membrane of PDMS) from the bulk of the stamp by an anti-adhesion layer ('No Stick'), and permanently seals it to an oxide bearing substrate via UV-Ozone (UVO) treatment. (ii) The bulk PDMS peels away at the anti-adhesion interface, leaving behind a PDMS decal pattern on the receiver. (iii) Reactive ion etching (RIE) removes the stabilizing PDMS membrane, to yield discrete PDMS decals, as shown in (iv). SEM images of (b) 5  $\mu\text{m}$  and (c) 300 nm wide lines of PDMS printed as a closed form decal on a  $\text{SiO}_2/\text{Al}/\text{Si}$  substrate, after removal of the connecting top layer of PDMS by RIE. The inset of (c) gives a high resolution cross-sectional SEM image. Reproduced with permission from Ref. [54]. Copyright 2006 American Institute of Physics.

selected regions of the stamp to UVO. Such microreactors provide enough oxygen to modify the PDMS surface while limiting diffusion of the reactive species outside of the pattern boundaries. Once activated in this way, the stamp is immediately placed in contact with an oxide bearing surface and modestly heated to bond it, selectively, in the patterned regions. Cohesive mechanical failure of the bulk of the PDMS upon peel-back represents the printing step. The heights of these features can be controlled by varying the contact time and the oxygen plasma treatment of the stamp as well as the receiving substrate.<sup>[317]</sup>

Even though thin films of PDMS can be printed using *additive transfers* described above, the stamp is gradually consumed with repeated use. PDMS coatings on the stamps can eliminate this disadvantage. In one example, a thin film of a monoglycidyl ether-terminated PDMS prepolymer is cast onto a pentaerythritol propoxylater triacrylate (PPT) stamp treated with 3-aminopropyl triethoxysilane.<sup>[318]</sup> The covalent bond formed by the epoxy-amine chemistry creates a stable patterned film. After deposition, sonication of the mold in solvent (IPA) removes any unreacted PDMS, and the stamp can then be used for repeated transfers.<sup>[318]</sup>

### 6.3. Other Organics and Polymers

A variety of organic materials and polymers, ranging from mesogenic liquid crystals,<sup>[319]</sup> to polyelectrolytes, and block copolymers can also be transfer printed.<sup>[320,321]</sup> These layers can play intrinsic roles in a device or structure, or they can be sacrificial. One example of the former is molecular transfer printing (MTP) whereby a master surface template of organized block copolymer domains is reproduced exactly on a rep-

lica substrate. This *additive transfer* process relies on selective segregation of block copolymer 'inks' in a blend film that is laminated between the template and replica surfaces. After annealing and rinsing, guided assembly of the polymer ink patterns and chemically binds to the replica surface to create a mirror image of the master template. After replication, both the original master and newly created replica can serve as templates for further assembly.<sup>[321]</sup> The patterned surfaces, which have features on the order of the domain size in the block copolymer film, can be coupled with traditional lithographic techniques to generate complex feature geometries, and can be extended to massively parallel processing schemes. Direct printing of block copolymers with ordered domains of sub-10 nm resolution has also been demonstrated.<sup>[322]</sup> Here, block copolymer blends fill microscopic recesses embossed in a PDMS stamp; annealing in a solvent environment encourages microphase-separation. The self-assembled block copolymer films are then transferred from the stamp onto a receiver, where plasma oxidation can preferentially remove one phase, leaving behind

ordered domains. For example,  $\text{SiO}_x$  nanowires converted from poly(styrene-*b*-dimethylsiloxane) (PS-PDMS) have been delivered onto a variety of substrates such as silver, silicon, PI, and soda cans in single and multilevel configurations as example model systems.<sup>[322]</sup>

Another interesting case of organic material printing is that of photoresist.<sup>[15]</sup> This process first uses *subtractive transfer* to pattern a photoresist film supported on a flat PDMS slab by placing it in contact with an etched silicon stamp, annealing, and then quickly removing the stamp to peel away all contacting regions of resist. The resulting pattern of photoresist on PDMS can then be delivered to a receiving substrate, in *additive transfer*, by applying heat while in contact and then slowly peeling the PDMS away, as per the printing step in Figure 2a. Demonstrations of photoresist patterns transferred to both planar and non-planar substrates are presented in Figures 13a–d. The significance of patterning photoresist without photolithography lies not only in the simplicity of processing, but also in the facile pathways for fabricating curved and multi-level patterns. Figure 13e, for example, is an image of an etched silicon wafer with photoresist stripes printed perpendicular to the silicon trenches, such that after etching by RIE, a two-level pattern in Figure 13f results.

Polyelectrolytes, such as poly(acrylic acid)/poly(allylamine hydrochloride) (PAA/PAH), can be printed onto appropriately functionalized substrates, e.g., amine-terminated surfaces in the case of PAA/PAH. The acid groups on the PAA bind via dipole-dipole interactions, hydrogen bonding, and/or ionic interactions with the amine groups on the substrate, and through the formation of amide groups.<sup>[320]</sup> To accomplish multi-level patterning, a PDMS stamp is inked with a polyelectrolyte multilayer by alternating adsorption of the polyanion/polycation pair

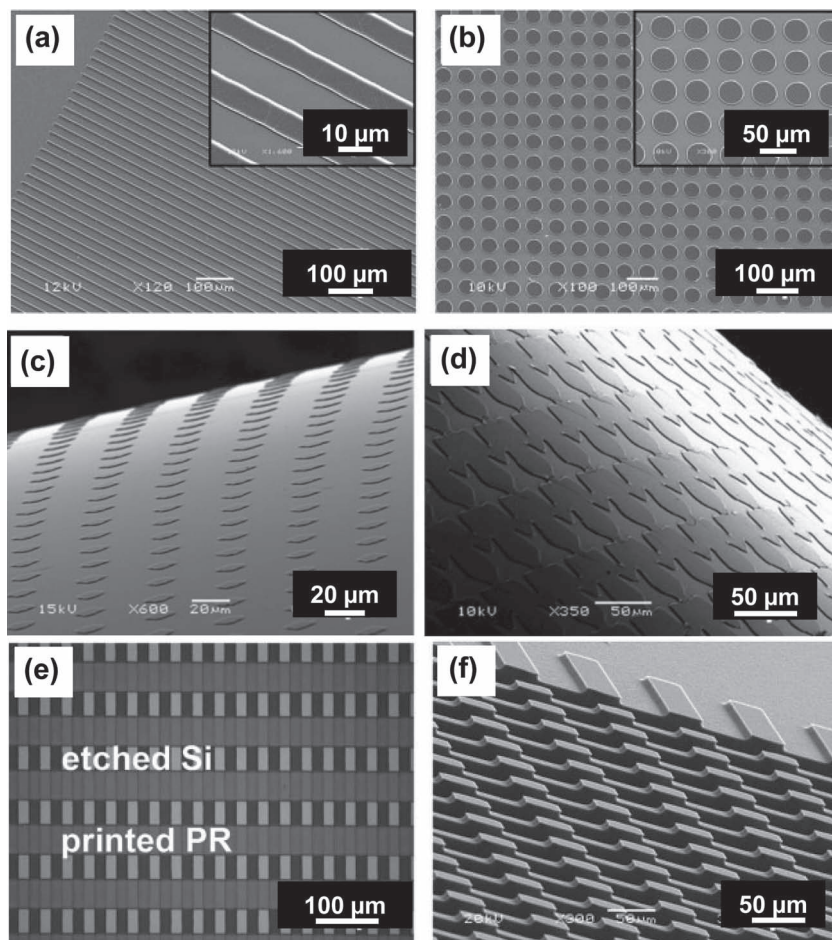


**Figure 13.** Diverse patterns of photoresist (PR) transfer printed onto various substrates. SEM images of a 0.85- $\mu\text{m}$ -thick structure of PR in an array of (a) 10  $\mu\text{m}$  lines separated by 20  $\mu\text{m}$  and (b) 50  $\mu\text{m}$  circles separated by 20  $\mu\text{m}$ . The insets provided magnified views. Slowly rolling a heated cylinder across the stamp transfers the PR to the surface of the cylinder. SEM images of (c) an array of 10  $\mu\text{m}$  x 10  $\mu\text{m}$  squares separated by 20  $\mu\text{m}$  and (d) an array of 50- $\mu\text{m}$ -wide star-shaped holes printed onto a glass cylinder with a diameter of 6 mm. (e) Optical micrograph of an array of 50- $\mu\text{m}$ -wide lines PR (2.7  $\mu\text{m}$  thick) on 200- $\mu\text{m}$  wide trenches etched into the surface of a silicon wafer. (f) Multiple levels of relief formed in the silicon by etching the substrate in (e) using the PR as a mask. Reproduced with permission from Ref. [15]. Copyright 2010 John Wiley and Sons.

directly onto the stamp surface. The inked stamp is brought into contact with the substrate, which is engineered to carry opposite charge as the top layer of the polyelectrolyte multilayer. For printing to occur, the hydrophobic interaction between the bottom layer of the polyelectrolyte and the PDMS stamp surface must be weaker than the electrostatic interactions between the top surface of the polyelectrolyte multilayer and the charged receiver substrate.<sup>[323]</sup> Three different types of patterns can be fabricated using the same stamp structure by optimizing the film thickness of the polyelectrolyte ink, processing times, and applied pressure: positive transfer; edge defined transfer; and negative molding and transfer.<sup>[324]</sup> For example, application of an inked stamp to a receiver under minimal or no external pressure transfers only regions of the polyelectrolyte film from raised relief on the PDMS surface (positive transfer). Under high pressures, entire embossed films are transferred (negative

molding and transfer) and for intermediate pressures, select regions of the surface relief are printed (edge defined transfer). Similar concepts of multilayer polyelectrolyte printing have been used to form self-assembled sheets of viruses that direct nanowire growth for fabrication of battery electrodes.<sup>[325]</sup> Polyelectrolyte films can also be printed directly onto the surfaces of individual colloidal particles. By using AFM tips modified with individual colloids, and controlling the applied force with a hybrid AFM/micro-interferometry setup, it is possible to define accurately the surface area of the colloidal particles that are contacted and thus coated with the polyelectrolyte ink.<sup>[326]</sup>

As with other material classes addressed in this review, alternative stamp materials are sometimes more desirable than PDMS for printing. For example, due to its relatively high modulus and ability to resist solvent swelling,<sup>[327]</sup> PMMA is useful for transfer printing of materials such as resists for electron beam lithography, hydrogen silsesquioxane (HSQ), and conductive silver paste.<sup>[327]</sup> Previously described PUA stamps have also been used to print polymers, by first coating their surfaces with aluminum to facilitate release, and then with a desired polymer film (such as poly(vinyl acetate) (PVAc)). Upon contact with a receiving substrate, followed by mild heating the patterned PVAc film detaches upon removal of the PUA stamp. Printing is once again driven by differential adhesion strength at the aluminum/PVAc and PVAc/substrate interfaces.<sup>[50,192]</sup> A double roller setup can press the inked PUA/PET stamp into contact with a moving, large area receiver substrate.<sup>[50]</sup>

A related procedure, also conducted with PUA stamps, is known as polymer spin transfer printing.<sup>[328]</sup> Here, spin-coating the stamp with a polymer to be printed and then exposing its surface to an oxygen plasma generates a negative charge that facilitates its transfer to a substrate coated with a polyelectrolyte that displays positive charge, such as poly(diallyldimethylammonium chloride) (PDAC). Mild heating softens the PUA to enhance release. This method has been used to transfer nanopatterned structures of a variety of polymers onto different substrates.<sup>[328]</sup> Subtractive transfer is also possible, due to the relatively high surface energy of PUA stamps (59.8  $\text{mJ}/\text{m}^2$ ).<sup>[15,66]</sup> When performed with a partially cured epoxy stamp, complete curing provides strong adhesion for this type of process.<sup>[67,329,330]</sup> Ultraviolet (UV) light can alternatively be used to mediate transfer,<sup>[331,332]</sup> in which a PDMS stamp coated with an organic material is brought into contact with a photocurable resin (e.g., acrylate) distributed on the receiver substrate, then exposed to UV light, allowing the resin to cure through radical polymerization.<sup>[331,332]</sup>

## 7. Colloids

Colloidal crystals<sup>[333,334]</sup> are ordered structures made up of arrayed polymeric or inorganic particles, useful for applications in chemical or biological sensing, optics, photonics (i.e., photonic band gap materials), high strength ceramics, battery electrodes, separation membranes and others.<sup>[335–338]</sup> To realize optimal properties, such crystals must be patterned in a controlled and spatially organized manner. Most techniques form colloidal crystals in desired geometries via directed self-assembly or using external stimuli based on electrostatics, topography,<sup>[339]</sup> or surface energy.<sup>[340]</sup> Soft lithography methods utilize microfluidic channels to physically confine colloids in the desired configuration. Such strategies require continuous flow pathways and channel geometries that promote capillary action of the colloidal suspensions.<sup>[98,341,342]</sup>

*Subtractive transfer* printing techniques provide useful, complementary capabilities.<sup>[343,344]</sup> The first step involves formation of close-packed crystals made up of inorganic or polymeric colloids by a traditional method, such as the solution evaporation technique.<sup>[337]</sup> The upper layer of the colloidal crystal can then be removed in selected regions by contact with a PDMS stamp under pressure and moderate heat. Multiple rounds of such patterning with accurate registration can yield crystals with complex patterns.<sup>[343]</sup> Similar steps, in *additive transfer* mode, can form patterned colloids on planar, non-planar, or topographically complex surfaces.<sup>[345]</sup> The parallel operation offers advantages compared to schemes that require individual placement of colloidal particles using optical tweezers,<sup>[346]</sup> or atomic force microscopy (AFM).<sup>[347]</sup> Furthermore, the inked PDMS stamp can be swelled with an organic solvent<sup>[213]</sup> or mechanically deformed (stretched) to alter the lattice spacing of the colloidal crystal while still preserving long range order in the array.<sup>[344]</sup>

In some examples, such printing occurs into a heated adhesive layer, such as poly(vinyl alcohol) (PVA).<sup>[345]</sup> Water can also be substituted as a transient adhesion promoter, in a process where hydrophilic colloids on a hydrophobic PDMS stamp move towards the hydrophilic receiving substrate by means of capillary action, forming a “liquid bridge.”<sup>[183,348]</sup> Evaporation of the water brings the colloids and the substrate into conformal contact. If the colloids and the substrate form strong physical or covalent linkages (such as that between silica and oxidized Si), the patterned colloidal crystal film will attach to the receiving substrate and become durably bonded.

The relief on the stamp can be exploited to yield printable clusters of colloids, using ideas similar to those described for the printing of metal nanoparticles.<sup>[349]</sup> The method involves a colloidal assembly step and subsequent binding of the resulting clusters to lock in the patterned assemblies and impart structural stability. A proof-of-concept system uses cyclodextrin-capped polystyrene colloids grouped into clusters by convective assembly within the relief features of a PDMS stamp.<sup>[349]</sup> A supramolecular glue (an adamantyl-terminated poly(propylene imine) dendrimer) infiltrated into the constrained clusters creates a strong bond between the particles by means of host-guest interactions involving the cyclodextrin and the dendrimer. The resulting 3D clusters are then directly printed from the reliefs of the PDMS stamp onto a cyclodextrin functionalized surface, where they are fixed and locked into their as-printed

configuration. These constructs can also be used as free-standing particle bridges that span relief features present on a receiving substrate.<sup>[350]</sup>

A related approach exploits segregation of colloids at a phase separated liquid-liquid interface, such as that between paraffin oil and water<sup>[351]</sup> or at the surface of a Langmuir-Blodgett style trough.<sup>[352]</sup> In the former case, colloids (e.g., polystyrene beads) collect at the oil-water interface to form a close-packed assembly. When a PDMS stamp is pushed through the liquid-particle-liquid interface, energy minimization redistributes the colloidal particles, confining them in the relief features of the stamp.<sup>[351]</sup> The particles remain on the stamp until it passes all the way through the liquids and comes into contact with a receiving substrate at the bottom of the container housing the liquids. Printing is achieved by heating the mixture slightly above the glass transition temperature of the colloids, allowing the particles to adhere to each other as well as the receiving substrate. When the PDMS stamp and both liquids are removed, a stable patterned array of molded particles remains on the substrate. A related approach also has been used to ink PDMS stamps.<sup>[353]</sup> Instead of utilizing heat to bond the confined material to a receiver, the inked stamp is allowed to dry and then is used to print the colloidal particles in a pattern following that of the relief of the PDMS stamp.

Similar inking and printing protocols can be used to assemble highly ordered configurations of FePt and Pt@Fe<sub>2</sub>O<sub>3</sub> core-shell nanoparticles on bare silicon substrates.<sup>[352,354]</sup> Here, single and multilayers of nanoparticles are lifted onto the surface of a structured PDMS stamp as it is passed through a Langmuir-Blodgett trough, conceptually similar to the approaches used with nanowires, described previously. Optimized surface pressure and retraction rates ensure that high-quality, densely packed layers of nanoparticles formed on the stamp surface.<sup>[354]</sup> The inked stamp is then immediately placed into contact with a plasma-activated silicon surface and transferred in a mode analogous to the *deterministic assembly* protocols of Figure 2. The resulting patterns demonstrate sub-micron resolution, low surface roughness, geometry-dependent edge-roughness, and the ability to be converted to high-quality FePt thin films under appropriate annealing conditions.<sup>[352,354]</sup> Such assembly techniques might be advantageous for developing ultrahigh-density magnetic storage devices or magneto-optical tools.<sup>[352]</sup>

## 8. Biological Materials and Living Cells

Applications in biotechnology demand the ability to pattern relevant bio-organic materials, ranging from small molecule drug candidates to living cells. Several transfer printing techniques are available for such purposes. Most simply, hydrophobic patterns achieved by transfer printing silicone oligomers from a PDMS stamp onto a hydrophilic substrate can facilitate assembly of stretched DNA molecules on patterned glass<sup>[12]</sup> and selective adsorption of proteins from solution.<sup>[355]</sup> PDMS stamps can also be used to print DNA and other biomaterials directly.<sup>[356–359]</sup> Depositing a DNA solution on unmodified PDMS yields highly aligned patterns of stretched DNA molecules, facilitating their use as probes for gene mapping. For accurate positioning of DNA into a precise array, a capillary assembly can be used to

deliver DNA solutions to specific regions on a PDMS stamp.<sup>[360]</sup> Contact with a receiving substrate, such as hydrophilic glass or mica, elicits printing.<sup>[13]</sup> When the substrate is coated with 3-aminopropyltrimethoxysilane, DNA transfer results from electrostatic binding;<sup>[360]</sup> sequential prints produce multi-layered DNA patterns.<sup>[13]</sup> Additionally, covalent attachment of dendrimers to PDMS can create patterns of positive charge on a stamp surface, which in turn can be used to bind negatively charged, amino-modified DNA or RNA molecules in a “layer-by-layer” arrangement. Arrays of this type can be printed onto aldehyde-functionalized surfaces.<sup>[361]</sup>

Oligonucleotide patterns can also be replicated at high resolution by other forms of printing. Supramolecular nanostamping encompasses a class of protocols that form patterns of single stranded DNA (ssDNA) molecules with exceptional resolution.<sup>[14,362–365]</sup> In a first step, complementary DNA molecules are hybridized to a master surface that supports a pattern of ssDNA. The complementary DNA molecules have end groups that covalently bond upon contact with a receiver. For example, a PMMA substrate functionalized with reactive aldehyde groups enables printing and capture of amine-terminated DNA via imine linkages.<sup>[363,364]</sup> Once contact is achieved, the sample is heated to dehybridize the DNA strands. Upon separation of the substrates, the ssDNA master is retained in its original form and the receiver hosts a complementary DNA strand pattern mimicking the spatial layout of the ssDNA master.<sup>[14,362]</sup>

Another transfer method applicable to biomaterials, known as affinity contact printing, uses non-covalent chemical recognition to select a specific target protein from a complex mixture. Here, a PDMS stamp is functionalized with appropriate capture molecules to drive high affinity selective binding,<sup>[366–368]</sup> after which the captured proteins are printed by contacting the inked stamp to the surface of a suitably modified receiving substrate.<sup>[366]</sup> This method can create patterns on a flat stamp by defining open microwells on its surface and filling each with a solution that affects the attachment of a specific capture molecule.<sup>[366]</sup> A *subtractive transfer* version of this patterning method uses a silicon stamp, which on contact with a planar PDMS slab captures specific protein targets. Complex arrays of capture molecules suitable for specific multi-protein inking from a solution can be fabricated in this way, with high selectivity over many patterning cycles.<sup>[366]</sup> Such printed protein patterns can immobilize and direct cell growth, define organization of focal adhesions, and guide axon outgrowth.<sup>[367]</sup> Printed DNA patterns have also been broadly used, most notably for genetic phenotyping and diagnostic sensing.<sup>[12,357,368]</sup>

The current literature suggests that affinity contact printing can be adapted to virtually any ligand-analyte pair with nanomolar range affinity, provided that background levels due to non-specific binding can be suitably controlled.<sup>[367]</sup> For this reason, and due to its more general importance to all other forms of biomolecular printing, much work focuses on the development of surface chemistries to resist such adsorption.<sup>[369–371]</sup> Hyaluronic acid (HA), a polysaccharide, is used extensively in processes for patterning proteins and cells, due to its ability to resist adsorption/adhesion to many biomolecular adsorbate materials.<sup>[372,373]</sup> This chemistry provides a control strategy for assembly in which well-defined patterns of HA are printed onto a substrate (including SiO<sub>2</sub>, poly-2-hydroxyethyl

methacrylate (poly(HEMA)), polystyrene culture dishes, and poly(lactic-co-glycolic acid) (PLGA)) through printing and application of a secondary adsorbate organized via orthogonal assembly.<sup>[370]</sup> In one such embodiment, a PDMS stamp is first rendered hydrophilic by an oxygen plasma treatment and then inked using an aqueous HA solution.<sup>[370]</sup>

Soft stamps of polar materials provide substitutes for PDMS, specifically engineered for use with biomolecular inks where requirements exist to maximize wetting while minimizing irreversible binding of adsorbates present in compositionally complex aqueous ink solutions. The most popular material for this purpose is agarose, a hydrogel material that can be molded with relief features using soft lithographic methods.<sup>[374]</sup> These stamps are remarkably durable<sup>[374–377]</sup> and can pattern a wide range of biomolecular inks, including proteins and cell membrane protein-receptor fragments, on various substrates (e.g., glass, plastic, etc.).<sup>[375,378]</sup> In general, agarose stamps use significantly less material during inking and printing than PDMS, which is especially important for efficient utilization of precious and/or difficult-to-harvest materials.<sup>[379]</sup> Agarose stamps also support the printing of protein gradients, a form of patterning mediated by diffusion within the stamp.<sup>[375]</sup> Delivering a printed gradient pattern to a receiving substrate provides a simple route to fabricate useful grayscale molecular patterns.

Perhaps the most remarkable property of agarose stamps is their ability to print patterns of living cells. Cell-inked agarose, a “living stamp,” can be used to fabricate patterns for a variety of cell types, including one exemplary model array of osteoblasts on hydroxyapatite scaffolds, as shown in **Figures 14a–b**.<sup>[380]</sup> Entire bacterial colonies can also be printed, as shown in **Figures 14c–f**.<sup>[376,377]</sup> Alternatively, printed patterns of cell adhesive proteins can elicit hierarchical organizations in plated cell cultures. One reported example immobilized these ligand proteins on a thermoresponsive poly(*N*-isopropylacrylamide) (PIPAAM) functionalized culture plate and subsequently used them to direct the growth of confluent aligned human aortic vascular smooth muscle cell sheets.<sup>[374]</sup> These sheets can be viably released from the culture surface via a polymer phase change (driven thermally by lowering the substrate temperature) and can further function as living inks for use in more complex forms of patterning.

## 9. Integrated Devices

The printing techniques highlighted in this review can be used to assemble diverse and disparate classes of materials, from GaAs nanowires, to graphene sheets and living cells, into single and multilevel functional systems. Such materials can serve a variety of roles in operational devices, from passive elements, such as electrodes or transparent contacts or photonic elements, to active semiconducting or sensing components. These assembly methods also provide an effective means to integrate different functionalities (electronic, optical, biological, mechanical, etc.) into heterogeneous configurations. Notable examples range from simple thin-film transistors (TFTs) and single level biological sensor elements to full arrays of multi-level logic structures designed to mimic high performance devices fabricated via traditional CMOS processes. In the following sections, examples

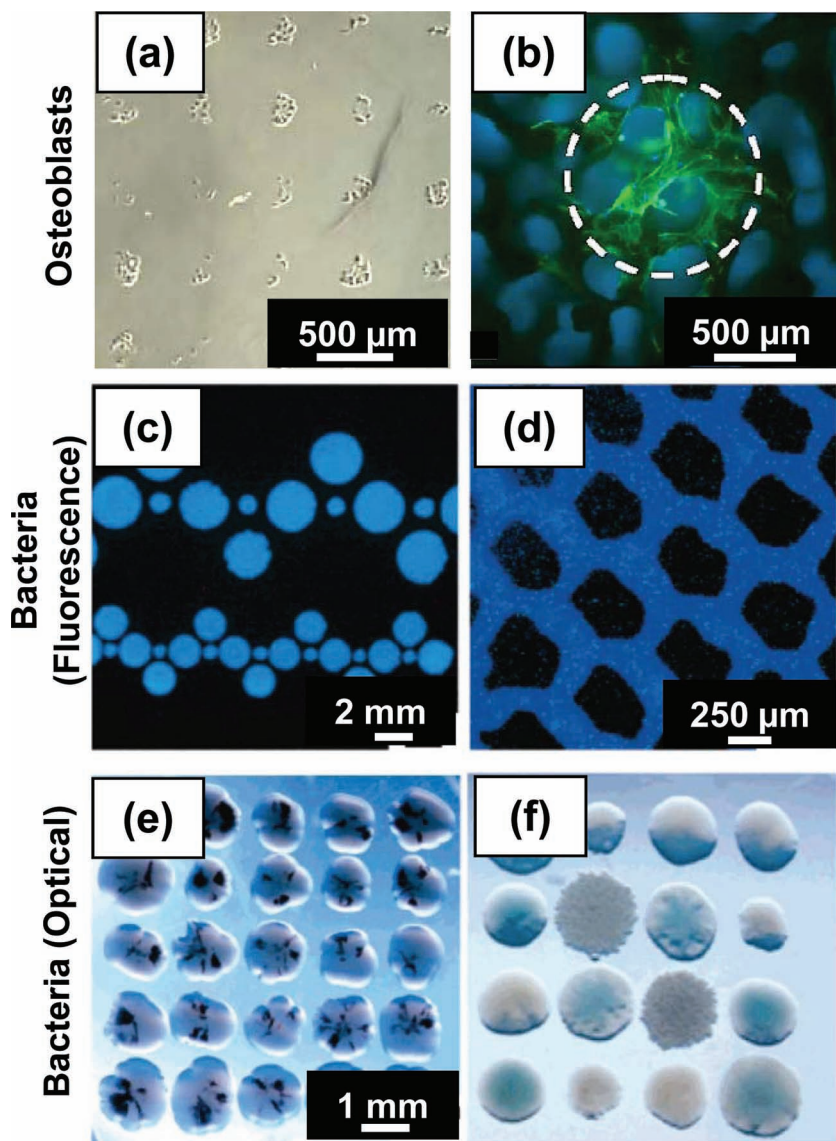


**Figure 14.** (a) Patterns of cells printed using an agarose stamp with 200  $\mu\text{m}$  features. (b) Scaffold with osteoblasts printed using an agarose stamp with 700  $\mu\text{m}$  diameter circular features. Actin is stained green; phalloidin and DNA are stained blue. The white dashed circle denotes the area patterned with cells. The blue features in the background are artifacts of fluorescence microscopy, resulting from light reflected from the white hydroxyapatite scaffolds. Reproduced with permission from Ref. [380]. Copyright 2005 Elsevier. (c)-(d) Images of patterns of *V. fischeri* printed onto a GVM-agar substrate using an agarose stamp. (e) Printed pattern of *E. coli* on LB-agar, with blue staining. (f) Array of 5 different printed colonies including *E. coli* clones that produce: N-acyl amino acid antibiotics (blue); violacein (purple), melanin (brown), and *B. subtilis*. Reproduced with permission from Ref. [376]. Copyright 2005 American Chemical Society.

of printed devices embedding challenging features, the printing techniques utilized in their fabrication, and their relative (and generally high level of) performance are discussed.

### 9.1. Transistors, Light Emitting Diodes and Solar Cells

Unique classes of large scale, heterogeneously integrated devices, specifically enabled by transfer printing, have been extensively

explored as a means to circumvent limitations in integration density, operation speed, and power consumption of current high performance electronics.<sup>[20,35,45,123]</sup> These systems also enable other useful properties, including flexible and even stretchable forms, curvilinear shapes, and lightweight, mechanically rugged construction. Inorganic semiconducting nanowires, nanoribbons and nanomembranes represent preferred materials in these applications, due to their favorable mechanics, ease of fabrication, and superior performance.<sup>[123,141,144]</sup> Printing techniques such as those discussed in Sections 3.1 and 3.2 have been utilized with exceptional success to pattern regions of single crystalline nanomaterials of InP, InAs, Ge, GaN, GaAs, and Si as active components of LEDs,<sup>[31,106]</sup> metal oxide semiconductor field effect transistors (MOSFETs),<sup>[27,30]</sup> metal semiconductor field effect transistors (MESFETs),<sup>[29,35]</sup> TFTs,<sup>[16,27,28,61,69]</sup> solar cells,<sup>[39]</sup> various sensors and other active and passive components.<sup>[123,381]</sup> As an example, printed top-gate silicon transistors on plastic exhibit mobilities of  $>600 \text{ cm}^2/\text{V-s}$  and  $530 \text{ cm}^2/\text{V-s}$  in the linear and saturation regimes, respectively, ON/OFF ratios  $>10^5$ , and switching frequencies of 515 MHz.<sup>[27]</sup> More recent results describe full radio frequency operation, with unity current gain at switching speeds greater than 10 GHz.<sup>[382]</sup> Compound semiconductor devices such as printed GaAs MESFETs<sup>[19,106]</sup> and InAs nanowire FETs<sup>[383]</sup> on plastic also offer GHz operation. In the latter case, transistors demonstrate high saturation velocities ( $>1.3 \times 10^7 \text{ cm/s}$  at a field of 16 kV/cm), maximum oscillation frequencies of 1.8 GHz, and a transconductance of 1.1 mS.<sup>[383]</sup> The devices are mechanically robust, with the ability to withstand mechanical bending cycles (radius of curvature of  $<18 \text{ mm}$ ) without performance degradation. Other flexible device geometries have also been realized, including GaAs and GaN HEMTs,<sup>[19,35]</sup> making them potentially useful platforms for ultra-high frequency electronics.

Transistors built on plastic and other substrates with printed films of SWNTs (networks, perfectly aligned arrays or anything in between) or graphene offer additional features.

In the former cases, GHz operation is possible in functional RF devices such as radios,<sup>[6,384]</sup> and full integrated circuits can be achieved.<sup>[6,44]</sup> Repetitive printing enables transparent, 'all-SWNT' transistors in which films of SWNTs serve not only as the semiconductor but also as the electrodes.<sup>[45]</sup> In conceptually similar integration schemes, transfer printing of high-quality graphene sheets can yield graphene-based CMOS-compatible electronic and optoelectronic devices,<sup>[263,271,274]</sup> in transistors that show ambipolar behavior,<sup>[263,270]</sup> and electron and hole mobilities of

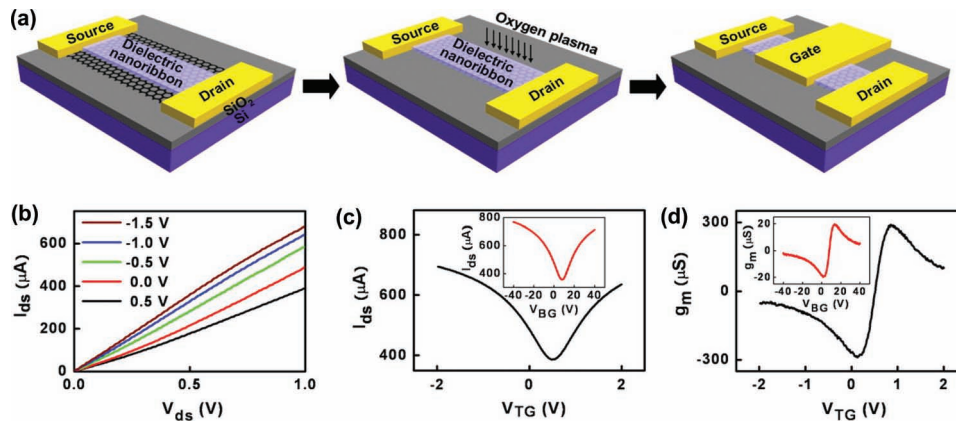


**Figure 15.** (a) Process for fabricating top gated graphene transistors using transfer printing of ultrathin, nanoribbon dielectrics of  $\text{Al}_2\text{O}_3$ . Definition of source and drain electrodes is followed by oxygen plasma etching to remove excess graphene. The top gate electrode is defined through lithography and metallization. (b) Room temperature current-voltage characteristics of a typical device. (c) Transfer characteristics of top-gated and back-gated (inset) devices at  $V_{DS} = 1$  V. (d) Transconductance,  $g_m$ , as a function of top-gate voltage  $V_{TG}$ . The inset plot shows  $g_m$  vs.  $V_{BG}$ , the voltage on the back-gate. Reproduced with permission from Ref. [385]. Copyright 2010 National Academy of Sciences.

$800 \text{ cm}^2/\text{V}\cdot\text{s}$  and  $\sim 3700 \text{ cm}^2/\text{V}\cdot\text{s}$ , respectively.<sup>[263]</sup> Top-gate dielectrics of  $\text{Al}_2\text{O}_3$  nanoribbons printed onto mechanically exfoliated graphene enable superior graphene-dielectric interface properties as well as enhanced device functionality.<sup>[385]</sup> Figure 15a provides a schematic illustration of the process flow to fabricate such devices, and Figures 15b–d show current-voltage characteristics. From these curves, an electron mobility of  $22600 \text{ cm}^2/\text{V}\cdot\text{s}$  was determined, one of the largest reported values for top-gate configurations. Figure 15c, d compare transfer characteristics and transconductances of top-gate and bottom-gate (inset) devices, demonstrating the advantages of the former.<sup>[385]</sup>

Printing techniques can also be used to form multilevel electronic devices that use multiple classes of semiconductor materials described above.<sup>[35,123,140]</sup> As an example of three dimensional heterogeneous integration (3D HGI) of this type,<sup>[35]</sup> three-layer stacks of high performance devices were constructed that integrate GaN nanoribbon HEMTs, Si nanoribbon MOSFETs, and SWNT network TFTs. Figures 16a, b present a plane view and a confocal 3D colorized image, respectively, which clearly illustrate the three distinct device layers printed on a  $25 \mu\text{m}$  thick PI substrate.<sup>[35]</sup> Figure 16c shows an optical image of the three device layers held in a bent configuration

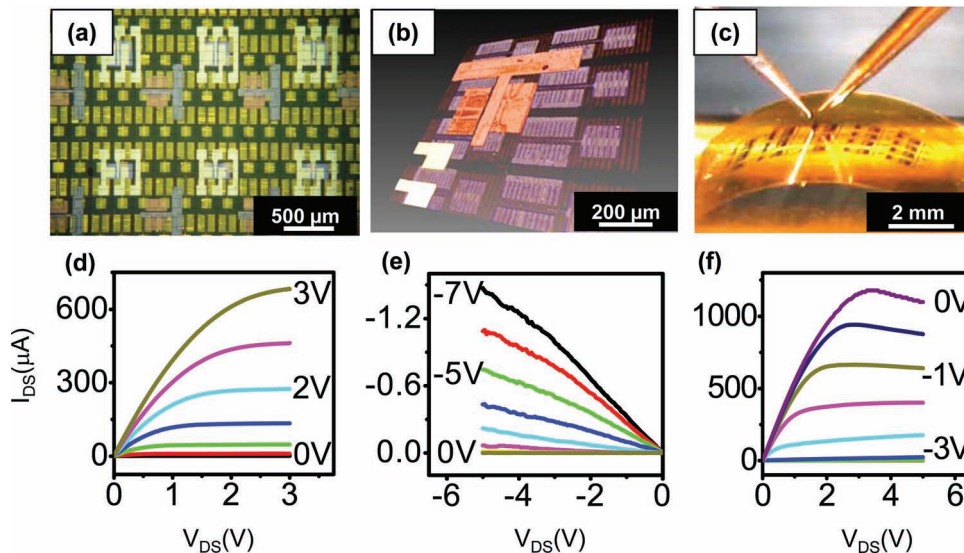


**Figure 16.** (a) Optical micrograph of 3D, heterogeneously integrated electronic devices formed by printing, in a sequential fashion, GaN nanoribbons for HEMTs, Si nanoribbons MOSFETs, and SWNT networks for TFTs, in a three-layer stack. (b) 3D image collected by confocal microscopy. The layers are colorized (gold: top layer, Si MOSFETs; red: middle layer, SWNT TFTs; pink: bottom layer GaN HEMTs) for ease of viewing. (c) Image of the system in a bent configuration, during electrical probing. (d) Electrical characteristics of a GaN HEMT from the first layer (channel lengths, widths and gate widths of 20, 170, and  $5 \mu\text{m}$ , respectively, and ribbon thicknesses, widths, and lengths of 1.2, 10, and  $150 \mu\text{m}$ , respectively), (e) a SWNT TFT on the second layer (channel lengths and widths of 50 and  $200 \mu\text{m}$ , respectively, and average tube diameters and lengths of 1.5 nm and  $10 \mu\text{m}$ , respectively) and (f) a Si MOSFET on the third layer (channel lengths and widths of 19 and  $200 \mu\text{m}$ , respectively). Reproduced with permission from Ref. [35]. Copyright 2006 The American Association for Advancement of Science.

during probing. Figures 16d-f provide device performances for the different layers: the GaN HEMTs have threshold voltages  $V_{TH} = -2.4 \pm 0.2$  V, ON/OFF ratio  $>10^6$ , and transconductances of  $0.6 \pm 0.05$  mS; the SWNT TFTs have  $V_{TH} = -5.3 \pm 1.5$  V, ON/OFF ratio  $> 10^5$ , and linear mobilities of  $5.9 \pm 2.0$  cm<sup>2</sup>/Vs; and the Si MOSFETs have  $V_{TH} = 0.2 \pm 0.3$  V, ON/OFF ratio  $> 10^4$ , and linear mobilities of  $500 \pm 30$  cm<sup>2</sup>/Vs, all consistent with performance of conventionally fabricated devices having the same geometries.<sup>[35]</sup>

Optoelectronic devices utilizing printed inorganic semiconductor materials can also be assembled into similar heterogeneous, mechanically flexible formats. Arrays of red (AlInGaP)<sup>[31]</sup> and blue (InGaN)<sup>[43]</sup> LEDs, visible<sup>[107]</sup> and near infrared<sup>[35,106]</sup> photodetectors and high performance solar cells<sup>[38]</sup>, have been printed into functional arrays on substrates ranging from glass to plastic to rubber. In all cases, performance comparable to or better than that of corresponding devices on wafer substrates is possible.

## 9.2. Negative Index Metamaterials

Optoelectronic systems that include devices such as those described in the previous section often require passive optical elements, such as lenses, waveguides, splitters, polarizers and other components. Negative index metamaterials (NIMs) enable classes of optical elements in which engineered structures offer optical properties not found in naturally occurring materials. Recent work shows that focused ion beam lithography, multi-layer electron beam lithography and related techniques can be used to achieve small-scale (i.e., smaller than a few hundred square micrometers) NIMs with interesting characteristics, including negative index behavior in the optical regime.<sup>[386]</sup> A key challenge is in fabrication with sizes and throughputs necessary for realistic applications in superlensing, invisibility cloaking and others. Printing techniques, such as the nTP method described in Section 4.1, have exceptional capabilities for forming large-area, high-quality NIMs with three-dimensional, multilayer mesh formats (i.e., fishnet NIMs).<sup>[41]</sup> The process involves blanket deposition of multilayer stacks of alternating layers of silver (Ag) and magnesium fluoride (MgF<sub>2</sub>), using a directional flux on top of a thin release layer (SiO<sub>2</sub>) on a silicon stamp.<sup>[41]</sup> Transfer printing patterned multilayer structures from the raised regions onto rigid or flexible substrates, facilitated by removal of the SiO<sub>2</sub> layer with hydrofluoric acid, completes the fabrication. Experimental and modeling results show that macroscale NIMs ( $>75$  cm<sup>2</sup>) formed in this way exhibit strong, negative index of refraction behavior in the near-IR spectral range, with excellent figures of merit, comparable to or better than those of small devices fabricated with much more complex techniques.<sup>[41]</sup> The materials can be formed on a variety of both flexible and rigid substrates.

## 9.3. Mechanical Energy Scavengers

In addition to electronic, optoelectronic and optical components, transfer printing can yield interesting mechanical devices. For example, spatially organized, printed arrays of lead zirconate titanate (PZT) ribbons enable fabrication of mechanical energy

harvesting devices supported on rubber or plastic substrates, suggesting new device platform possibilities.<sup>[387–392]</sup> The resulting generators demonstrate high efficiencies, in flexible/stretchable, wearable, and potentially implantable formats. Figure 17a provides a schematic view of a printing process for integrating PZT transducers on plastic.<sup>[389,390]</sup> PZT films (500 nm thick) are deposited, thermally annealed and patterned into arrays of strips (5 μm wide) onto a MgO (100) donor wafer which also provides a sacrificial layer for release.<sup>[389,390]</sup> Etching of the underlying surface regions of MgO releases the ribbons from the substrate sufficiently to enable retrieval with a flat PDMS stamp. The aligned orientation of the ribbons is maintained over large areas during retrieval with the stamp as shown in Figure 17a. Subsequent transfer onto an epoxy coated film of Kapton, followed by formation of interdigitated Cr/Au (10/250 nm thick) electrodes yields the mechanical energy harvester shown in Figures 17b,c. Poling (field strength  $\sim 100$  kV cm<sup>-1</sup>) the ribbons ensures a maximum piezoelectric constant,  $d_{33}$ , in the plane of the device.<sup>[388,390]</sup> Figure 17d shows the open circuit voltage for stresses applied at 0.8 Hz, 1.6 Hz, and 3.2 Hz. Maximum output currents and voltages are  $\sim 40$  nA and 0.25 V, respectively, at frequencies of 3.2 Hz and strains of 0.05%.<sup>[390]</sup> More recent work demonstrates the ability to achieve similar performance, but in fully stretchable configurations using buckled PZT ribbons printed onto PDMS substrates.<sup>[391,392]</sup>

## 10. Advanced Systems

Not only are individual device components possible, as highlighted in the previous sections, but full integrated systems that contain many thousands of such devices can be realized. This scaling provides strong evidence for printing as a core, enabling manufacturing process for new kinds of applications. The following sections review a few examples.

### 10.1. Quantum Dot Displays

Printed films of QDs provide the starting point for fabricating arrays of QD LEDs in full, active matrix displays. Figure 7c demonstrates simultaneous operation of RGB pixels formed using this approach, described in detail in Section 3.3. After transfer of registered QD pixel layers onto an organic hole-transporting layer (HTL), the QDs are cross-linked and thermally annealed to reduce the hole injection barriers and interfacial electrical resistivities, respectively. An electron-transporting layer (ETL) of sol-gel TiO<sub>2</sub> applied to the QD surface along with aluminum cathodes and an encapsulation of cover glass under a nitrogen environment completes the fabrication of QD LEDs. Hafnium-indium-zinc oxide (HIZO) TFT arrays serve to drive the QD LED pixels in advanced switching modes. The transistors exhibit superior current stability and each pixel emits over a surface area of  $\sim 46$  μm × 96 μm, comparable to the resolution in state-of-the-art high definition televisions. 4" (diagonal) full color active matrix displays with 320 × 240 pixels provide system level examples, as presented in Figure 1e.<sup>[46]</sup> These materials and fabrication techniques have potential for scale-up in next generation displays.

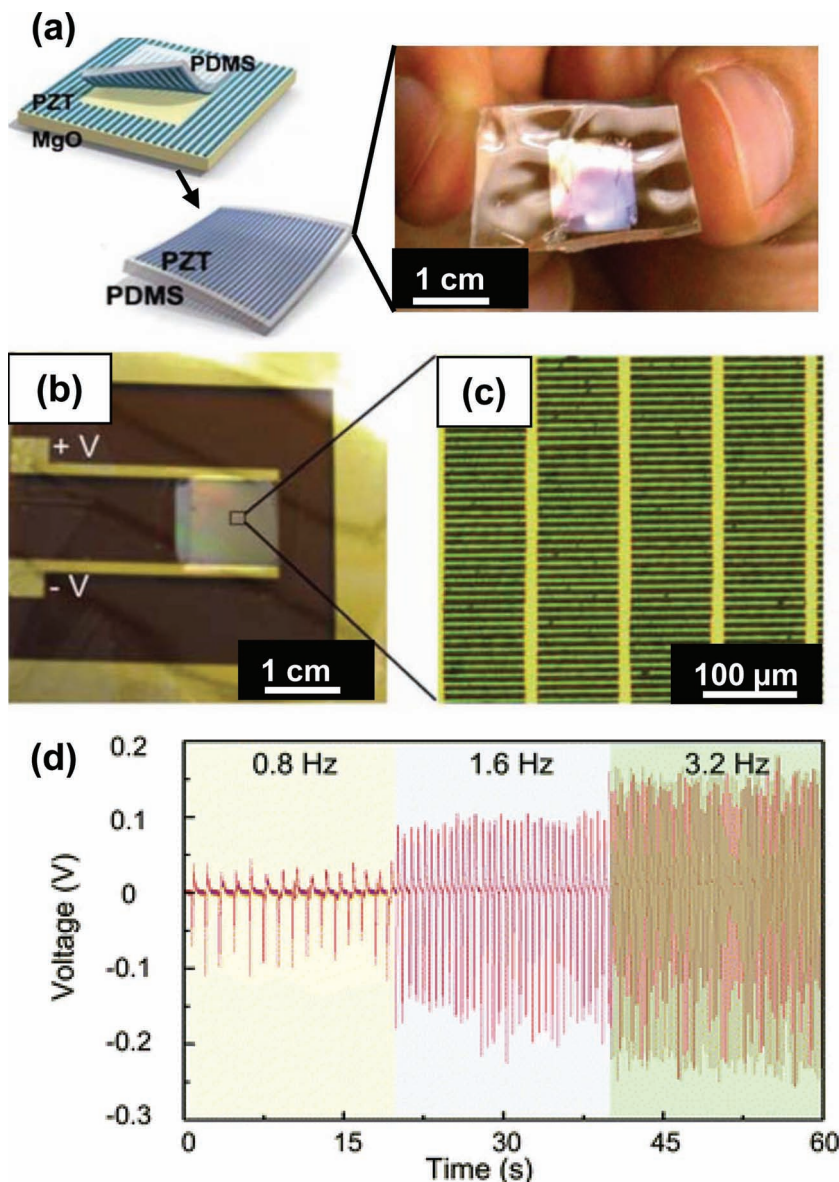


**Figure 17.** Nanogenerator device made of PZT ribbons formed on a substrate of MgO and then transfer printed onto a sheet of PDMS. Reproduced with permission from Ref. [390]. Copyright 2010 The Royal Society of Chemistry. (a) Schematic illustration of the printing process, and photograph of a resulting device. (b) Optical micrograph of an interconnected array of PZT ribbons onto a thin sheet of polyimide and (c) magnified view. (d) Measured open-circuit voltage during deformation at three different frequencies.

## 10.2. Flexible Pressure Sensor Arrays

Transistors for the active matrix display in Figure 1e use conventional planar processing techniques on rigid substrates. Transfer printing enables similar functionality on arbitrary surfaces. In one example, printed nanowire arrays serve as the active materials for such circuits, where potential applications include not only displays but also other systems such as arrays of pressure sensors, strain gauges and photodetectors.<sup>[107,393]</sup> A recently reported example of the first possibility is a large-area, pressure mapping device that incorporates printed arrays of

Ge/Si core/shell (30 nm diameter) nanowires as channel materials for transistors on a thin polyimide substrate in a  $19 \times 18$  active matrix array. The sensors in this case use a top layer of pressure sensitive rubber which also encapsulates and isolates individual pixels during operation.<sup>[393]</sup> Figure 18a provides an optical image of one such fabricated device during extreme mechanical flexure while Figure 18b shows a pressure map of the same device when embossed with a molded PDMS stamp. The system can provide fast mapping of distributions of pressure in the range from 0 and 15 kPa.

## 10.3. Bio-Integrated Electronics

Flexibility, such as that achieved by the pressure sensor arrays described in the previous section, is important for many applications. The optimal mode for integration with the human body, on the other hand, requires stretchability, in the sense of linear elastic mechanical response to large strain deformation. The capabilities of transfer printing enable devices that bond to and accommodate the motions of soft, elastomeric substrates, to provide 'tissue-like' physical properties (i.e., thin, soft, curvilinear), and resulting capacities to integrate intimately with organs of the body without any significant mechanical or mass loading effects. These characteristics enable conformable adhesion with electrical, thermal, optical and chemical access, and robust binding without irritation. Such devices can provide thousands or millions of interface points, with local electronics for advanced processing, monitoring, stimulating or other functions, along with multiplexed readout to minimize the number of wire connections. Examples include high resolution sensor sheets that laminate, like pieces of Saran Wrap, onto the surfaces of the heart<sup>[394]</sup> and the brain<sup>[395]</sup> for mapping electrophysiology, with unmatched temporal and spatial resolution. Example systems of this type include electronics with thousands of printed silicon nanomembrane MOSFETs.

An important mode of operation for cardiac devices involves endocardial access, obtained through arteries or veins. Here, transfer printing allows integration of sophisticated device functionality onto the surfaces of otherwise conventional catheter balloons.<sup>[396,397]</sup> Insertion of such 'instrumented' catheters into the interior of the heart, followed by inflation softly presses the deformable membrane of the balloon against the endocardial surface, in a configuration where a surgeon can perform a range of sensing and therapeutic operations. An example of such a device appears in Figure 19, where the functionality

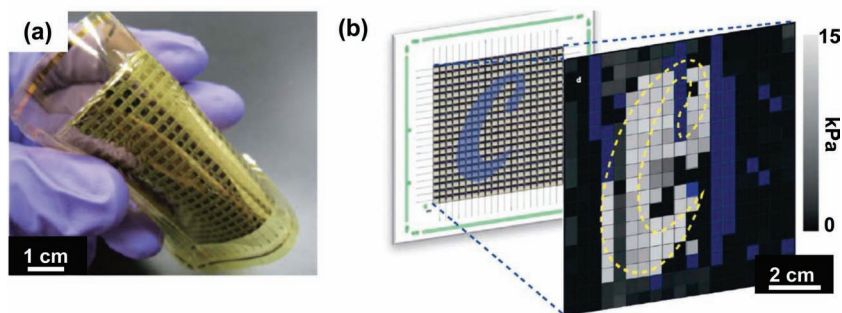


**Figure 18.** (a) Array of pressure sensors on a flexible substrate, with active matrix addressing using printed arrays of semiconductor nanowires (7 cm × 7 cm with a 19 × 18 pixel array). (b) Measured response of the device under compression in the geometry of a ‘C’ character. The blue pixels represent defects. Reproduced with permission from Ref. [393]. Copyright 2010 Nature Publishing Group.

ranges from ECG mapping to temperature and tactile sensing, to flow monitoring, tissue ablation and LED-based activation of photosensitive drugs. The images show the balloon in deflated (top) and inflated (bottom) states.

In a most recent demonstration, advanced designs in related circuits enable physical properties, ranging from modulus to degree of stretchability, areal mass density, thickness and flexural rigidity, that match the epidermis.<sup>[42]</sup> Here, lamination mounts the devices on the surface of the skin, in a manner much like a child’s temporary transfer tattoo, to provide various types of healthcare and non-healthcare related functions, using demonstrated building blocks such as antennas, wireless power coils, silicon nanomembrane MOSFETs and diodes, strain and temperature gauges, along with RF inductors, capacitors and oscillators (Figure 1c). Contact mounting yields low-impedance

level designs including classes of biologically inspired devices, such as hemispherical and parabolic imagers, that meld the high performance of conventional, wafer-based CMOS technology with form factors that mimic geometries optimized by evolution. In fabrication flows for such devices, the PDMS stamps not only provide tools for transfer, but also for geometry transformation (i.e., planar to curvilinear). For example, a thin PDMS stamp can be formed by molding against a substrate with a desired final geometry (hemisphere, paraboloid, golf ball, etc.). Placing the membrane in a state of radial tension flattens it into a drumhead shape, allowing conformal contact with a fully formed circuit or detector array in the form of a thin, open mesh. Peeling the stretched PDMS membrane away carries the mesh with it. Relaxation back to the original shape transforms the geometry of the mesh to the molded shape, in a process

where engineered deformation and buckling of non-coplanar interconnects accommodates the associated strains.<sup>[399]</sup> For the case of matrix addressed arrays of photodetectors, transfer of the geometry-transformed mesh to a rigid substrate with the same shape as the relaxed PDMS stamp followed by external connection to a printed circuit board (PCB) for computer control and data acquisition yields a curved-surface, digital imager.

Figure 20a shows a demonstrated electronic ‘eyeball’ camera that incorporates a hemispherically curved photodetector array with the size and shape of the human retina, coupled to a simple, plano-convex lens fixed in a transparent hemispherical shell.<sup>[37,398]</sup> The fields of view, levels of aberration and illumination uniformity all exceed those achievable with otherwise similar, flat photodetector arrays when the same, simple optics are used. Figure 20b presents a picture captured with a similar camera, rendered in the hemispherical geometry of the detector (top), and as a planar projection (bottom); the actual object appears in the right inset. The key feature of this device is that the shape

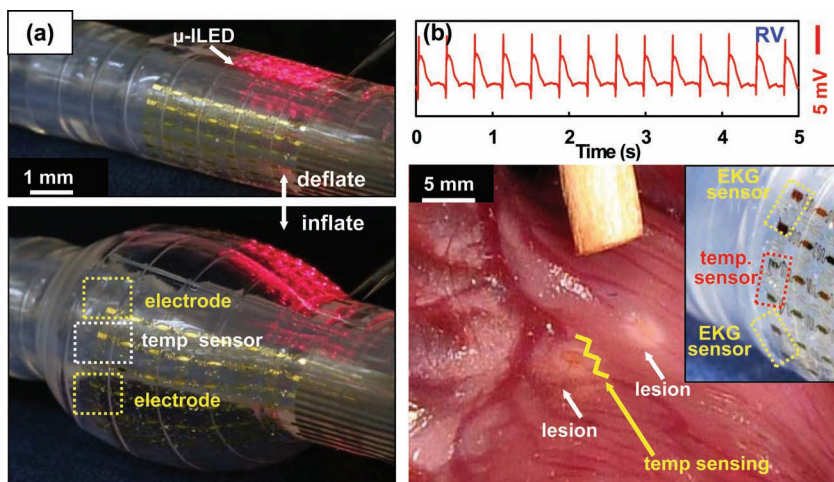


**Figure 19.** (a) Optical image of a multifunctional, ‘instrumented’ balloon catheter in deflated (top panel) and inflated (bottom panel) states. The device integrates interconnected arrays of printed components, including temperature sensors (anterior), microscale inorganic LEDs (μ-ILEDs) (posterior) and EP sensors (facing downward) (b) *In vivo* epicardial recordings of electrophysiological responses in a beating rabbit heart appears in the top panel. The bottom panel shows an optical image of epicardial lesions (white discoloration) created by two pairs of RF ablation electrodes. The yellow line denotes the region of temperature sensing. The inset shows an image of representative EKG sensors co-located with temperature sensors. Reproduced with permission from Ref. [396]. Copyright 2011 Nature Publishing Group.

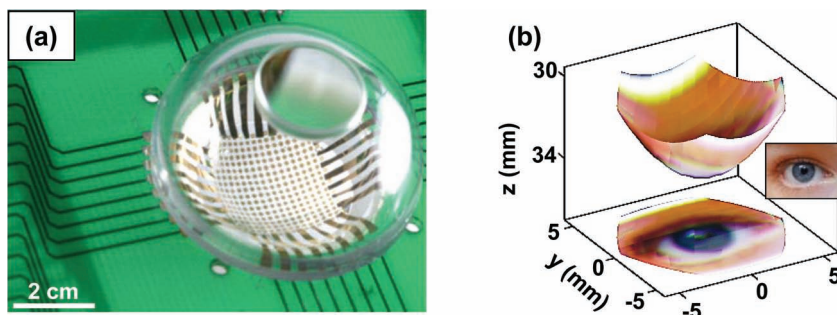


**Figure 20.** (a) Photograph of an electronic eyeball camera, consisting of an array of silicon photodiodes printed onto the hemispherical surface of a glass substrate. A transparent hemispherical cap (for ease of viewing) supports a simple, single-component plano-convex imaging lens. (b) Example of a color picture collected with a camera similar to the one in (a) but with a paraboloid curvature. The top part of this frame corresponds to the image itself, while the bottom frame provides a planar projection. The inset at the right shows the object. Reproduced with permission from Ref. [36]. Copyright 2010 American Institute of Physics.

of the photodetector array approximately matches that of the image formed with the lens (i.e., the Petzval surface).<sup>[37]</sup> Precise matching for the case of the plano-convex lens involves surfaces in the shapes of elliptic paraboloids. Paths to more sophisticated devices, such as those with improved fill-factor<sup>[36,399]</sup> and tunable curvature have recently been reported, along with quantitative experimental and theoretical analysis of the optics.<sup>[400]</sup>

### 10.5. Microconcentrator Photovoltaics

The most technically mature example of transfer printing exists as part of a manufacturing flow for a class of high concentration photovoltaic module. Here, automated transfer printing tools,

integrated optics and high precision load cells provide alignment monitoring and force-feedback sensing to determine contact between a stamp and substrate on length scales ranging from microns up to centimeters or longer. Micron scale registration and positioning accuracy across stamp/substrate contact and a repeatable overlay accuracy (the ability to automatically return to the same location on a substrate) of less than 500 nm are characteristic staging requirements. An example of a completed microconcentrator photovoltaic module is shown in Figure 21b.<sup>[401]</sup> The small surface area of each individual device provides efficient heat transfer without integration of a separate heat sink, lower series resistance as compared to larger devices, and most notably allows the use of small, lightweight concentrating optical elements (corresponding, in this case, to 1000x) with wide angle of acceptance, and optimized incident light intensity onto the microcells. The integrated modules (Figure 21c) fabricated in this way incorporate ~100,000 printed microcells and provide a route to high volume production at low costs with impressive resulting energy conversion efficiencies at the level of the individual cells (>41.7%) and world record results at the module level (>33.9%), the latter of which exceeds the 1/3 conversion milestone for the first time. These attributes, combined with low materials and manufacturing costs, yield an affordable source of energy at low start-up and lifetime costs.<sup>[402]</sup> Such strategies toward industrial scale-up of device module fabrication have strong potential to be extended to other application spaces, including those presented in other sections.

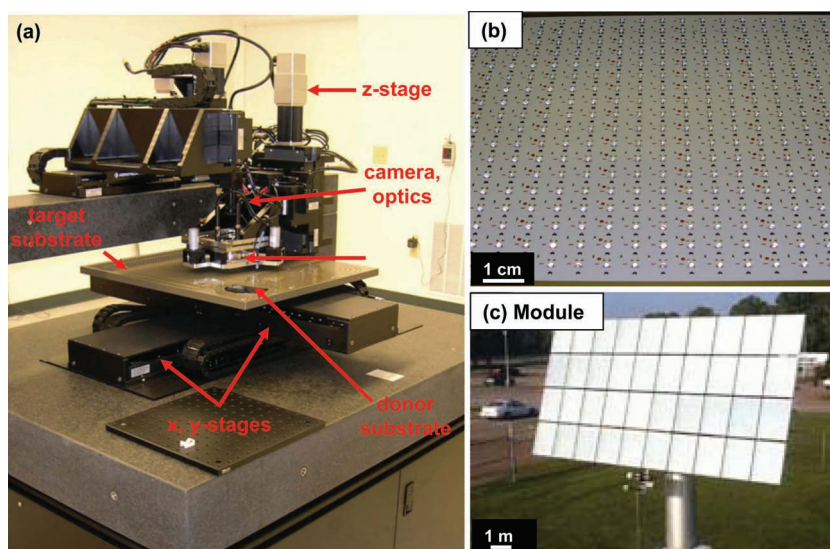


**Figure 21.** (a) Picture of a high-throughput, automated tool for transfer printing, designed specifically for a type of high concentration, microscale photovoltaic technology. (b) Image of a backplane consisting of a large-area array of interconnected, microscale multijunction solar cells with glass spheres as focusing elements. (c) Image of a completed module that incorporates ~100,000 printed microcells. Reproduced with permission from Ref. [401]. Copyright 2010 IEEE.

similar to the example shown in Figure 21a, utilize composite stamp designs of molded thin elastomeric layers supported on high-modulus, flexible backing layers,<sup>[20,171]</sup> to retrieve and print selected elements from a densely packed array of inks consisting of multi-junction compound semiconductor microscale solar cells (microcells), similar in dimensions to those reported in Reference [38]. Repetition of this printing process in a parallel mode rapidly deploys the microcells over large areas ('area multiplication', Figure 3) for direct integration into final devices that include microscale focusing elements. Such tools are nominally comprised of  $x$ -,  $y$ -, and  $z$ -axis linear stages with additional tilt- and rotation staging to enable controlled and reproducible manipulation of a stamp element independent of a host or receiving

substrate. Integrated optics and high precision load cells provide alignment monitoring and force-feedback sensing to determine contact between a stamp and substrate on length scales ranging from microns up to centimeters or longer. Micron scale registration and positioning accuracy across stamp/substrate contact and a repeatable overlay accuracy (the ability to automatically return to the same location on a substrate) of less than 500 nm are characteristic staging requirements. An example of a completed microconcentrator photovoltaic module is shown in Figure 21b.<sup>[401]</sup> The small surface area of each individual device provides efficient heat transfer without integration of a separate heat sink, lower series resistance as compared to larger devices, and most notably allows the use of small, lightweight concentrating optical elements (corresponding, in this case, to 1000x) with wide angle of acceptance, and optimized incident light intensity onto the microcells. The integrated modules (Figure 21c) fabricated in this way incorporate ~100,000 printed microcells and provide a route to high volume production at low costs with impressive resulting energy conversion efficiencies at the level of the individual cells (>41.7%) and world record results at the module level (>33.9%), the latter of which exceeds the 1/3 conversion milestone for the first time. These attributes, combined with low materials and manufacturing costs, yield an affordable source of energy at low start-up and lifetime costs.<sup>[402]</sup> Such strategies toward industrial scale-up of device module fabrication have strong potential to be extended to other application spaces, including those presented in other sections.

## 11. Concluding Remarks

Results discussed in this Review capture the wide-ranging and rapid developments in the field of transfer printing. The advances enable

broad application spaces, encompassing virtually all classes of materials. The ease with which most of these techniques can be implemented with high throughput and engineering control suggest their applicability not only in basic scientific studies and engineering prototyping, but also volume manufacturing. A key feature is that printing broadens the range of materials that can be patterned (as well as patterned on), and allows for demanding applications to be realized with materials that were previously rendered useless due to incompatibility with patterning and deposition protocols. In particular, materials prone to degradation during processing and chemical exposure can now be utilized in capacities not previously possible, through decoupling of the deposition, processing, patterning, and printing steps. Already, the ability to transfer print microstructures layer-by-layer with precise spatial orientation, has led to elegant implementations of heterogeneous integration for unusual electronic, optoelectronic, photovoltaic and photonic systems, as addressed in the Review. Further, these patterning platforms have enabled important developments in the field of non-planar and flexible electronics, not only as a method for printing and integrating microscale device arrays but also as a scheme for realizing stretchable forms of silicon and other brittle inorganic materials. Most of these engineering capabilities have, at their origins, advanced fundamental understanding in the interface chemistries, materials, adhesion physics and fracture mechanics associated with the process. Many additional opportunities exist for basic research in these areas. Engineering efforts might establish new modes of operation, such as programmable stamps with actively controlled surfaces. These collective considerations suggest that this field of study will remain active and dynamic, promising even more complex constructs and advanced patterning schemes in the near future.

## Acknowledgements

The writing of this review was supported by a MURI-funded AFRL-managed Silicon Nanomembrane Macroelectronics Contract FA9550-08-1-0394, the Frederick Seitz Materials Research Lab and the Center for Microanalysis of Materials in University of Illinois, which is funded by U.S. Department of Energy through grant DE-FG02-07ER46453 and DE-FG02-07ER46471, and the Center for Nanoscale Chemical Electrical Mechanical Manufacturing Systems in University of Illinois, which is funded by the NSF through grant CMMI-0328162.

Received: April 5, 2012

Published online: August 31, 2012

- [1] Y. Xia, G. M. Whitesides, *Angew. Chem. Int. Ed.* **1998**, *37*, 551.
- [2] Y. Xia, G. M. Whitesides, *Annu. Rev. Mater. Sci.* **1998**, *28*, 153.
- [3] J. A. Rogers, R. G. Nuzzo, *Mater. Today* **2005**, *8*, 50.
- [4] E. Menard, M. A. Meitl, Y. Sun, J.-U. Park, D. J. Shir, Y.-S. Nam, S. Jeon, J. A. Rogers, *Chem. Rev.* **2007**, *107*, 1117.
- [5] R. H. Baughman, A. A. Zakhidov, W. A. deHeer, *Science* **2002**, *297*, 787.
- [6] Q. Cao, J. A. Rogers, *Adv. Mater.* **2009**, *21*, 29.
- [7] T. Dürkop, S. A. Getty, E. Cobas, M. S. Fuhrer, *Nano Lett.* **2004**, *4*, 35.
- [8] J. Kong, N. R. Franklin, C. Zhou, M. G. Chapline, S. Peng, K. Cho, H. Dai, *Science* **2000**, *287*, 622.

- [9] G. Malliaras, R. Friend, *Phys. Today* **2005**, *58*, 53.
- [10] T. W. Kelley, P. F. Baude, C. Gerlach, D. E. Ender, D. Muyres, M. A. Haase, D. E. Vogel, S. D. Theiss, *Chem. Rev.* **2004**, *16*, 4413.
- [11] J. M. J. Frechet, *Science* **1994**, *263*, 1710.
- [12] P. Bjork, S. Holmstrom, O. Inganas, *Small* **2006**, *2*, 1068.
- [13] H. Nakao, M. Gad, S. Sugiyama, K. Otobe, T. Ohtani, *J. Am. Chem. Soc.* **2003**, *125*, 7162.
- [14] A. A. Yu, F. Stellacci, *J. Mater. Chem.* **2006**, *16*, 2868.
- [15] J. Yeom, M. A. Shannon, *Adv. Funct. Mater.* **2010**, *20*, 289.
- [16] E. Menard, K. J. Lee, D.-Y. Khang, R. G. Nuzzo, J. A. Rogers, *Appl. Phys. Lett.* **2004**, *84*, 5398.
- [17] K. J. Lee, J. Lee, H. Hwang, Z. J. Reitmeier, R. F. Davis, J. A. Rogers, R. G. Nuzzo, *Small* **2005**, *1*, 1164.
- [18] Y. Sun, J. A. Rogers, *Adv. Mater.* **2007**, *19*, 1897.
- [19] Y. Sun, H.-S. Kim, E. Menard, S. Kim, I. Adesida, J. A. Rogers, *Small* **2006**, *2*, 1330.
- [20] A. J. Baca, J.-H. Ahn, Y. Sun, M. A. Meitl, E. Menard, H.-S. Kim, W. M. Choi, D.-H. Kim, Y. Huang, J. A. Rogers, *Angew. Chem. Int. Ed.* **2008**, *47*, 5524.
- [21] Y.-L. Loo, R. L. Willett, K. W. Baldwin, J. A. Rogers, *J. Am. Chem. Soc.* **2002**, *124*, 7654.
- [22] E. J. Smythe, M. D. Dickey, G. M. Whitesides, F. Capasso, *ACS Nano* **2009**, *3*, 59.
- [23] K. Felmet, Y.-L. Loo, Y. Sun, *Appl. Phys. Lett.* **2004**, *85*, 3316.
- [24] H. Schmid, H. Wolf, R. Allenspach, H. Riel, S. Karg, B. Michel, E. Delamarque, *Adv. Funct. Mater.* **2003**, *13*, 145.
- [25] T.-H. Kim, W. M. Choi, D.-H. Kim, M. A. Meitl, E. Menard, H. Jiang, J. A. Carlisle, J. A. Rogers, *Adv. Mater.* **2008**, *20*, 2171.
- [26] A. Kawahara, H. Katsuki, M. Egashira, *Sens. Actuator, B* **1998**, *49*, 273.
- [27] J.-H. Ahn, H.-S. Kim, K. J. Lee, Z. Zhu, E. Menard, R. G. Nuzzo, J. A. Rogers, *IEEE Electron Device Lett.* **2006**, *27*, 460.
- [28] S. Mack, M. A. Meitl, A. J. Baca, Z.-T. Zhu, J. A. Rogers, *Appl. Phys. Lett.* **2006**, *88*, 213101.
- [29] K. J. Lee, M. A. Meitl, J.-H. Ahn, J. A. Rogers, R. G. Nuzzo, V. Kumar, I. Adesida, *J. Appl. Phys.* **2006**, *100*, 124507.
- [30] E. Menard, R. G. Nuzzo, J. A. Rogers, *Appl. Phys. Lett.* **2005**, *86*, 093507.
- [31] S.-I. Park, Y. Xiong, R.-H. Kim, P. Elvikis, M. Meitl, D.-H. Kim, J. Wu, J. Yoon, C.-J. Yu, Z. Liu, Y. Huang, K.-C. Hwang, P. Ferreira, X. Li, K. Choquette, J. A. Rogers, *Science* **2009**, *325*, 977.
- [32] J.-H. Choi, K.-H. Kim, S.-J. Choi, H. H. Lee, *Nanotechnology* **2006**, *17*, 2246.
- [33] D.-H. Kim, Y.-S. Kim, J. Wu, Z. Liu, J. Song, H.-S. Kim, Y. Y. Huang, K.-C. Hwang, J. A. Rogers, *Adv. Mater.* **2009**, *21*, 3703.
- [34] D.-H. Kim, J.-H. Ahn, H.-S. Kim, K. J. Lee, T.-H. Kim, C.-J. Yu, R. G. Nuzzo, J. A. Rogers, *IEEE Electron Device Lett.* **2008**, *29*, 73.
- [35] J.-H. Ahn, H.-S. Kim, K. J. Lee, S. Jeon, S. J. Kang, Y. Sun, R. G. Nuzzo, J. A. Rogers, *Science* **2006**, *314*, 1754.
- [36] I. Jung, G. Shin, V. Malyarchuk, J. S. Ha, J. A. Rogers, *Appl. Phys. Lett.* **2010**, *96*, 021110.
- [37] H. C. Ko, M. P. Stoykovich, J. Song, V. Malyarchuk, W. M. Choi, C.-J. Yu, J. B. Geddes III, J. Xiao, S. Wang, Y. Huang, J. A. Rogers, *Nature* **2008**, *454*, 748.
- [38] J. Yoon, A. J. Baca, S.-I. Park, P. Elvikis, J. B. Geddes III, L. Li, R. H. Kim, J. Xiao, S. Wang, T.-H. Kim, M. J. Motala, B. Y. Ahn, E. B. Duoss, J. A. Lewis, R. G. Nuzzo, P. M. Ferreira, Y. Huang, A. Rockett, J. A. Rogers, *Nat. Mater.* **2008**, *7*, 907.
- [39] A. J. Baca, K. J. Yu, J. Xiao, S. Wang, J. Yoon, J. H. Ryu, D. Stevenson, R. G. Nuzzo, A. A. Rockett, Y. Huang, J. A. Rogers, *Energy Environ. Sci.* **2010**, *3*, 208.
- [40] S. Kim, J. Wu, A. Carlson, S. H. Jin, A. Kovalsky, P. Glass, Z. Liu, N. Ahmed, S. L. Elgan, W. Chen, P. M. Ferreira, M. Sitti, Y. Huang, J. A. Rogers, *Proc. Natl. Acad. Sci. U.S.A.* **2010**, *107*, 17095.

- [41] D. Chanda, K. Shigeta, S. Gupta, T. Can, A. Carlson, A. Mihi, A. J. Baca, G. R. Bogart, P. Braun, J. A. Rogers, *Nat. Nanotechnol.* **2011**, *6*, 402.
- [42] D.-H. Kim, N. Lu, R. Ma, Y.-S. Kim, R.-H. Kim, S. Wang, J. Wu, S. M. Won, H. Tao, A. Islam, K. J. Yu, T.-I. Kim, R. Chowdhury, M. Ying, L. Xu, M. Li, H.-J. Chung, H. Keum, M. McCormick, P. Liu, Y.-W. Zhang, F. G. Omenetto, Y. Huang, T. Coleman, J. A. Rogers, *Science* **2011**, *333*, 838.
- [43] H. Kim, E. Brueckner, J. Song, Y. Li, S. Kim, C. Lu, J. sulking, K. Choquette, Y. Huang, R. G. Nuzzo, J. A. Rogers, *Proc. Natl. Acad. Sci. U.S.A.* **2011**, *108*, 10072.
- [44] Q. Cao, H.-S. Kim, N. Pimparkar, J. P. Kulkarni, C. Wang, M. Shim, K. Roy, M. A. Alam, J. A. Rogers, *Nature* **2008**, *454*, 495.
- [45] Q. Cao, J. A. Rogers, *Nano Res.* **2008**, *1*, 259.
- [46] T.-H. Kim, K.-S. Cho, E. K. Lee, S. J. Lee, J. Chae, J. W. Kim, D. H. Kim, J.-Y. Kwon, G. Amaratunga, S. Y. Lee, B. L. Choi, Y. Kuk, J. M. Kim, K. Kim, *Nat. Photonics* **2011**, *5*, 176.
- [47] M. A. Meitl, Z.-T. Zhu, V. Kumar, K. J. Lee, X. Feng, Y. Y. Huang, I. Adesida, R. G. Nuzzo, J. A. Rogers, *Nat. Mater.* **2006**, *5*, 33.
- [48] Y. Sun, S. Kim, I. Adesida, J. A. Rogers, *Appl. Phys. Lett.* **2005**, *87*, 083501.
- [49] Y.-L. Loo, R. L. Willett, K. W. Baldwin, J. A. Rogers, *Appl. Phys. Lett.* **2002**, *81*, 562.
- [50] D. Suh, S.-J. Choi, H. H. Lee, *Adv. Mater.* **2005**, *17*, 1554.
- [51] D. R. Hines, S. Mezheny, M. Breban, E. D. Williams, V. W. Ballarotto, G. Esen, A. Southard, M. S. Fuhrer, *Appl. Phys. Lett.* **2005**, *86*, 163101.
- [52] J. Zausmeil, M. A. Meitl, J. W. P. Hsu, B. R. Acharya, K. W. Baldwin, Y.-L. Loo, J. A. Rogers, *Nano Lett.* **2003**, *3*, 1223.
- [53] S.-H. Hur, D.-Y. Khang, C. Kocabas, J. A. Rogers, *Appl. Phys. Lett.* **2004**, *85*, 5730.
- [54] H. Ahn, K. J. Lee, W. R. Childs, J. A. Rogers, R. G. Nuzzo, A. Shim, J. *Appl. Phys.* **2006**, *100*, 0849071.
- [55] W. R. Childs, M. J. Motala, K. J. Lee, R. G. Nuzzo, *Langmuir* **2005**, *21*, 10096.
- [56] W. R. Childs, R. G. Nuzzo, *J. Am. Chem. Soc.* **2002**, *124*, 13583.
- [57] W. R. Childs, R. G. Nuzzo, *Adv. Mater.* **2004**, *16*, 1323.
- [58] W. R. Childs, R. G. Nuzzo, *Langmuir* **2005**, *21*, 195.
- [59] M. A. Meitl, Y. Zhou, A. Gaur, S. Jeon, M. L. Usrey, M. S. Strano, J. A. Rogers, *Nano Lett.* **2004**, *4*, 1643.
- [60] T. Kraus, L. Malaquin, H. Schmid, W. Riess, N. D. Spencer, H. Wolf, *Nat. Nanotechnol.* **2007**, *2*, 570.
- [61] K. J. Lee, H. Ahn, M. J. Motala, R. G. Nuzzo, E. Menard, J. A. Rogers, *J. Micromech. Microeng.* **2010**, *20*, 075018.
- [62] S. Y. Park, T. Kwon, H. H. Lee, *Adv. Mater.* **2006**, *18*, 1861.
- [63] S.-M. Seo, J. H. Kim, H. H. Lee, *Appl. Phys. Lett.* **2006**, *89*, 253515.
- [64] K.-H. Kim, S.-Y. Huh, S.-M. Seo, H. H. Lee, *Org. Electron.* **2008**, *9*, 1118.
- [65] J. A. Rogers, H. H. Lee, *Unconventional nanopatterning techniques and applications*, John Wiley & Sons, Inc, Hoboken **2008**.
- [66] J. K. Kim, J. W. Park, H. Yang, M. Choi, J. H. Choi, K. Y. Suh, *Nanotechnology* **2006**, *17*, 940.
- [67] Z. Wang, J. Zhang, R. Xing, J. Yuan, D. Yan, Y. Han, *J. Am. Chem. Soc.* **2003**, *125*, 15278.
- [68] A. J. Baca, M. A. Meitl, H. C. Ko, S. Mack, H.-S. Kim, J. Dong, P. M. Ferreira, J. A. Rogers, *Adv. Funct. Mater.* **2007**, *17*, 3051.
- [69] K. J. Lee, M. J. Motala, M. A. Meitl, W. R. Childs, E. Menard, A. K. Shim, J. A. Rogers, R. G. Nuzzo, *Adv. Mater.* **2005**, *17*, 2332.
- [70] X. Feng, M. A. Meitl, A. M. Bowen, Y. Huang, R. G. Nuzzo, J. A. Rogers, *Langmuir* **2007**, *23*, 12555.
- [71] T. L. Anderson, *Fracture mechanics: fundamentals and applications*, CRC Press, Boca Raton **1995**.
- [72] J. W. Hutchinson, Z. Suo, *Adv. Appl. Mech.* **1992**, *29*, 63.
- [73] A. N. Gent, *J. Polym. Sci. B: Polym. Phys.* **1994**, *32*, 1543.
- [74] J.-H. Ahn, H.-S. Kim, E. Menard, K. J. Lee, Z. Zhu, D.-H. Kim, R. G. Nuzzo, J. A. Rogers, I. Amlani, V. Kushner, S. G. Thomas, T. Duenas, *Appl. Phys. Lett.* **2007**, *90*, 2135011.
- [75] Y. Sun, E. Menard, J. A. Rogers, H.-S. Kim, S. Kim, G. Chen, I. Adesida, R. Dettmer, R. Cortez, A. Tewksbury, *Appl. Phys. Lett.* **2006**, *88*, 183509.
- [76] H. C. Ko, A. J. Baca, J. A. Rogers, *Nano Lett.* **2006**, *6*, 2318.
- [77] Y. Sun, D.-Y. Khang, F. Hua, K. Hurley, R. G. Nuzzo, J. A. Rogers, *Adv. Funct. Mater.* **2005**, *15*, 30.
- [78] Y. Sun, J. A. Rogers, *Nano Lett.* **2004**, *4*, 1953.
- [79] H.-C. Yuan, J. Shin, G. Qin, L. Sun, P. Bhattacharya, M. G. Lagally, G. K. Celler, Z. Ma, *Appl. Phys. Lett.* **2009**, *94*, 013102.
- [80] T.-H. Kim, A. Carlson, J.-H. Ahn, S. M. Won, S. Wang, Y. Huang, J. A. Rogers, *Appl. Phys. Lett.* **2009**, *94*, 113502.
- [81] K. H. Tsai, K. S. Kim, *Int. J. Solids. Struct.* **1993**, *30*, 1789.
- [82] A. N. Gent, *Langmuir* **1996**, *12*, 4492.
- [83] K. S. Kim, J. Kim, *J. Eng. Mater. Technol.* **1988**, *110*, 266.
- [84] K. Shull, D. Ahn, W.-L. Chem, C. M. Flanagan, A. Crosby, *Macromol. Chem. Phys.* **1998**, *199*, 489.
- [85] R. Saeidpourazar, R. Li, Y. Li, M. D. Sangid, S. Kim, C. Lu, H.-S. Kim, J. Song, Y. Huang, J. A. Rogers, P. M. Ferreira, *J. Microelectromech S* **2011**, submitted.
- [86] J. Wu, S. Kim, A. Carlson, C. F. Lu, K.-C. Hwang, Y. Huang, J. A. Rogers, *Theor. Appl.* **2011**, *1*, 011001.
- [87] J. Wu, S. Kim, W. Chen, A. Carlson, K.-C. Hwang, Y. Huang, J. A. Rogers, *Soft Matter* **2011**, *7*, 8657.
- [88] A. Carlson, H.-J. Kim-Lee, J. Wu, P. Elvikis, H. Cheng, A. Kovalsky, S. Elgan, Q. Yu, P. M. Ferreira, Y. Huang, K. T. Turner, J. A. Rogers, *Appl. Phys. Lett.* **2011**, *98*, 264104.
- [89] I. McMackin, J. Choi, P. Schumaker, V. Nguyen, F. Xu, E. Thompson, D. Babbs, S. V. Sreenivasan, M. Watts, N. Schumaker, *Proc. of SPIE* **2004**, *5374*, 222.
- [90] Y. Yin, B. Gates, Y. Xia, *Adv. Mater.* **2000**, *12*, 1426.
- [91] Z.-T. Zhu, E. Menard, K. Hurley, R. G. Nuzzo, J. A. Rogers, *Appl. Phys. Lett.* **2005**, *86*, 133507.
- [92] M. A. Meitl, X. Feng, J. Dong, E. Menard, P. M. Ferreira, Y. Huang, J. A. Rogers, *Appl. Phys. Lett.* **2007**, *90*, 083110.
- [93] H. Onoe, E. Iwase, K. Matsumoto, I. Shimoyama, *J. Microeng. Microeng.* **2007**, *17*, 1818.
- [94] Y. Yang, Y. Hwang, H. A. Cho, J.-H. Song, S.-J. Park, J. A. Rogers, H. C. Ko, *Small* **2011**, *7*, 484.
- [95] C. L. Mirley, J. T. Koberstein, *Langmuir* **1995**, *11*, 1049.
- [96] M. Ouyang, C. Yuan, R. J. Muisener, A. Boulares, J. T. Koberstein, *Chem. Mater.* **2000**, *12*, 1591.
- [97] K. Efimenko, W. E. Wallace, J. Genzer, *J. Colloid Interface Sci.* **2002**, *254*, 306.
- [98] D. C. Duffy, J. C. McDonald, O. J. A. Schueller, G. M. Whitesides, *Anal. Chem.* **1998**, *70*, 4974.
- [99] M. M. Roberts, L. J. Klein, D. E. Savage, K. A. Slinker, M. Friesen, G. Celler, M. A. Eriksson, M. G. Lagally, *Nat. Mater.* **2006**, *5*, 388.
- [100] J. L. Hoyt, H. M. Nayfeh, S. Eguchi, I. Aberg, G. Xia, T. Drake, E. A. Fitzgerald, D. A. Antoniadis, *Tech. Dig. - Int. Electron Devices Meet.* **2002**, 23.
- [101] H.-C. Yuan, Z. Ma, M. M. Roberts, D. E. Savage, M. G. Lagally, *J. Appl. Phys.* **2006**, *100*, 013708.
- [102] H. Yang, H. Pan, Z. Qiang, Z. Ma, W. Zhou, *Electron. Letters* **2008**, *44*, 858.
- [103] J. A. Rogers, M. G. Lagally, R. G. Nuzzo, *Nature* **2011**, *477*, 45.
- [104] Z. Qiang, H. Yang, L. Chen, H. Pang, Z. Ma, W. Zhou, *Appl. Phys. Lett.* **2008**, *93*, 061106.
- [105] Y. Sun, R. A. Graff, M. S. Strano, J. A. Rogers, *Small* **2005**, *1*, 1052.
- [106] J. Yoon, S. Jo, I. S. Chun, I. Jung, H.-S. Kim, M. Meitl, E. Menard, X. Li, J. J. Coleman, U. Paik, J. A. Rogers, *Nature* **2010**, *465*, 329.
- [107] Z. Fan, J. C. Ho, Z. A. Jacobson, H. Razavi, A. Javey, *Proc. Natl. Acad. Sci. U.S.A.* **2008**, *105*, 11066.

- [108] J. J. Cole, C. R. Bary, R. J. Knuesel, X. Wang, H. O. Jacobs, *Langmuir* **2010**, *27*, 7321.
- [109] D. J. Sirbuly, G. M. Lowman, B. Scott, G. D. Stucky, S. K. Buratto, *Adv. Mater.* **2003**, *15*, 149.
- [110] D. J. Gargas, O. Muresan, D. J. Sirbuly, S. K. Buratto, *Adv. Mater.* **2006**, *18*, 3164.
- [111] Y. Y. Li, P. Kim, M. J. Sailor, *Phys. Status. Solidi A: Appl. Mater. Sci.* **2005**, *202*, 1616.
- [112] C. Baratto, G. Faglia, G. Sberveglieri, Z. Gaburro, L. Pancheri, C. Oton, L. Pavesi, *Sensors* **2002**, *2*, 121.
- [113] A. Loni, L. T. Canham, M. G. Berger, R. Arens-Fischer, H. Munder, H. Luth, H. F. Arrand, T. M. Benson, *Thin Solid Films* **1996**, *276*, 143.
- [114] H. Ouyang, C. C. Striemer, P. M. Fauchet, *Appl. Phys. Lett.* **2006**, *88*, 163108.
- [115] S. O. Meade, M. S. Yoon, K. H. Ahn, M. J. Sailor, *Adv. Mater.* **2004**, *16*, 1811.
- [116] C. Mazzoleni, L. Pavesi, *Appl. Phys. Lett.* **1995**, *67*, 2983.
- [117] J. Volk, J. Balázs, A. L. Tóth, I. Bársony, *Sens. Actuators, B* **2004**, *100*, 163.
- [118] E. Xifré-Pérez, L. F. Marsal, J. Ferré-Borrull, J. Pallarès, *J. Appl. Phys.* **2007**, *102*, 063111.
- [119] D. Mangaiyarkarasi, M. B. H. Breese, Y. S. Ow, *Appl. Phys. Lett.* **2008**, *93*, 221905.
- [120] F. Cunin, T. A. Schmedake, J. R. Link, Y. Y. Li, J. Koh, S. N. Bhatia, M. J. Sailor, *Nat. Mater.* **2002**, *1*, 39.
- [121] A. C. Ford, J. C. Ho, Z. Fan, O. Ergen, V. Altoe, S. Aloni, H. Razavi, A. Javey, *Nano Res.* **2008**, *1*, 32.
- [122] A. C. Ford, J. C. Ho, Y.-L. Chueh, Y.-C. Tseng, Z. Y. Fan, J. Guo, J. Bokor, A. Javey, *Nano Lett.* **2009**, *9*, 360.
- [123] A. Javey, S. Nam, R. S. Friedman, H. Yan, C. M. Lieber, *Nano Lett.* **2007**, *7*, 773.
- [124] Y. Huang, X. Duan, C. Lieber, *Small* **2005**, *1*, 142.
- [125] O. L. Muskens, S. L. Diedenhofen, B. C. Kaas, R. E. Algra, E. P. A. M. Bakkers, J. G. Rivas, A. Lagendijk, *Nano Lett.* **2009**, *9*, 930.
- [126] Z. Y. Fan, J. G. Lu, *Appl. Phys. Lett.* **2005**, *86*, 123510.
- [127] D. H. Zhang, Z. Liu, C. Li, T. Tang, X. Liu, S. Han, B. Lei, C. Zhou, *Nano Lett.* **2004**, *4*, 1919.
- [128] H. Tang, M. Yan, X. Ma, H. Zhang, M. Wang, D. Yang, *Sens. and Actuators B* **2005**, *113*, 324.
- [129] C. K. Chan, H. Peng, G. Liu, K. Mclwrath, X. F. Zhang, R. A. Huggins, Y. Cui, *Nature* **2008**, *3*, 31.
- [130] W. Lu, J. Xiang, B. P. Timko, Y. Wu, C. M. Lieber, *Proc. Natl. Acad. Sci. USA* **2005**, *102*, 10046.
- [131] K. Heo, C.-J. Kim, M.-H. Jo, S. Hong, *J. Mater. Chem.* **2009**, *19*, 901.
- [132] W. Lu, C. M. Lieber, *J. Phys. D: Appl. Phys.* **2006**, *39*, R387.
- [133] H. J. Fan, P. Wener, M. Zacharias, *Small* **2006**, *2*, 700.
- [134] Y. Cui, M. T. Björk, J. A. Liddle, C. Sönnichsen, B. Boussert, A. P. Alivisatos, *Nano Lett.* **2004**, *4*, 1093.
- [135] P. A. Smith, C. D. Nordquist, T. N. Jackson, T. S. Mayer, B. R. Martin, J. Mbindyo, T. E. Mallouk, *Appl. Phys. Lett.* **2000**, *77*, 1290272.
- [136] B. Messer, J. H. Song, P. Yang, *J. Am. Chem. Soc.* **2000**, *122*, 10232.
- [137] S. Myung, M. Lee, G. T. Kim, J. S. Ha, S. Hong, *Adv. Mater.* **2005**, *17*, 2361.
- [138] B. Y. Yoo, Y. W. Rheem, W. P. Beyermann, N. V. Myung, S. Hong, *Nanotechnology* **2006**, *17*, 2512.
- [139] C. H. Lee, D. R. Kim, X. Zheng, *Proc. Natl. Acad. Sci. U.S.A.* **2010**, *107*, 9950.
- [140] S. W. Nam, X. Jiang, Q. Xiong, D. Ham, C. Lieber, *Proc. Natl. Acad. Sci. U.S.A.* **2009**, *106*, 1035.
- [141] Z. Fan, J. C. Ho, Z. A. Jacobson, R. Yerushalmi, R. L. Alley, H. Razavi, A. Javey, *Nano Lett.* **2008**, *8*, 20.
- [142] T. Takahashi, K. Takei, J. C. Ho, Y.-L. Chueh, Z. Fan, A. Javey, *J. Am. Chem. Soc.* **2009**, *131*, 2102.
- [143] Z. Fan, J. C. Ho, T. Takahashi, R. Yerushalmi, K. Takei, A. C. Ford, Y.-L. Chueh, A. Javey, *Adv. Mater.* **2009**, *21*, 3730.
- [144] R. Yerushalmi, Z. A. Jacobson, J. C. Ho, Z. Fan, A. Javey, *Appl. Phys. Lett.* **2007**, *91*, 203104.
- [145] S. J. Park, J. S. Ha, Y. J. Chang, G. T. Kim, *Chem. Phys. Lett.* **2004**, *390*, 199.
- [146] Y.-K. Kim, P. S. Kang, D.-I. Kim, G. Shin, G. T. Kim, J. S. Ha, *Small* **2009**, *5*, 727.
- [147] Y. K. Kim, S. J. Park, J. P. Koo, D. J. Oh, G. T. Kim, S. Hong, J. S. Ha, *Nanotechnology* **2006**, *17*, 1375.
- [148] S. A. Fortuna, J. Wen, I. S. Chun, X. Li, *Nano Lett.* **2008**, *8*, 4421.
- [149] P. Alivisatos, *Pure Appl. Phys.* **2000**, *72*, 3.
- [150] C. B. Murray, C. R. Kagan, M. G. Bawendi, *Science* **1995**, *270*, 1335.
- [151] J. Hu, L. Li, W. Yang, L. Manna, L. Wang, A. P. Alivisatos, *Science* **2001**, *292*, 2060.
- [152] A. P. Alivisatos, *Science* **1996**, *271*, 933.
- [153] S. Coe, W.-K. Woo, M. Bawendi, V. Bulovic, *Nature* **2002**, *420*, 800.
- [154] P. O. Anikeeva, J. E. Halpert, M. G. Bawendi, V. Bulovic, *Nano Lett.* **2007**, *7*, 2196.
- [155] A. Rizzo, Y. Li, S. Kudera, F. Della-Sala, M. Zanella, W. J. Parak, R. Cingolani, L. Manna, G. Gigli, *Appl. Phys. Lett.* **2007**, *90*, 051106.
- [156] J. Zhao, J. A. Bardecker, A. M. Munro, M. S. Liu, Y. Niu, I. K. Ding, J. Luo, B. Chen, A. K. Jen, D. S. Ginger, *Nano Lett.* **2006**, *6*, 463.
- [157] Y. Li, A. Rizzo, M. Mazzeo, L. Carbone, L. Manna, R. Cingolani, G. Gigli, *J. Appl. Phys.* **2005**, *97*, 113501.
- [158] Y. Q. Li, A. Rizzo, R. Cingolani, G. Gigli, *Adv. Mater.* **2006**, *18*, 2545.
- [159] M. A. Islam, I. P. Herman, *Appl. Phys. Lett.* **2002**, *80*, 3823.
- [160] V. Santhanam, R. P. Andres, *Nano Lett.* **2004**, *4*, 41.
- [161] V. Santhanam, J. Liu, R. Agarwal, R. P. Andres, *Langmuir* **2003**, *19*, 7881.
- [162] B. O. Dabbousi, C. B. Murray, M. F. Rubner, M. G. Bawendi, *Chem. Mater.* **1994**, *6*, 216.
- [163] S. Coe-Sullivan, J. S. Steckel, W.-K. Woo, M. G. Bawendi, V. Bulovic, *Adv. Funct. Mater.* **2005**, *15*, 1117.
- [164] A. Rizzo, M. Mazzeo, M. Palumbo, G. Lerario, S. D'Amone, R. Cingolani, G. Gigli, *Adv. Mater.* **2008**, *20*, 1886.
- [165] L. Kim, P. O. Anikeeva, S. A. Coe-Sullivan, J. S. Steckel, M. G. Bawendi, V. Bulovic, *Nano Lett.* **2008**, *8*, 4513.
- [166] A. Rizzo, M. Mazzeo, M. Biasiucci, R. Cingolani, G. Gigli, *Small* **2008**, *4*, 2143.
- [167] R. C. Dunn, *Chem. Rev.* **1999**, *99*, 2891.
- [168] S. K. Buratto, *Curr. Opin. Solid St. M.* **1996**, *1*, 485.
- [169] L. Novotny, S. J. Stranick, *Annu. Rev. Phys. Chem.* **2006**, *57*, 303.
- [170] K. Hoshino, T. C. Turner, S. Kim, A. Gopal, X. Zhang, *Langmuir* **2008**, *24*, 13804.
- [171] E. Menard, L. Bilhaut, J. Zaumseil, J. A. Rogers, *Langmuir* **2004**, *20*, 6871.
- [172] Y.-L. Loo, D. V. Lang, J. A. Rogers, J. W. P. Hsu, *Nano Lett.* **2003**, *3*, 913.
- [173] Y.-L. Loo, J. W. P. Hsu, R. L. Willett, K. W. Baldwin, K. W. West, J. A. Rogers, *J. Vac. Sci. Technol. B* **2002**, *20*, 2853.
- [174] N. A. Abu-Hatab, J. M. Oran, M. J. Sepaniak, *ACS Nano* **2008**, *2*, 377.
- [175] T.-I. Kim, J.-H. Kim, S. J. Son, S.-M. Seo, *Nanotechnology* **2008**, *19*, 1.
- [176] M. Xue, Y. Yang, T. Cao, *Adv. Mater.* **2008**, *20*, 596.
- [177] J. C. Love, L. A. Estroff, J. K. Kriebel, R. G. Nuzzo, G. M. Whitesides, *Chem. Rev.* **2005**, *105*, 1103.
- [178] S. L. Lehoczkya, R. J. Ledericha, J. J. Bellina Jr., *Thin Solid Films* **1978**, *55*, 125.
- [179] O. J. A. Schueller, D. C. Duffy, J. A. Rogers, S. T. Brittain, G. M. Whitesides, *Sens. Actuators, A* **1999**, *78*, 149.
- [180] A. Plecis, Y. Chen, *Microelectron. Eng.* **2007**, *84*, 1265.
- [181] Y. Berdichevsky, J. Khandurina, A. Guttman, Y.-H. Lo, *Sensor. Actuat. B-Chem* **2004**, *97*, 402.

- [182] J.-W. Kim, K.-Y. Yang, S.-H. Hong, H. Lee, *Appl. Surf. Sci.* **2008**, *254*, 5607.
- [183] B. H. Lee, Y. H. Cho, H. Lee, K.-D. Lee, S. H. Kim, M. M. Sung, *Adv. Mater.* **2007**, *19*, 1714.
- [184] K. Oh, B. H. Lee, J. K. Hwang, H. Lee, K. H. Lee, S. Im, M. M. Sung, *Small* **2009**, *5*, 558.
- [185] C.-H. Chen, Y.-C. Lee, *J. Micromech. Microeng.* **2007**, *17*, 1252.
- [186] A. Pique, H. Kim, R. Auyeung, A. Birnbaum, N. Charipar, K. Metkus, S. Mathews, *Proc. of SPIE* **2011**, 7921.
- [187] J. Wang, R. C. Y. Auyeung, H. Kim, N. A. Charipar, A. Pique, *Adv. Mater.* **2010**, *22*, 4462.
- [188] B. LeDrogoff, B. Cui, T. Veres, *Appl. Phys. Lett.* **2006**, *89*, 113103.
- [189] Z. Wang, J. Yuan, J. Zhang, R. Xing, D. Yan, Y. Han, *Adv. Mater.* **2003**, *15*, 1009.
- [190] M.-G. Kang, L. J. Guo, *J. Vac. Sci. Technol. B* **2008**, *26*, 2421.
- [191] A. J. Tunnell, V. W. Ballarotto, D. R. Hines, E. D. Williams, *Appl. Phys. Lett.* **2008**, *93*, 193113.
- [192] D. Suh, J. Rhee, H. H. Lee, *Nanotechnology* **2004**, *15*, 1103.
- [193] X. Yu, S. Yu, Z. Wang, D. Ma, Y. Han, *Appl. Phys. Lett.* **2006**, *88*, 263517.
- [194] F. Zhang, H. Y. Low, *Nanotechnology* **2008**, *19*, 415305.
- [195] C. D. Schaper, *Nano Lett.* **2003**, *3*, 1305.
- [196] J. Yu, V. Bulovic, *Appl. Phys. Lett.* **2007**, *91*, 043102.
- [197] C. E. Packard, A. Murarka, E. W. Lam, M. A. Schmidt, V. Bulovic, *Adv. Mater.* **2010**, *22*, 1.
- [198] C. Kim, P. E. Burrows, S. R. Forrest, *Science* **2000**, *288*, 831.
- [199] T.-W. Lee, J. Zauseil, Z. Bao, J. W. P. Hsu, J. A. Rogers, *Proc. Natl. Acad. Sci. U.S.A.* **2004**, *101*, 429.
- [200] J. Zauseil, K. W. Baldwin, J. A. Rogers, *J. Appl. Phys.* **2003**, *93*, 6117.
- [201] C. Kim, M. Shtein, S. R. Forrest, *Appl. Phys. Lett.* **2002**, *80*, 4051.
- [202] G. S. Ferguson, M. K. Chaudhury, G. B. Sigal, G. M. Whitesides, *Science* **1991**, *253*, 776.
- [203] C. Kim, S. R. Forrest, *Adv. Mater.* **2003**, *15*, 541.
- [204] A. Erbe, W. Jiang, Z. Bao, D. Abusch-Magder, D. M. Tennant, E. Garfunkel, N. Zhitenev, *J. Vac. Sci. Technol. B* **2005**, *23*, 3132.
- [205] W. T. S. Huck, N. Bowden, P. Onck, T. Pardoen, J. W. Hutchinson, G. M. Whitesides, *Langmuir* **2000**, *16*, 3497.
- [206] M. V. Kunnavakkam, F. M. Houlihan, M. Schlax, J. A. Liddle, P. Kolodner, O. Nalamasu, J. A. Rogers, *Appl. Phys. Lett.* **2003**, *82*, 1152.
- [207] N. Bowden, W. T. S. Huck, K. E. Paul, G. M. Whitesides, *Appl. Phys. Lett.* **1999**, *75*, 2557.
- [208] N. Bowden, S. Brittain, A. G. Evans, J. W. Hutchinson, G. M. Whitesides, *Nature* **1998**, *393*, 146.
- [209] T. T. Truong, R. Lin, S. Jeon, H. H. Lee, J. Maria, A. Gaur, F. Hua, I. Meinel, J. A. Rogers, *Langmuir* **2007**, *23*, 2898.
- [210] S. S. Williams, S. Retterer, R. Lopez, R. Ruiz, E. T. Samulski, J. M. DeSimone, *Nano Lett.* **2010**, *10*, 1421.
- [211] M. K. Kwak, T.-I. Kim, P. Kim, H. H. Lee, K. Y. Suh, *Small* **2009**, *5*, 928.
- [212] M. K. Kwak, P. Kim, J. K. Kim, C. I. Park, H. S. Cho, K. Y. Suh, *Proc. of SPIE* **2008**, 7039, 70390D.
- [213] J. N. Lee, C. Park, G. M. Whitesides, *Anal. Chem.* **2003**, *75*, 6544.
- [214] J. Kim, M. K. Chaudhury, M. J. Owen, T. Orbeck, *J. Colloid Interf. Sci.* **2001**, *244*, 200.
- [215] D. Bodas, C. Khan-Malek, *Sens. Actuators, B* **2007**, *123*, 368.
- [216] J. L. Fritz, M. J. Owen, *J. Adhesion* **1995**, *54*, 33.
- [217] D. T. Eddington, J. P. Puccinelli, D. J. Beebe, *Sens. Actuators, B* **2006**, *114*, 170.
- [218] A. Oláh, H. Hillborg, G. J. Vancso, *Appl. Surf. Sci.* **2005**, *239*, 410.
- [219] H. Hillborg, J. F. Ankner, U. W. Gedde, G. D. Smith, H. K. Yasuda, K. Wikstrom, *Polymer* **2000**, *41*, 6851.
- [220] S. Olcum, A. Kocabas, G. Ertas, A. Atalar, A. Aydinli, *Opt. Express* **2009**, *17*, 8542.
- [221] R. M. Cole, S. Mahajan, J. J. Baumberg, *Appl. Phys. Lett.* **2009**, *95*, 154103.
- [222] S. R. Forrest, *Nature* **2004**, *428*, 911.
- [223] J. Kim, S. Yun, *Macromolecules* **2006**, *39*, 4202.
- [224] H. S. Kim, J. Kim, W. Jung, J. Ampofo, W. Craft, J. Sankar, *Smart Mater. Struct.* **2008**, *17*, 015029.
- [225] J. Kim, Y. B. Seo, *Smart Mater. Struct.* **2002**, *11*, 355.
- [226] S. Yun, Y. Chen, J. N. Nayak, J. Kim, *Sens. Actuators, B* **2008**, *129*, 652.
- [227] H. G. Lim, G. Y. Cho, J. Kim, K. S. Kang, *J. Micromech. Microeng.* **2007**, *17*, 1415.
- [228] J. Kim, S.-H. Bae, H.-G. Lim, *Smart Mater. Struct.* **2006**, *15*, 889.
- [229] A. M. Bowen, R. G. Nuzzo, *Adv. Funct. Mater.* **2009**, *19*, 3243.
- [230] K. W. Rhee, L. M. Shirey, P. I. Isaacson, C. F. Korngay, W. J. Dressick, M.-S. Chen, S. L. Brandow, *J. Vac. Sci. Technol. B* **2000**, *18*, 3569.
- [231] Y. Y. Huang, W. Zhou, K. J. Hsia, E. Menard, J.-U. Park, J. A. Rogers, A. G. Alleyne, *Langmuir* **2005**, *21*, 8058.
- [232] J. P. Folkers, C. B. Gorman, P. E. Laibinis, S. Buchholz, G. M. Whitesides, *Langmuir* **1995**, *11*, 813.
- [233] N. Adden, L. J. Gamble, D. G. Castner, A. Hoffmann, G. Gross, H. Menzel, *Langmuir* **2006**, *22*, 8197.
- [234] J. W. P. Hsu, Y. L. Loo, D. V. Lang, J. A. Rogers, *J. Vac. Sci. Technol. B* **2003**, *21*, 1928.
- [235] D.-W. Oh, S. Kim, J. A. Rogers, D. G. Cahill, S. Sinha, *Adv. Mater.* **2011**, *23*, 5028.
- [236] N. Sanetra, Z. Karipidou, R. Wirtz, N. Knorr, S. Rosselli, G. Nelles, A. Offenhausser, D. Mayer, *Adv. Funct. Mater.* **2012**, *22*, 1129.
- [237] C.-H. Chen, Y.-C. Lee, *J. Microelectromech. S.* **2011**, *20*, 37.
- [238] L. J. Guo, *Adv. Mater.* **2007**, *19*, 495.
- [239] C. M. Sotomayor-Torres, S. Zankovych, J. Seekamp, A. P. Kam, C. Clavijo-Cedeño, T. Hoffmann, J. Ahopelto, F. Reuther, K. Pfeiffer, G. Bleidiessell, G. Gruetzner, M. V. Maximov, B. Heidari, *Mat. Sci. Eng. C* **2003**, *23*, 23.
- [240] S. Zankovych, T. Hoffmann, J. Seekamp, J.-U. Bruch, C. M. Sotomayor-Torres, *Nanotechnology* **2001**, *12*, 91.
- [241] M. Xue, Z. Zhang, N. Zhu, F. Wang, X. Zhao, T. Cao, *Langmuir* **2009**, *25*, 4347.
- [242] M. Xue, S. Guo, X. S. Zhao, T. Cao, *Scripta Mater.* **2008**, *58*, 854.
- [243] N. A. Melosh, A. Boukai, F. Diana, B. Gerardot, A. Badolato, P. M. Petroff, J. R. Heath, *Science* **2003**, *300*, 112.
- [244] J. R. Heath, *Acc. Chem. Res.* **2008**, *41*, 1609.
- [245] M. C. McAlpine, H. Ahmad, D. Wang, J. R. Heath, *Nat. Mater.* **2007**, *6*, 379.
- [246] D. Wang, B. A. Sheriff, M. C. McAlpine, J. R. Heath, *Nano Res.* **2008**, *1*, 9.
- [247] J. Aizenberg, P. V. Braun, P. Wiltzius, *Phys. Rev. Lett.* **2000**, *84*, 2997.
- [248] N. V. Dziomkina, G. J. Vancso, *Soft Matter* **2005**, *1*, 265.
- [249] S. Srinivasan, J. Hiller, B. Kabius, O. Auciello, *Appl. Phys. Lett.* **2007**, *90*, 134101.
- [250] H. D. Espinosa, B. C. Prorok, B. Peng, K. H. Kim, N. Moldovan, O. Auciello, J. A. Carlisle, D. M. Gruen, D. C. Mancini, *Exp. Mech.* **2003**, *43*, 256.
- [251] O. A. Williams, *Semicond. Sci. Technol.* **2006**, *21*, R49.
- [252] O. Auciello, A. V. Sumant, *Diamond. Relat. Mater.* **2010**, *19*, 699.
- [253] W. Yang, O. Auciello, J. E. Butler, W. Cai, J. A. Carlisle, J. E. Gerbi, D. M. Gruen, T. Knickerbocker, T. L. Lasseter, J. J. N. Russell, L. M. Smith, R. J. Hamers, *Nat. Mater.* **2002**, *1*, 253.
- [254] S. Park, R. S. Ruoff, *Nat. Nanotech.* **2009**, *4*, 217.
- [255] C. Soldano, A. Mahmood, E. Dujardin, *Carbon* **2010**, *48*, 2127.
- [256] X. Huang, Z. Yin, S. Wu, X. Qi, Q. Zhang, Q. Yan, F. Boey, H. Zhang, *Small* **2011**, *7*, 1876.
- [257] Y. Zhu, S. Murali, W. Cai, X. Li, J. W. Suk, J. R. Potts, R. S. Ruoff, *Adv. Mater.* **2010**, *22*, 3906.

- [258] X. Li, Y. Zhu, W. Cai, M. Borysiak, B. Han, D. Chen, R. D. Piner, L. Colombo, R. S. Ruoff, *Nano Lett.* **2009**, *9*, 4359.
- [259] K. S. Kim, Y. Zhao, H. Jang, S. Y. Lee, J. M. Kim, K. S. Kim, J.-H. Ahn, P. Kim, J.-Y. Choi, B. H. Hong, *Nature* **2009**, *457*, 706.
- [260] Y. Zhou, K. P. Loh, *Adv. Mater.* **2010**, *22*, 3615.
- [261] X. Liang, A. S. P. Chang, Y. Zhang, B. D. Harteneck, H. Choo, D. L. Olynick, S. Cabrini, *Nano Lett.* **2009**, *9*, 467.
- [262] D. Li, W. Windl, N. P. Padture, *Adv. Mater.* **2009**, *20*, 1243.
- [263] X. Liang, Z. Fu, S. Y. Chou, *Nano Lett.* **2007**, *7*, 3840.
- [264] G. Eda, G. Fanchini, M. Chhowalla, *Nat. Nanotech.* **2008**, *3*, 270.
- [265] M. J. Allen, V. C. Tung, L. Gomez, Z. Xu, L.-M. Chen, K. S. Nelson, C. Zhou, R. B. Kaner, Y. Yang, *Adv. Mater.* **2009**, *21*, 1.
- [266] D. Wei, Y. Liu, *Adv. Mater.* **2010**, *22*, 3225.
- [267] J. W. Suk, A. Kitt, C. W. Magnusson, Y. Hao, S. Ahmed, J. An, A. K. Swan, B. B. Goldberg, R. S. Ruoff, *ACS Nano* **2011**, *5*, 6916.
- [268] T. R. Hendricks, J. Lu, L. T. Drzal, I. Lee, *Adv. Mater.* **2008**, *20*, 2008.
- [269] S. Bae, H. Kim, Y. Lee, X. Xu, J.-S. Park, Y. Zheng, J. Balakrishnan, T. Lei, H. R. Kim, Y. I. Song, Y.-J. Kim, K. S. Kim, B. Ozylmaz, J.-H. Ahn, B. H. Hong, S. Iijima, *Nat. Nanotechnol.* **2010**, *5*, 574.
- [270] Y. Lee, S. Bae, H. Jang, S. Jang, S.-E. Zhu, S. H. Sim, Y. I. Song, B. H. Hong, J.-H. Ahn, *Nano Lett.* **2010**, *10*, 490.
- [271] L. Song, L. Ci, W. Gao, P. M. Ajayan, *ACS Nano* **2009**, *3*, 1353.
- [272] K. V. Emtsev, A. Bostwick, K. Horn, J. Jobst, G. L. Kellogg, L. Ley, J. L. McChesney, T. Ohta, S. A. Reshanov, J. Röhr, E. Rotenberg, A. K. Schmid, D. Waldmann, H. B. Weber, T. Seyller, *Nat. Mater.* **2009**, *8*, 203.
- [273] J. D. Caldwell, T. J. Anderson, J. C. Culbertson, G. G. Jernigan, K. D. Hobart, F. J. Kub, M. J. Tadjer, J. L. Tedesco, J. K. Hite, M. A. Mastro, R. L. Myers-Ward, C. R. Eddy, P. M. Campbell, D. K. Gaskill, *ACS Nano* **2010**, *4*, 1108.
- [274] J.-H. Chen, M. Ishigami, C. Jang, D. R. Hines, M. S. Fuhrer, E. D. Williams, *Adv. Mater.* **2007**, *19*, 3623.
- [275] V. K. Sangwan, D. R. Hines, V. W. Ballarotto, G. Esen, M. S. Fuhrer, E. D. Williams, *Mater. Res. Soc. Symp. Proc. Vol.* **2007**, *963*, 0963Q1057.
- [276] S. J. Kang, C. Kocabas, T. Ozel, M. Shim, N. Pimparkar, M. A. Alam, S. V. Rotkin, J. A. Rogers, *Nat. Nanotechnol.* **2007**, *2*, 230.
- [277] D. Zhang, K. Ryu, X. Liu, E. Polikarpov, J. Ly, M. E. Tompson, C. Zhou, *Nano Lett.* **2006**, *6*, 1880.
- [278] S. Li, Y. Yan, N. Liu, M. B. Chan-Park, Q. Zhang, *Small* **2007**, *3*, 616.
- [279] C. L. Pint, Y.-Q. Xu, S. Moghazy, T. Cherukuri, N. T. Alvarez, E. H. Haroz, S. Mahzooni, S. K. Doorn, J. Kono, M. Pasquali, R. H. Hauge, *ACS Nano* **2010**, *4*, 1131.
- [280] S. Tawfick, K. O'Brien, A. J. Hart, *Small* **2009**, *5*, 2467.
- [281] H. Liu, D. Takagi, S. Chiashi, Y. Homma, *ACS Nano* **2010**, *4*, 933.
- [282] Y. Zhou, L. Hu, G. Gruner, *Appl. Phys. Lett.* **2006**, *88*, 123109.
- [283] S. J. Kang, C. Kocabas, H.-S. Kim, Q. Cao, M. A. Meitl, D.-Y. Khang, J. A. Rogers, *Nano Lett.* **2007**, *7*, 3343.
- [284] S. J. Kang, C. Kocabas, T. Ozel, M. Shim, N. Pimparkar, M. A. Alam, S. V. Rotkin, J. A. Rogers, *Nat. Nanotech.* **2007**, *2*, 230.
- [285] S.-H. Hur, O. O. Park, J. A. Rogers, *Appl. Phys. Lett.* **2005**, *86*, 243502.
- [286] C. Kocabas, S. J. Kang, T. Ozel, M. Shim, J. A. Rogers, *J. Phys. Chem. C* **2007**, *111*, 17879.
- [287] F. N. Ishikawa, H.-K. Chang, K. Ryu, P.-C. Chen, A. Badmaev, L. G. DeArco, G. Shen, C. Zhou, *ACS Nano* **2009**, *3*, 73.
- [288] C. C. Wu, C. H. Liu, Z. Zhong, *Nano Lett.* **2010**, *10*, 1032.
- [289] V. K. Sangwan, V. W. Ballarotto, M. S. Fuhrer, E. D. Williams, *Appl. Phys. Lett.* **2008**, *93*, 113112.
- [290] L. Jiao, B. Fan, X. Xian, Z. Wu, J. Zhang, Z. Liu, *J. Am. Chem. Soc.* **2008**, *130*, 12612.
- [291] G. B. Blanchet, Y.-L. Loo, J. A. Rogers, F. Gao, C. R. Fincher, *Appl. Phys. Lett.* **2003**, *82*, 463.
- [292] G. B. Blanchet, C. R. Fincher, F. Gao, *Appl. Phys. Lett.* **2003**, *82*, 1290.
- [293] M. M. Ling, Z. Bao, *Chem. Mater.* **2004**, *16*, 4824.
- [294] S. H. Ko, Ed. *Organic Light Emitting Diode - Material, Process, and Devices*, InTech, **2011**.
- [295] C. Kim, Y. Cao, W. O. Soboyejo, S. R. Forrest, *J. Appl. Phys.* **2005**, *97*, 113512.
- [296] H. Kim, B. Yoon, J. Sung, D.-G. Choi, C. Park, *J. Mater. Chem.* **2008**, *18*, 3489.
- [297] D. Li, L. J. Guo, *J. Phys. D: Appl. Phys.* **2008**, *41*, 105115.
- [298] K.-H. Yim, Z. Zheng, Z. Liang, R. H. Friend, W. T. S. Huck, J.-S. Kim, *Adv. Funct. Mater.* **2008**, *18*, 1012.
- [299] D. Li, L. J. Guo, *Appl. Phys. Lett.* **2006**, *88*, 063513.
- [300] D. R. Hines, A. E. Southard, A. Tunnell, V. Sangwan, T. Moore, J.-H. Chen, M. S. Fuhrer, E. D. Williams, *Proc. of SPIE* **2007**, *6658*, 66580Y.
- [301] D. R. Hines, A. Southard, M. S. Fuhrer, *J. Appl. Phys.* **2008**, *104*, 024510.
- [302] J. Park, S.-O. Shim, H. H. Lee, *Appl. Phys. Lett.* **2005**, *86*, 073505.
- [303] K.-H. Kim, K.-W. Bong, H. H. Lee, *Appl. Phys. Lett.* **2007**, *90*, 093505.
- [304] S. Liu, H. A. Becerril, M. C. LeMieux, W. M. Wang, J. H. Oh, Z. Bao, *Adv. Mater.* **2009**, *21*, 1266.
- [305] K. C. Dickey, S. Subramanian, J. E. Anthony, L.-H. Han, S. Chen, Y.-L. Loo, *Appl. Phys. Lett.* **2007**, *90*, 244103.
- [306] S. Yunus, C. de Crombrughe-de Looinghe, C. Poleunis, A. Delcorte, *Surf. Interface Anal.* **2007**, *39*, 922.
- [307] A. L. Briseno, M. Roberts, M.-M. Ling, H. Moon, E. J. Nemanick, Z. Bao, *J. Am. Chem. Soc.* **2006**, *128*, 3880.
- [308] K. S. Park, E. K. Seo, Y. R. Do, K. Kim, M. M. Sung, *J. Am. Chem. Soc.* **2006**, *128*, 858.
- [309] Y. Berdichevsky, J. Khandurina, A. Guttman, Y.-H. Lo, *Sens. Actuators, B-Chem* **2004**, *97*, 402.
- [310] H. Ahn, K. J. Lee, A. Shim, J. A. Rogers, R. G. Nuzzo, *Nano Lett.* **2005**, *5*, 2533.
- [311] Y.-K. Kim, J.-H. Park, G.-C. Shin, J. S. Ha, S. J. Park, S. M. Yi, G. T. Kim, *J. Phys.* **2007**, *61*, 560.
- [312] Y.-K. Kim, G. T. Kim, J. S. Ha, *Adv. Funct. Mater.* **2007**, *17*, 2125.
- [313] Z. Zheng, O. Azzaroni, F. Zhou, W. T. S. Huck, *J. Am. Chem. Soc.* **2006**, *128*, 7730.
- [314] I.-S. Park, M. Jang, J. Ahn, *Microelectron. Eng.* **2007**, *84*, 1511.
- [315] A. L. Thangawng, M. A. Swartz, M. R. Glucksberg, R. S. Ruoff, *Small* **2007**, *3*, 132.
- [316] S. Takayama, E. Ostuni, X. Qian, J. C. McDonald, X. Jiang, P. LeDuc, M.-H. Wu, D. E. Ingber, G. M. Whitesides, *Adv. Mater.* **2001**, *13*, 570.
- [317] B. Cortese, C. Piliago, I. Viola, S. D'Amone, R. Cingolani, G. Gigli, *Langmuir*, Article ASAP.
- [318] M. Kim, Y. S. Kim, *J. Am. Chem. Soc.* **2007**, *129*, 11304.
- [319] C. Sanchez, F. Verbakel, M. J. Escuti, C. W. M. Bastiaansen, D. J. Boer, *Adv. Mater.* **2008**, *20*, 74.
- [320] X. Jiang, H. Zheng, S. Gourdin, P. T. Hammond, *Langmuir* **2002**, *18*, 2607.
- [321] S. Ji, C.-C. Liu, G. Liu, P. F. Nealey, *ACS Nano* **2010**, *4*, 599.
- [322] J. W. Jeong, W. I. Park, L.-M. Do, J.-H. Park, T.-H. Kim, G. Chae, Y. S. Jung, *Adv. Mater.* **2012**, submitted.
- [323] J. Park, P. T. Hammond, *Adv. Mater.* **2004**, *16*, 520.
- [324] J. S. Park, S. M. Cho, G. Y. Han, S. J. Sim, J. Park, P. J. Yoo, *Langmuir* **2009**, *25*, 2575.
- [325] K. T. Nam, R. Wartena, P. J. Yoo, F. W. Liau, Y. J. Lee, Y.-M. Chiang, P. T. Hammond, A. M. Belcher, *Proc. Natl. Acad. Sci. U.S.A.* **2008**, *105*, 17227.
- [326] S. Schmidt, M. Nolte, A. Fery, *Phys. Chem. Phys.* **2007**, *9*, 4967.
- [327] K. Nakamatsu, K. Tone, H. Namatsu, S. Matsui, *J. Vac. Sci. Technol. B* **2006**, *24*, 195.

- [328] Y. S. Kim, S. J. Baek, P. T. Hammond, *Adv. Mater.* **2004**, *16*, 581.
- [329] S.-M. Seo, J.-Y. Park, H. H. Lee, *Appl. Phys. Lett.* **2005**, *86*, 133114.
- [330] J.-H. Choi, D. Kim, P. J. Yoo, H. H. Lee, *Adv. Mater.* **2005**, *17*, 166.
- [331] J. Zhang, C. M. Li, M. B. Chan-Park, Q. Zhou, Y. Gan, F. Qin, B. Ong, T. Chen, *Appl. Phys. Lett.* **2007**, *90*, 243502.
- [332] H. Kang, T.-I. Kim, H. H. Lee, *Appl. Phys. Lett.* **2008**, *93*, 203308.
- [333] P. Pieranski, *Contemp. Phys.* **1983**, *24*, 25.
- [334] A. van Blaaderen, R. Ruel, P. Wiltzius, *Nature* **1997**, *385*, 321.
- [335] J. D. Joannopoulos, P. R. Villeneuve, S. Fan, *Nature* **1997**, *386*, 143.
- [336] J. E. G. J. Wijnhoven, W. L. Vos, *Science* **1998**, *281*, 802.
- [337] S.-H. Kim, S. Y. Lee, S.-M. Yang, G.-R. Yi, *NPG Asia Mater.* **2011**, *3*, 25.
- [338] M. D. Sacks, T. Y. Tseng, *J. Am. Ceram. Soc.* **1984**, *67*, 526.
- [339] E. Kim, Y. Xia, G. M. Whitesides, *Adv. Mater.* **1996**, *8*, 245.
- [340] Z.-Z. Gu, A. Fujishima, O. Sato, *Angew. Chem. Int. Ed.* **2002**, *41*, 2067.
- [341] E. Kim, Y. Xia, G. M. Whitesides, *J. Am. Chem. Soc.* **1996**, *118*, 5722.
- [342] P. Kim, K. W. Kwon, M. C. Park, S. H. Lee, S. M. Kim, K. Y. Suh, *Biochip J.* **2008**, *2*, 1.
- [343] J. Yao, X. Yan, G. Lu, K. Zhang, X. Chen, L. Jiang, B. Yang, *Adv. Mater.* **2004**, *16*, 81.
- [344] X. Yan, J. Yao, G. Lu, X. Li, J. Zhang, K. Han, B. Yang, *J. Am. Chem. Soc.* **2005**, *127*, 7688.
- [345] X. Yan, J. Yao, G. Lu, X. Chen, K. Zhang, B. Yang, *J. Am. Chem. Soc.* **2004**, *126*, 10510.
- [346] J. P. Hoogenboom, D. L. J. Vossen, C. Faivre-Moskalenko, M. Dogterom, A. van-Blaaderen, *Appl. Phys. Lett.* **2002**, *80*, 4828.
- [347] T. Junno, K. Keepert, L. Montelius, L. Samuelson, *Appl. Phys. Lett.* **1995**, *66*, 3627.
- [348] B. H. Lee, H. Shin, M. M. Sung, *Chem. Mater.* **2007**, *19*, 5553.
- [349] X. Y. Ling, I. Y. Phang, D. N. Reinhoudt, G. J. Vancso, J. Huskens, *ACS Appl. Mater. Interfaces* **2009**, *1*, 960.
- [350] X. Y. Ling, I. Y. Phang, H. Schonherr, D. N. Reinhoudt, G. J. Vancso, J. Huskens, *Small* **2009**, *5*, 1428.
- [351] N. R. Sieb, B. D. Gates, *Adv. Mater.* **2008**, *20*, 1376.
- [352] Q. Guo, X. Teng, S. Rahman, H. Yang, *J. Am. Chem. Soc.* **2003**, *125*, 630.
- [353] B. Kowalczyk, M. M. Apodaca, H. Nakanishi, S. K. Smoukov, B. A. Grzybowski, *Small* **2009**, *5*, 1970.
- [354] Q. Guo, X. Teng, H. Yang, *Adv. Mater.* **2004**, *16*, 1337.
- [355] J. A. Wigenius, S. Fransson, F. von Post, O. Inganas, *Biointerphases* **2008**, *3*, 75.
- [356] D. J. Solis, S. R. Coyer, A. J. Garcia, E. Delamarche, *Adv. Mater.* **2010**, *22*, 111.
- [357] C. Thibault, V. LeBerre, S. Casimirius, E. Trevisiol, J. Francois, C. Vieu, *J. Nanobiotechnology* **2005**, *3*, 7.
- [358] S. A. Lange, V. Benes, D. P. Kern, J. K. Heinrich-Hörber, A. Bernard, *Anal. Chem.* **2004**, *76*, 1641.
- [359] S. A. Ruiz, C. S. Chen, *Soft Matter* **2007**, *3*, 168.
- [360] A. Cerf, C. Thibault, M. Genevieve, C. Vieu, *Microelectron. Eng.* **2009**, *86*, 1419.
- [361] D. I. Rozkiewicz, W. Brugman, R. M. Kerkhoven, B. J. Ravoo, D. N. Reinhoudt, *J. Am. Chem. Soc.* **2007**, *129*, 11593.
- [362] A. A. Yu, T. A. Savas, G. S. Taylor, A. Guiseppe-Elie, H. I. Smith, F. Stellacci, *Nano Lett.* **2005**, *5*, 1061.
- [363] A. A. Yu, T. Savas, S. Cabrini, E. diFabrizio, H. I. Smith, F. Stellacci, *J. Am. Chem. Soc.* **2005**, *127*, 16774.
- [364] S. Thevenet, H.-Y. Chen, J. Lahann, F. Stellacci, *Adv. Mater.* **2007**, *19*, 41333.
- [365] A. A. Yu, F. Stellacci, *Adv. Mater.* **2007**, *19*, 4338.
- [366] J. P. Renault, A. Bernard, D. Juncker, B. Michel, H. R. Bosshard, E. Delamarche, *Angew. Chem. Int. Ed.* **2002**, *41*, 2320.
- [367] A. Bernard, D. Fitzli, P. Sonderegger, E. Delamarche, B. Michel, H. R. Bosshard, H. Biebuyck, *Nature Biotech.* **2001**, *19*, 866.
- [368] H. Tan, S. Huang, K.-L. Yang, *Langmuir* **2007**, *23*, 8607.
- [369] L. B. Thompson, N. H. Mack, R. G. Nuzzo, *Phys. Chem. Chem. Phys.* **2010**, *12*, 4301.
- [370] K. Y. Suh, A. Khademhosseini, J. M. Yang, G. Eng, R. Langer, *Adv. Mater.* **2004**, *16*, 584.
- [371] W. Senaratne, L. Andruzzi, C. K. Ober, *Biomacromolecules* **2005**, *6*, 2427.
- [372] M. Morra, C. Cassinelli, *J. Biomater. Sci. Polym. Ed.* **1999**, *10*, 1107.
- [373] M. Morra, C. Cassinelli, A. Pavesio, D. Renier, *J. Colloid Interf. Sci.* **2003**, *259*, 236.
- [374] D. B. Weibel, W. R. DiLuzio, G. M. Whitesides, *Nat. Rev. Microbiol.* **2007**, *5*, 209.
- [375] M. Mayer, J. Yang, I. Gitlin, D. H. Gracias, G. M. Whitesides, *Proteomics* **2004**, *4*, 2366.
- [376] D. B. Weibel, A. Lee, M. Mayer, S. F. Brady, D. Bruzewicz, J. Yang, W. R. DiLuzio, J. Clardy, G. M. Whitesides, *Langmuir* **2005**, *21*, 6436.
- [377] H. Xu, X. Y. Ling, J. van Bennekom, X. Duan, M. J. W. Ludden, D. N. Reinhoudt, M. Wessling, R. G. H. Lammertink, J. Huskens, *J. Am. Chem. Soc.* **2009**, *131*, 797.
- [378] C. Williams, Y. Tsuda, B. C. Isenberg, M. Yamato, T. Shimizu, T. Okano, J. Y. Wong, *Adv. Mater.* **2009**, *21*, 2161.
- [379] S. Majid, M. Mayer, *J. Am. Chem. Soc.* **2008**, *130*, 16060.
- [380] M. M. Stevens, M. Mayer, D. G. Anderson, D. B. Weibel, G. M. Whitesides, R. Langer, *Biomaterials* **2005**, *26*, 7636.
- [381] J. Xiang, W. Lu, Y. Hu, Y. Wu, H. Yan, C. Lieber, *Nature* **2006**, *441*, 489.
- [382] L. Sun, G. Qin, J.-H. Seo, G. K. Celler, W. Zhou, Z. Ma, *Small* **2010**, *6*, 2553.
- [383] T. Takahashi, K. Takei, E. Adabi, Z. Fan, A. M. Niknejad, A. Javey, *ACS Nano* **2010**, *4*, 5855.
- [384] C. Kocabas, H.-S. Kim, T. Banks, J. A. Rogers, A. A. Pesetski, J. E. Baumgardner, S. V. Krishnaswamy, H. Zhang, *Proc. Natl. Acad. Sci. U.S.A.* **2008**, *105*, 1405.
- [385] L. Liao, J. Bai, Y. Qu, Y.-C. Lin, Y. Li, Y. Huang, X. Duan, *P. Natl. Acad. Sci. U.S.A.* **2010**, *107*, 6711.
- [386] J. Valentine, S. Zhang, T. Zentgraf, E. Ulin-Avila, D. A. Genov, G. Bartai, X. Zhang, *Nature* **2008**, *455*, 376.
- [387] R. Service, *Science* **2010**, *328*, 304.
- [388] J. M. Nguyen, Y. Nagarah, Y. Qi, S. S. Nonnenmann, A. V. Morozov, S. Li, C. B. Arnold, M. C. McAlpine, *Nano Lett.* **2010**, *10*, 4595.
- [389] Y. Qi, N. T. Jafferis, K. Lyons, C. M. Lee, H. Ahmad, M. C. McAlpine, *Nano Lett.* **2010**, *10*, 524.
- [390] Y. Qi, M. C. McAlpine, *Energy Environ. Sci.* **2010**, *3*, 1275.
- [391] Y. Qi, J. Kim, T. D. Nguyen, B. Lisko, P. K. Purohit, M. C. McAlpine, *Nano Lett.* **2011**, *11*, 1331.
- [392] X. Feng, B. D. Yang, Y. Liu, Y. Wang, C. Dagdeviren, Z. Liu, A. Carlson, J. Li, Y. Huang, J. A. Rogers, *ACS Nano* **2011**, *4*, 3326.
- [393] K. Takei, T. Takahashi, J. C. Ho, H. Ko, A. G. Gillies, P. W. Leu, R. S. Fearing, A. Javey, *Nat. Mater.* **2010**, *9*, 821.
- [394] J. Viventi, D.-H. Kim, J. D. Moss, Y.-S. Kim, J. A. Blanco, N. Annetta, A. Hicks, J. Xiao, Y. Huang, D. J. Callans, J. A. Rogers, B. Litt, *Sci. Transl. Med.* **2010**, *2*, 24ra22.
- [395] J. Viventi, D.-H. Kim, L. Vigeland, E. S. Frechette, J. A. Blanco, Y.-S. Kim, A. E. Avrin, V. R. Tiruvadi, S.-W. Hwang, A. C. Vanleer, D. F. Wulsin, K. Davis, C. E. Gelber, L. Palmer, J. V. d. Spiegel, J. Wu, J. Xiao, Y. Huang, D. Contreras, J. A. Rogers, B. Litt, *Nat. Neurosci.* **2011**, *14*, 1599.

- [396] D.-H. Kim, N. Lu, R. Ghaffari, Y.-S. Kim, S. P. Lee, L. Xu, J. Wu, R.-H. Kim, J. Song, Z. Liu, J. Viventi, B. d. Graff, B. Elolampi, M. Mansour, M. J. Slepian, S. Hwang, J. D. Moss, S.-M. Won, Y. Huang, B. Litt, J. A. Rogers, *Nat. Mater.* **2011**, *10*, 316.
- [397] M. J. Slepian, R. Ghaffari, J. A. Rogers, *Interv. Cardiol.* **2011**, *3*, 417.
- [398] H. C. Ko, G. Shin, S. Wang, M. P. Stoykovich, J. W. Lee, D.-H. Kim, J. S. Ha, Y. Huang, K.-C. Hwang, J. A. Rogers, *Small* **2009**, *5*, 2703.
- [399] G. Shin, I. Jung, V. Malyarchuk, J. Song, S. Wang, H. C. Ko, Y. Huang, J. S. Ha, J. A. Rogers, *Small* **2010**, *6*, 851.
- [400] I. Jung, J. Xiao, V. Malyarchuk, C. Lub, M. Li, Z. Liu, J. Yoon, Y. Huang, J. A. Rogers, *Proc. Natl. Acad. Sci. U.S.A.* **2011**, *108*, 1788.
- [401] B. Furman, E. Menard, A. Gray, M. Meitl, S. Bonafede, D. Kneeburg, K. Ghosal, R. Bukovnik, W. Wagner, J. Gabriel, S. Seel, S. Burroughs, in *Photovoltaic Specialists Conference (PVSC), 2010 35th IEEE.* **2010**, 000475.
- [402] S. Burroughs, R. Conner, B. Furman, E. Menard, A. Gray, M. Meitl, S. Bonafede, D. Kneeburg, K. Ghosal, R. Bukovnic, W. Wagner, S. Seel, M. Sullivan, in *CPV-6, Freiburg, Germany* **2010**.
-